COMPUTER SIMULATED LEARNING: A DIGITAL SIMULATION OF EMBEDDING FIELD OUTSTAR NETWORKS

Charles C. Frasier

COMPUTER SIMULATED LEARNING: A DIGITAL SIMULATION OF EMBEDDING FIELD OUTSTAR NETWORKS

By

CHARLES C. FRASIER, JR.

B.S., MASSACHUSETTS INSTITUTE OF TECHNOLOGY

(1965)

SUBMITTED IN PARTIAL FULFILLMENT

OF THE REQUIREMENTS FOR THE

DEGREES OF NAVAL ENGINEER

AND MASTER OF SCIENCE IN

ELECTRICAL ENGINEERING

at the

MASSACHUSETTS INSTITUTE OF

TECHNOLOGY

June 1970

COMPUTER SIMULATED LEARNING: A DIGITAL SIMULATION OF EMBEDDING FIELD OUTSTAR NETWORKS

By

CHARLES C. FRASIER

Submitted to the Department of Naval Architecture and Marine Engineering and the Department of Electrical Engineering on June 4, 1970 in partial fulfillment of the requirements for the degrees of Naval Engineer and Master of Science in Electrical Engineering.

ABSTRACT

This thesis reports the results of digitally simulating outstar embedding field learning networks. An outstar is a device that is capable of inductively learning to associate the occurance of a command event with a pattern of events. Once this association is learned, the outstar will reproduce tha pattern whenever the command event occurs.

A simple outstar was studied. It was found that a fast rate for forgetting accumulated experience is necessary to maintain control of the amplitudes of the outstar's responses. It was further found that a fast rate for forgetting accumulated experience results in poor noise resistance but good adaptability. A slow forgetting rate results in good noise resistance but poor adaptability. The practical aspects of thresholds was studied.

A laterally inhibiting outstar was studied. It was found that the active process of lateral inhibition results in both good noise resistance and good adaptability.

A short study of outstar avalanches was made. An outstar avalanche is a cascade of outstars which can learn and reproduce time varying patterns. It was found that a command node cascade avalanche does not work well because of pulse lengthening. A "long axon with collaterals" avalanche was studied.

A virtual laterally inhibiting outstar was studied.

A convenient method for analyzing new formulations for the learning process in an outstar was developed. A "generalized" learning process was developed and studied.

The analogy between embedding field theory and the nervous system of living organisms was introduced. The theoretical proposal that learning on the neurophysiological level is due to the production of transmitter in a synaptic cleft proportional to the correlation between presynaptic and postsynaptic membrane potentials was used to simplistically model a learning process for outstars.

Thesis Supervisor: Ian T. Young
Title: Professor of Electrical Engineering

TABLE OF CONTENTS

CHAPTER 1 EMBEDDING FIELD NETWORKS

section 1.1 Introduction

Grossberg has developed a theory for learning called embedding field theory. (Refs. 1 - 10) He has proposed several devices designed in accordance with this theory to handle broad categories of learning phenomena. These devices are inductive learning machines which are governed by a set of deterministic equations. He has qualitatively demonstrated their learning abilities. He has further drawn an analogy between embedding field theory and the nervous system of living organisms. Based on this analogy, he has made a concrete proposal for the neurophysiological phenomena underlying learning in living organisms.

By means of a digital simulation, this thesis experimentally studies one embedding field device called an outstar, and it will examine a combination of outstars called an outstar avalanche. The analogy between the nervous system of living organisms and embedding field theory will be introduced and examined.

For the uninitiated, we will begin by deriving the basic concepts of embedding field theory from intuitive ideas about learning.

section 1.2 Illustrative Derivation of an Embedding Field Network

Embedding Field theory is a mathematical model for learning. To gain an operational appreciation of this model, consider modeling the following learning experiment:

An experimenter teaches a subject an arbitrary time sequential list of letters of the alphabet by saying the list to the subject several times. At the end of this instruction, the subject is requested to repeat the list. If he can, then it is concluded that he has learned the list.

In order for the subject to learn the list, the letters composing the list must be familiar to him and must appear to be separate events. One of the tasks of this experiment will be to teach the subject to combine the separate letters of the alphabet into a new event which is the list. We expect that after instruction, presentation of the first letter of the list will automatically result in the subject expecting to hear the succeeding letters of this list.

We begin our description by modeling the subject's state before the experiment has begun. He is familiar with the letters of the alphabet and recognizes them as separate events. We model this by assigning a distinct point in space to each letter of the alphabet and calling these points nodes. To denote recognition of a letter of the alphabet, A_i, we assign a time varying process $x_i(t)$ to each node V_i. $x_i(t)$ has the properties:

(a) $x_i(t) \sim 0$ when the letter A_i has not been presented to the subject recently.

(b) $x_i(t) > 0$ when the letter A_i has been presented to the subject

recently.

As $x_i(t)$ indicates only the two conditions (a) and (b) above, we may constrain $x_i(t)$ to be non negative.

We model the experimenter's ability to communicate with the subject similarly. When the experimenter says the letter A_i to the subject, a non negative input pulse $P_i(t)$ is delivered to the appropriate node V_i in the subject. The pulse $P_i(t)$ has the properties:

(c) $P_i(t) > 0$ when the experimenter says A_i.

(d) $P_i(t) = 0$ all other times.

It will require a small, but finite, time interval for the experimenter to say A_i. $P_i(t)$ is non zero during this time interval.

We are now in a position to write a differential equation for $x_i(t)$:

eqn (1) $\dot{x}_i(t) = -\alpha x_i(t) + P_i(t)$

Equation (1) was chosen to model the response of V_i to presentation of the letter A_i because it is the simplest continuous representation for $x_i(t)$ satisfying conditions (a) and (b) on $x_i(t)$.

The experiment is now begun. The experimenter says a list A_1, A_2, ... A_n to the subject. There will be a time interval, w_i, between the presentation of each letter. For simplicity, we assume that these time intervals are all the same.

At the beginning of the experiment the subject has no idea of what the experimenter's list is. Therefore, when A_i is presented the subject can only guess, with probability 1/26 of success, what the experimenter's selection for the second letter A_2 is. This carries throughout the list. If the experimenter has presented letter A_j, the subject can only guess with probability 1/26 of success, what the A_{j+1} letter is.

However, when the experimenter presents the list for the second time, we expect the subject to be able to predict the succeeding letters of this list with much greater accuracy. When the subject has learned the list, he will be able to predict all the letters in the list, in their correct order, with certainty.

We must now model this process.

Firstly, we have said that the subject has the ability to predict what the succeeding letters of the list are, and this ability becomes more successful after each presentation of the list.

Let us model this prediction process by connecting each of our nodes to every other node with transmission lines which we shall call edges. We allow the signal $x_i(t)$ from a node to travel away from that node along the edges to each of the other nodes where it can act as input to these nodes. The actual prediction of the letter following the A_j letter is modeled in the same manner as awareness of a letter being presented by the experimenter. The appropriate $x_i(t)$ process is excited by the prediction signals arriving via the edge from V_j.

The subject's ability to only blindly guess what each succeeding letter is when the list is first presented means that equal prediction signals are received at all nodes at the beginning of the experiment. His ability to predict the entire list in the correct order after learning means that after excitation of the V_j node, a prediction signal is received only at the correct V_{j+1} node.

Prediction of the letters of the list in their correct order requires that the V_j node be excited by prediction signals before the V_{j+1} node. To accomplish this, we constrain the prediction signals traveling along the edges to a finite transmission velocity. That is, the signal $x_j(t)$

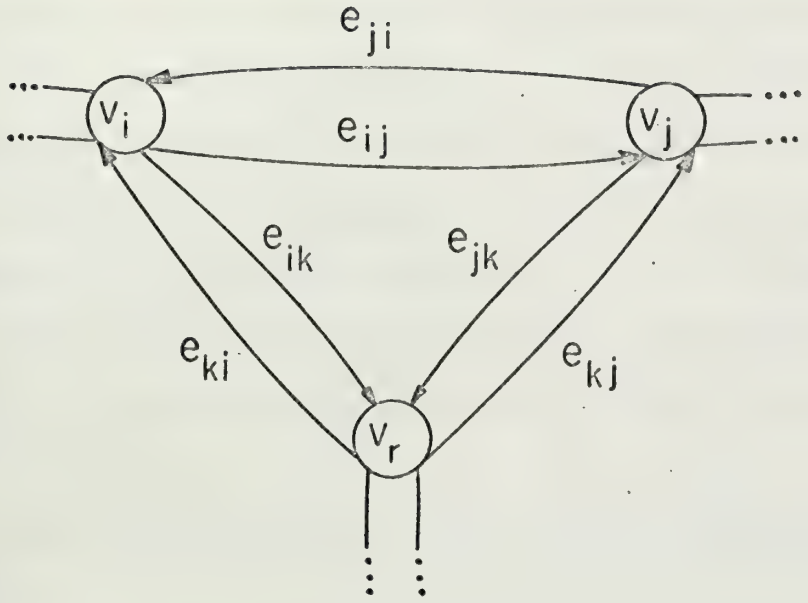

Figure 1.2.1. Geometric schematic of nodes and directed edges.

originating at node V_j arrives at node V_{j+1} after a time delay of $\tau_{j,j+1}$ time units.

The situation we have described so far is pictured in figure 1.2.1.

In figure 1.2.1 we have drawn the edge e_{ij} as two directed edges, e_{ij} and e_{ji} to stress that the lists A_iA_j and A_jA_i are distinct. The arrowhead indicates the direction of transmission along the directed edge.

Refering to figure 1.2.1 one can easily see how the subject predicts the succeeding letters of the list after he has learned it. If he has learned the list ... $A_iA_kA_j$..., excitement of $x_i(t)$ will result in a signal traveling to V_k. It will arrive at V_k, τ_{ik} time units later and $x_k(t)$ will be excited and a signal will be sent to V_j and so on. For simplicity, we shall assume that all the transmission delays are equal, or $\tau_{ij} = \tau$ for all i and j.

The effect of learning on the subject's prediction process is as follows:

(e) Before learning, excitement of the V_j node by presentation of the A_j letter results in equal prediction signals arriving at all nodes to which V_j is connected by edges τ time units after presentation of the A_i letter.

(f) After learning, excitement of the V_j node by presentation of the letter A_j results in a large prediction signal being delivered to the V_{j+1} node from V_j τ time units after presentation of A_j. No prediction signals, or at least small prediction signals, are delivered to the other nodes connected to V_j by edges.

Now, we must develop a mechanism which connects the subject's prediction process from state (e) to state (f) as the list is repeatedly presented.

To develop this mechanism, we note that the experimenter is presenting letters to the subject every w time units. If w is too small, say 1 millisecond, the subject will be unable to distinguish the separate letters of the list and it will be impossible for him to learn the list. On the other hand, if w is too large, say 24 hours, we expect the subject to have lost the context of the experiment. That is, if the experimenter said "A" yesterday, and then says "C" today, we would not be surprised if the subject responded, "See what?"... Again, we do not expect the subject to learn the list when w is too large. In between these extremes we expect the subject to do very well.

We now analyze this dependence of the subject's learning ability on the presentation interval w.

If w is large, say $w >> \tau$, then the process $x_j(t)$ has long ago decayed to zero before the next letter is presented to the subject and x_{j+1} becomes large. Additionally, the prediction signals from V_j have long since traveled to the ends of the edges from V_j, performed their prediction excitement of the other nodes, and decayed. As w is shortened we begin to arrive at the situation where the prediction signal from V_j arriving at the other nodes is still large when V_{j+1} is excited by presentation of the A_{j+1} letter. When $w = \tau$ the signal from V_j arriving at the other nodes exactly correlates with the x_{j+1} process. Making w smaller yet, such that $w << \tau$, means that many nodes are large when the prediction signals from any one of the excited nodes arrives at any other.

It seems likely that the subject's learning ability is dependent on the correlation between his prediction signal arriving at the V_{j+1} node from the V_j node and excitement of the x_{j+1} process by presentation

of the A_{j+1} letter. Assuming that this is the key to the subject's learning ability, we may write down some properties for his learning mechanism:

(g) If in one presentation of the list $\ldots A_j A_{j+1} \ldots$ the prediction signal arriving at the V_{j+1} node from the V_j node is large at the same time that the x_{j+1} process is large, then on subsequent predictions of the list a large prediction signal is delivered to V_{j+1} from the V_j node.

(h) If condition (e) is not met, then on subsequent predictions, a small prediction signal is delivered to the V_{j+1} node.

In condition (g) and (h) we have gotten in some geometrical difficulty. Previously we had decided that the prediction signal traveling along an edge e_{ij} is the x_i process from the V_i node suitably time delayed to account for the finite transmission velocity. If this signal is allowed to arrive at the V_j node unchanged it will always be large τ time units after excitement of V_i. Yet in condition (g) and (h) we have described a process which determines the amplitude of the prediction signal being delivered to V_j based on the past correlations between the prediction signal and the x_j process. The difficulty is that we must now require V_j to perform two functions: That of keeping track of recent presentations to, or predictions by, the subject of the A_j letter via the x_j process; and that of determining how vigorously the subject should predict the A_j letter based on past experience. The second of these functions was placed at V_j because it requires both the prediction signal $x_i(t - \tau)$ and the x_j process be simultaneously available for correlation.

Reference to figure 1.2.1 shows that besides V_j, the other place where $x_i(t - \tau)$ and x_j are simultaneously available for correlation is

the arrowhead of the e_{ij} directed edge. In order to maintain one function per element of figure 1.2.1., we shall locate a process, z_{ij}, in the arrowheads of the directed edges with properties (g) and (h). This simplifies things considerably, because we can make this process an amplifier of prediction signals with the further properties:

(i) When z_{ij} is large, a large prediction signal is delivered to V_j from V_i.

(j) When z_{ij} is small, a small prediction signal is delivered to V_j from V_i.

A modification of eqn (1) is now in order to account for conditions (i) and (j) above:

eqn (2) $$\dot{x}_j(t) = -\alpha x_j(t) + P_j(t) + \sum_i z_{ij}x_i(t - \tau)$$

Considering conditions (e), (f), (g), and (h) we may formulate an equation for z_{ij} as a function of time.

Condition (e) implies that before the experiment begins, $z_{ij}(t) \sim 0$. That is, the initial conditions on the z_{ij} are:

$$z_{ij}(0) \sim 0$$

Conditions (f) and (g) imply that $z_{ij}(t)$ gets large only when the predicting signal $x_i(t - \tau)$ and process $x_j(t)$ are large at the same time, and that $z_{ij}(t)$ remains large for a long time afterward. That is:

$$\dot{z}_{ij}(t) \sim x_i(t - \tau)x_j(t)$$

Condition (h) implies that when $x_i(t - \tau)$ and $x_j(t)$ are not large at the same time, then $z_{ij}(t)$ decays toward zero. That is:

$$\dot{z}_{ij}(t) \sim -uz_{ij}(t)$$

Combining the above results, we have:

eqn (3) $$\dot{z}_{ij}(t) = -uz_{ij}(t) + x_i(t - \tau)x_j(t)$$

with initial conditions $z_{ij}(0) \sim 0$.

Equations (2) and (3) are sufficient to describe the subject's learning process and its dependence on the experimenter's presentation interval w. If the experimenter presents the letters of the list with a time interval between each letter of approximately τ time units, then when the A_{j+1} letter is presented, the prediction signal from the V_j node has arrived at the arrowhead of the $e_{j,j+1}$ node and the product $x_{j+1}(t)x_j(t - \tau)$ is large. From eqn (3) $z_{j,j+1}(t)$ grows. On subsequent repetitions of the list the same conditions are met and $z_{j,j+1}(t)$ grows larger yet. On the other hand, $x_k(t)$ for the nodes V_k, $k \neq j + 1$, corresponding to letters of the alphabet other than A_{j+1} are small when A_{j+1} is presented and from eqn (3), $z_{jk}(t)$ decays toward zero for $k \neq j+1$. When the subject is asked to recall the list, he uses his prediction process, starting at the first letter A_1 and sequentially excites each of the nodes corresponding to letters in the list in their correct order by following the path of large z_{ij}'s until the end of the list is reached. To prevent saddling ourselves with a cumbersome output mechanism, we assume that the experimenter can read the amplitudes of the $x_j(t)$ processes and considers a large $x_j(t)$ as a response by the subject.

One can easily see that when $w >> \tau$, none of the products $x_i(t - \tau)x_j(t)$ are large and the subject learns nothing. On the other hand when $w << \tau$, many nodes, V_k, are excited before the prediction signals from the node associated with the first letter in the list arrive at their corresponding arrowheads. Thus the associated $z_{ik}(t)$'s grow large. This situation continues as the prediction signals from the subsequent letters of the list arrive at their arrowheads. Called upon to repeat the list, the subject's prediction process will equally excite many nodes at the same time. To the subject, it will appear

that every letter of this list succeeds every other letter. Although he has limited his guesses to the letters in the list, the subject is no better off than he was at the beginning of the experiment in being able to repeat the list.

section 1.3 Generalized Embedding Fields

The embedding field network derived in section 1.2 to model learning of an alphabetic list is a specialized example of embedding field networks. This particular network was derived because it illustrates vividly the major ideas behind embedding field theory and its derivation depends only upon intuitive ideas about learning. It is not the only embedding field network which can learn time sequential lists and it may not be the best network for this purpose. The alert reader may have noticed that it can not repeat a list in which a letter is repeated. In addition to being dependent on the experimenter's presentation interval w, its performance is highly dependent on the time delay γ and the parameters α and u in eqns (2) and (3). It has other problems, but remarkably, Grossberg has shown that these problems are qualitatively similar to problems experienced by human subjects trying to learn an alphabetic list. (The interested reader is refered to references 1 and 3 for a detailed analysis of networks similar to that derived in section 1.2.)

However, the network of section 1.2 contains most of the elements of embedding field theory and we shall pause here to list them. Figure 1.3.1 shows the pictoral representation of these elements.

(1) A node V_i representing an elemental event which the network is capable of recognizing and responding to.

(2) A directed edge e_{ij} allowing transmission of signals at a finite velocity in one direction from node V_i to node V_j. Pictorally, a directed edge is drawn as an arrow shaft with the arrowhead indicating the transmission direction.

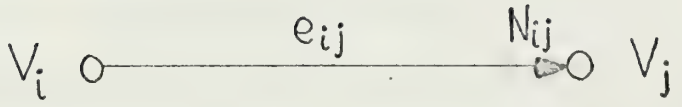

Figure 1.3.1. Elements of an embedding field network.

The process $x_i(t)$ is located at the V_i node.

The process $x_j(t)$ is located at the V_j node.

The process $z_{ij}(t)$ is located at the arrow head N_{ij}.

The prediction signal $x_i(t - \tau)$ is arriving at the arrow head N_{ij}.

(3) Arrowheads N_{ij} representing the termination of directed edge e_{ij} on the node V_j. Because the directed edges transmit signals without effecting them, it will not be necessary to reference signals traveling along a directed edge until they reach the arrowhead. In all subsequent equations in this paper, signals which have been transmitted along a directed edge will be identified by the effect of the transmission delay on them, i.e. $x_i(t - \tau)$.

(4) Input pulses $P_i(t)$ to node V_i indicating the occurance of the elemental event represented by V_i in the environment external to the network. Input pulses will always be non negative and identically zero except in a small time interval around the occurance of event i. It is assumed throughout this paper that $P_i(t)$ is immediately available at V_i whenever event i occurs. Because embedding field theory does not deal with the input apparatus necessary to deliver inputs to nodes, no geometric symbol has been developed for this purpose.

(5) A process $x_j(t)$ located at V_j with the general formulation:

1.3.1 $$\dot{x}_j(t) = -a(t) + \sum_i b_i(t - \tau) + P_j(t)$$

The amplitude of $x_j(t)$ indicates whether the event represented by V_j has recently been observed or predicted by the network.

The term $a(t)$ is designed such that $x_j(t)$ always returns to some ambient state indicative of no recent occurance or prediction of event j.

The term $b_i(t - \tau)$ is the effect of prediction signals on V_j. The summation is taken over every arrowhead N_{ij} impinging on V_j. $b_i(t - \tau)$ is the modified prediction signal received by V_j from the arrowheads N_{ij} impinging on it.

We will most frequently use the following formulations for these functions:

$$a(t) = \alpha x_j(t)$$

$$b_i(t - \tau) = \beta z_{ij}(t) x_i(t - \tau)$$

With these formulations, equation 1.3.1 is:

$$\dot{x}_j(t) = -\alpha x_j(t) + \beta \sum_i z_{ij}(t) x_i(t - \tau) + P_j(t)$$

(6) A prediction signal modification process $z_{ij}(t)$ located in the N_{ij} arrowhead with the general formulation:

1.3.2 $$\dot{z}_{ij}(t) = -u(t) + f(x_i(t - \tau), x_j(t))$$

The $z_{ij}(t)$'s are the memory of the network. In general $z_{ij}(t)$ will correlate prediction signals signals $x_i(t - \tau)$ with the process $x_j(t)$ via function f, and deliver a suitably modified prediction signal $b_i(t - \tau)$ to V_j. The amplitude of $z_{ij}(t)$ is the network's memory of how well $x_i(t - \tau)$ and $x_j(t)$ have correlated in the past. The term $u(t)$ is the network's "forgetfulness". We will most frequently use the following formulations for these functions:

$$u(t) = -uz_{ij}(t)$$

$$f(x_i(t - \tau), x_j(t)) = vx_i(t - \tau) x_j(t)$$

With these formulations, equation 1.3.2 is:

$$\dot{z}_{ij}(t) = -uz_{ij}(t) + vx_i(t) x_j(t - \tau)$$

Combining the geometric elements of figure 1.3.1 in various ways and suitably defining the terms of eqns 1.3.1 and 1.3.2, Grossberg has developed networks which qualitatively model many general categories of learning phenomena. In addition to describing learning phenomena on the psychological level as in section 1.2, Grossberg has drawn an analogy between embedding field networks and nerve networks in living organisms which is a concrete theoretical proposal for the neurophys-

iological phenomena underlying learning in living organisms. (See references 2 and 4.)

The power of embedding field theory is that it is a generalized theory describing learning with deterministic equations. The equations are simple enough to allow mathematical analyses and the establishment of the conditions necessary for them to perform the tasks desired of them. Due to the large number of nodes and arrowheads necessary to model a particular learning phenomena, exact analytic descriptions of their performance are difficult. However, the basic simplicity of the equations makes the simulation of their performance straightforward on a high speed computer.

CHAPTER 2 THE OUTSTAR AND THE OUTSTAR AVALANCHE EMBEDDING FIELD NETWORKS

section 2.1 Description of the Networks

The embedding field network of section 1.2 was derived to illustrate the concepts of embedding field theory. Combining the elements of his theory in another way, Grossberg has proposed two very interesting networks which this paper will study. The outstar network, and a combination of outstars called an outstar avalanche, are networks capable of learning and reproducing any number of complicated space-time patterns.

Figure 2.1.1 presents the geometric schematic for an outstar and the basic equations governing its performance. The N grid nodes V_1, V_2, ...V_n represent the set of elemental events the network is capable of recognizing. Each of the distinct combinations of elemental events taken singly or several at a time is a distinct pattern.

The command node V_c represents an event which always precedes a particular pattern of grid elemental events. The function of the outstar is to learn to associate the occurance of the event associated with the command node causally with the occurance of the grid pattern. After learning this "causal" association, the occurance of the command node event will result in the associated pattern occuring on the grid - even though there are no external inputs to the grid.

As an illustration, the outstar may be used to model a pianist playing a piano from a score. Excitement of the x_c process at the command node represents the event of reading the notes associated with a chord on his score. The grid nodes represent his fingers and a large

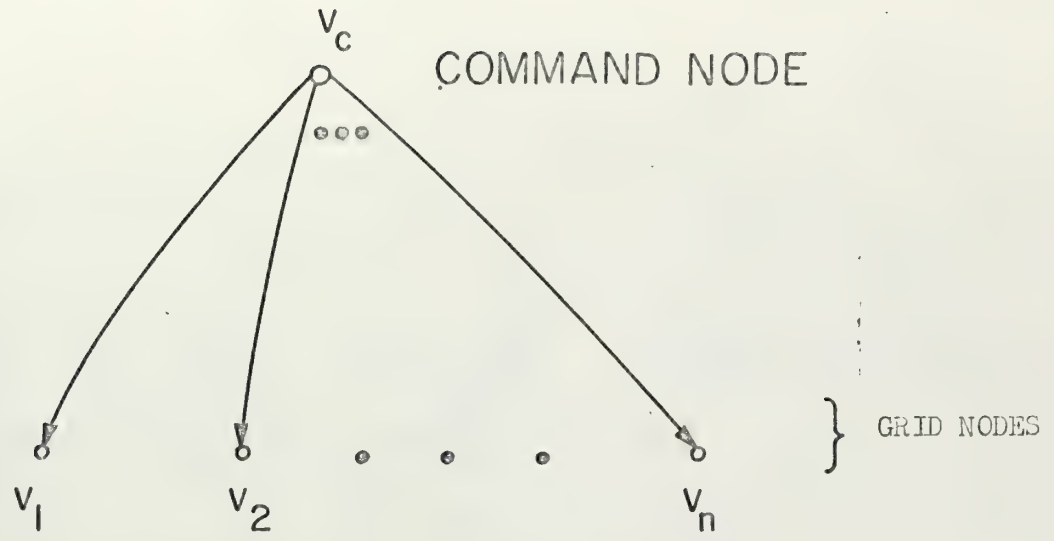

EQUATIONS GOVERNING NETWORK PERFORMANCE

2.1.1 $\dot{x}_c(t) = -\alpha x_c(t) + P_c(t)$

2.1.2 $\dot{x}_i(t) = -\alpha x_i(t) + \beta z_{ci}(t) x_c(t-\tau) + P_i(t)$

2.1.3 $\dot{z}_{ci}(t) = -u z_{ci}(t) + v x_c(t-\tau) x_i(t)$

Figure 2.1.1. An outstar network and the equations governing its performance.

STARTING NODE

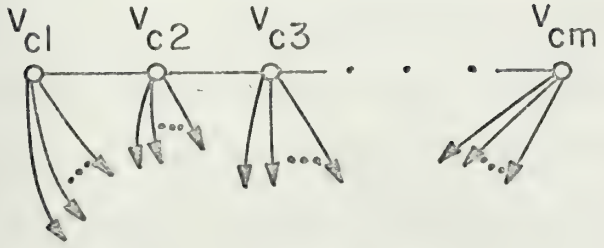

COMMAND NODE CASCADE

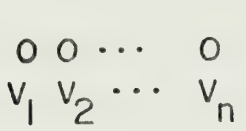

} GRID NODES

EQUATIONS GOVERNING NETWORK PERFORMANCE

2.1.4 $\dot{x}_{c1}(t) = -\alpha x_{c1}(t) + P_{c1}(t)$

2.1.5 $\dot{x}_{ci}(t) = -\alpha x_{ci}(t) + \beta x_{ci-1}(t - \tau)$ for $1 < i \leq M$

2.1.6 $\dot{x}_j(t) = -\alpha x_j(t) + \beta \sum_{i=1}^{M} z_{ci,j}(t) x_{ci}(t - \tau) + P_j(t)$ for $1 \leq j \leq N$

2.1.7 $\dot{z}_{ci,j}(t) = -uz_{ci,j}(t) + vx_{ci}(t - \tau)x_j(t)$

Figure 2.1.2. An outstar avalanche and the equations governing its performance.

$x_i(t)$ is interpreted as the ith finger being lowered to strike a piano key. A small $x_j(t)$ represents the jth finger being raised so as not to strike a key. By practice the piano player will learn the proper finger positions associated with the written chord in the musical score. The outstar will learn the proper finger positions by reading the chord on the score and having its fingers placed in the proper positions sufficiently often. This finger pattern will be remembered by large and small $z_{ci}(t)$'s at the appropriate arrowheads impinging on the grid nodes. After having learned the association between the written chord on the score, both the pianist's and the outstar's fingers will automatically assume the proper position when the chord is read.

Figure 2.1.2 presents the geometric schematic of an outstar avalanche and the basic equations governing its behavior. An outstar avalanche is a cascaded series of outstars. Each outstar learns and is capable of reproducing the pattern on the grid approximately time units after its command node is excited. The command nodes are deterministically cascaded. That is, excitation of the starting node V_{c1} by an input will always result in a prediction signal going to V_{c2} which will send one to V_{c3} and so on. There is no learning associated with this. The command node cascade is an embedding field clock. Because the prediction signals travel along directed edges at constant velocities, excitement of the starting node results in a prediction signal arriving at command node V_{ci}, $(i - 1)\gamma$ time units later. If a time varying pattern of elemental events is being played on the grid, then each command node takes a picture of that pattern when it is excited. Thus associating the start of a particular time varying pattern, say a piano sonata, with excitement of the starting node will

result in a time sequential series of pictures approximating that pattern being learned by the network. If many command nodes are cascaded in this manner and γ is made sufficiently small, the sampled data approximation of the pattern can be made arbitrarily close to the pattern.

section 2.2 Theoretical Work on Outstars and Outstar Avalanches

Grossberg has mathematically analyzed the pattern learning abilities of outstars and outstar avalanches extensively. (Refs 7 and 8). In the process of this analysis he developed particularly handy mathematical descriptions of a pattern of elemental events, the pattern learned by the outstar to approximate this pattern, and the pattern reproduced by the outstar on its grid when predicting the elemental event pattern.

An elemental event pattern is defined by the values of the input pulses $P_i(t)$ at the grid nodes. Although their amplitudes may be different, all input pulses have the same shape. We can describe the relation of the ith input pulse to the other N - 1 inputs (consisting of non zero pulses $P_j(t)$ indicating that event j is part of the pattern and zero pulses $P_k(t)$ indicating that event k is not part of the pattern) by forming the probability:

$$\theta_i = \frac{P_i(t)}{\sum_{j=1}^{N} P_j(t)}$$ when any $P_i(t)$ comprising the pattern is non zero

The elemental pattern can be completely described by the N dimensional vector,

$$\vec{\theta} = \theta_1, \theta_2, \ldots, \theta_n$$

Note that this description of the pattern is amplitude independent. That is, $\vec{\theta}$ defines the pattern whether that pattern is presented vigorously or not. Additionally note that by the definition of the θ_i, $\vec{\theta}$ not only describes a pattern by the occurance or non occurance of elemental events in it, but also by the relative strength of the occurance of those events. In the piano playing example, this corresponds to describing the finger positions for a chord by indicating

which fingers are raised so as not to strike keys and which fingers are lowered to strike keys, plus the relative pressure each of the lowered fingers is to exert on the keys.

Since the $P_i(t)$'s have the same shape, and differ only in amplitude, the θ_i's are constants during presentation of the pattern.

In a similar manner the outstars' response to presentation or prediction of this pattern can be described by the probability vector:

$$\vec{X}(t) = X_1(t), X_2(t), \ldots, X_n(t)$$

where $$X_i(t) = \frac{x_i(t)}{\sum_{j=1}^{N} x_j(t)}$$

The pattern learned by the outstar to approximate this pattern can be described by the probability vector:

$$\vec{Y}(t) = y_1(t), y_2(t), \ldots, y_n(t)$$

where $$y_i(t) = \frac{z_{ci}(t)}{\sum_{j=1}^{N} z_{cj}(t)}$$

Now suppose that the pattern $\vec{\theta}$ has been presented to the outstar M times. Then Grossberg has proved that starting with arbitrary initial data for the $x_i(t)$'s and $z_{ci}(t)$'s:

(a) For every M = 1, the limits:

$$Q_i^{(M)} = \lim_{t\to\infty} X_i^{(M)}(t)$$

and

$$R_i^{(M)} = \lim_{t\to\infty} y_i(t)$$

exist.

(b) For every M = 1 and for all times t after the last presentation of the pattern, the probabilities $X_i(t)$ and $y_i(t)$ are monotonic in opposite senses with $|y_i(t) - X_i(t)|$ non increasing and are constant on intervals where the prediction signal from V_c is zero.

(c) $\lim_{M\to\infty} m_i^{(M)} = \lim_{M\to\infty} M_i^{(M)} = \theta_i$

where

$m_i^{(M)}$ = minimum of $X_i^{(M)}(t_0)$ or $y_i^{(M)}(t_0)$

and t_0 is the instant the last presentation of the pattern was completed.

And

$M_i^{(M)}$ = maximum of $X_i^{(M)}(t_0)$ or $y_i^{(M)}(t_0)$

Thus by (a) - (c),

$$\lim_{M\to\infty}\lim_{t\to\infty} X_i^{(M)}(t) = \lim_{M\to\infty}\lim_{t\to\infty} y_i^{(M)}(t) = \theta_i$$

(d) The functions $\dot{y}_i(t)$, $f_i^{(M)} = y_i^{(M)}(t) - X_i^{(M)}(t)$ and $g_i^{(M)} = X_i^{(M)}(t) - \theta_i$ change sign at most once and not at all if $f_i^{(M)}(t=0)g_i^{(M)}(t=0) \geq 0$. Moreover, $f_i^{(M)}(t=0)g_i^{(M)}(t=0) > 0$ implies $f_i^{(M)}(t)g_i^{(M)}(t) > 0$ for all $t \geq 0$.

Interpreting these results, we see that (c) implies that the network's memory of the pattern and its predictions of the pattern converge to the pattern as the number of times the pattern is presented increases, or "practice makes perfect". (a) and (b) insures that the network's memory of and prediction of the pattern after the last presentation of the pattern will get no worse than it was immediately after that last presentation. (d) shows that there is at most one oscilation in the convergence and therefore the network's learning ability is stable.

An additional benefit of result (c) is that if the network started associating one pattern with the command node event and it is decided that association is an error, then a new pattern, the correct one, may be learned over the old one with sufficient practice. That is, all errors are correctable.

section 2.3 Approach to the Study

Grossberg's theoretical results greatly enhance the attractiveness of outstars and avalanches as devices for modeling certain categories of learning phenomena. As qualitative models they have wide application. (See refs 6 and 9) However, beyond the qualitative insight that they provide, are they practical? The mathematics guarantee that an avalanche will learn a piano sonata with sufficient practice. If sufficient practice means forty years, we would do well to go shopping for another model - not because they do not work, but because they do not work well enough.

Thus the question "How well do they work?" is pertinent. This is the question that this paper addresses. It is a practical question and outstars and avalanches are considered as practical devices that learn throughout the rest of this paper.

In order to accomplish this study, a digital simulation of the networks was programed onto a computer. The details of this simulation and an evaluation of its accuracy are provided in appendix A. All attempts were made to reduce the artificialities and errors introduced by this method of study. However, constraints were forced on the study by the digital simulation and these constraints will be noted and explained as they occur in this paper.

As an outstar avalanche is a cascade of outstars, the primary emphasis of this study is on outstars. In studying the outstars, attention is devoted to the possible interactions of one outstar in an avalanche with another. Where avalanches are presented, they are more or less used as tests to confirm the conclusions established while

studying the outstars composing them.

CHAPTER 3 THE SIMPLE OUTSTAR

section 3.1 Specification of Parameters for the Study

The geometric schematic and equations in figure 2.1.1 describe the simplest outstar. The equations are repeated here for easy reference:

3.1.1 $\dot{x}_c(t) = -\alpha x_c(t) + P_c(t)$

3.1.2 $\dot{x}_i(t) = -\alpha x_i(t) + P_i(t) + \beta z_{ci}(t) x_c(t - \tau)$

3.1.3 $\dot{z}_{ci}(t) = -u z_{ci}(t) + v x_i(t) x_c(t - \tau)$

In order to study this outstar, we must assign numbers to the constants α, β, u, v, and τ; initial conditions must be assigned to the variables x_c, x_i, and z_{ci}; a shape and amplitude for the inputs P_c and P_i must be selected; and the numbers of pattern nodes, N, must be specified. Additionally, the test pattern to be taught to the outstar must be decided upon.

A great deal of experimental time can be saved if these parameters are specified in a somewhat rational way. A rationale can be developed for any method of specifying the parameters, so we shall arbitrarily begin with the inputs.

Firstly, the inputs are only used to indicate the occurance of elemental events external to the outstar. All we require of them is that they be non negative in an interval around the occurance of the elemental event and zero at all other times. Also, we would like them to reflect the strength of presentation of the events they represent. For a first try we will make them identical in shape, duration and amplitude for both the grid inputs $P_i(t)$ and the command input $P_c(t)$.

An impulse might be good shape for them, but there might be effects associated with duration that would be interesting to see. On the other hand, if we want to analytically check our results, then we want the inputs' shape to be simple enough to make the analysis tractable. A rectangular pulse of amplitude A and duration δ is suitable. Note that with this selection for inputs we have implied that our input apparatus is a digital sampling device which samples the continuous variation of events in the external environment at time t_0, sets the inputs to nodes corresponding to events present in the environment at t_0 to value A, and holds these values until the next sample is taken at time $t_0 + \delta$. If we recall that an avalanche performs a similar digital approximation to time varying events, this selection for inputs is not too bad.

As the direct response to the inputs is linear, we may leave the amplitude, A, of the input pulses arbitrary. In selection of the duration δ, we run into a compromise with the digital simulation. An accurate simulation of the response to a long duration pulse requires considerable computation time. Thus to minimize computation time, δ should be short. Yet the pulses were given a finite duration to study possible effects of duration. We do not want δ to be too short. With this trade off in mind, a good selection for δ would be the shortest rise time in the outstar. The rise times of the outstar are $1/\alpha$ for the x processes at the nodes, and $1/u$ for the z processes at the arrowheads. u is the "forgetting rate" of the outstar and it would be expected that the forgetting rate of the outstar should be slower than the response rate, α, of the x processes. Therefore it is reasonable that α should be greater than u. This implies that $1/\alpha$ is the shortest rise time

in the outstar and we shall set $\delta = 1/\alpha$.

The x processes at the command node and the grid nodes indicate the recent presentation to or prediction by the outstar of events. At the beginning of a learning experiment it is reasonable to assume that there has been no recent presentations or predictions of the events to be learned. The initial conditions for the x processes can be assumed zero, i.e. $x_c(0) = 0 = x_i(0)$ for all i.

The response time α of the x processes has already been specified as $\alpha = 1/\delta$. Thus all the parameters for the command nodes x_c process have been spedified. For the grid nodes τ , β , and the initial conditions on the z's still must be specified. To save computation time, τ should be small. As there is no feedback from the grid to the command node, there is no necessity for τ to be non zero in this simple outstar. In a digital simulation, however, the accuracy is improved if there is a time delay between simultaneous processes and making $\tau > 0$ is advantageous. A suitable selection for τ is $\tau = \delta$.

From equation 3.1.2 it can be seen that β and $z_{ci}(t)$ determine the amplitude of the prediction signal being admitted to grid node V_i. As the outstar's memory is the $z_{ci}(t)$'s, it is the most important factor in this prediction signal amplitude determination. Setting $\beta = 1$ will make analyzing the effect of the z's on the prediction signals easier.

The parameters associated with the z processes, u, v, and initial conditions $z_{ci}(0)$, must be specified. u is the "forgetting rate" of the outstar. As we want the outstar to remember what it has learned, we want u to be small. Remembering that computation time is scarce, a small u for this experiment is anything such that the decay time

1/u of the z processes is several times longer than the length of the experiment.

Selecting v is a problem. As can be seen from equation 3.1.3, v determines the rise rate and amplitude of the z process given an $x_i(t)$ response and the prediction signal $x_c(t - \tau)$. In presenting a pattern to the outstar to be learned, the best learning should occur when the inputs to the grid nodes are presented at the same time as the prediction signals from the command node arrives at the arrowheads. The problem is that in this situation, how well should the outstar learn the pattern on the first presentation? To answer this question, we need some way of measuring how well the outstar has learned a pattern after presentation.

A tentative operational measurement would be to say that the outstar has learned a pattern well when the prediction process drives the amplitudes of the grid node x processes to at least the same values as they are driven to by the event inputs. Using this measurement we can specify v's which result in well learning in one presentation or two presentations and so on.

However, this does not end the problem associated with "rationally" selecting an initial v for an experiment. Suppose we specify a v which results in well learning in one presentation. What value should this v have? A rational selection of an initial v requires solving the outstar equations. The reason why the outstar is being simulated is the difficulty of analytically solving these equations. To avoid these difficulties, the procedure taken in this study was to specify all other parameters in the outstar including the numbers of presentations required for well learning. A guess is then made for a v and an

experiment is performed to see what amplitude the prediction process will drive the grid nodes to after one pattern presentation. The guessed v is then appropriately scaled to result in the specified well learning criteria.

For the current experiment, v was selected to result in well learning in two pattern presentations.

Concerning the initial conditions for the z processes, we expect on the first presentation of the pattern that the network has not previously learned anything about the pattern. That is $z_{ci}(0) = 0$ for all i. However, we would like to see what happens if one of the z_{ci}'s is not zero at the beginning of the experiment. Therefore we will make one of the $z_{ci}(0)$ non zero, but small.

Only the number, N, of grid nodes and the test pattern to be taught the outstar remain to be specified. As we are only performing this experiment as an initial look at an outstar, a good test pattern would be presentations of one event which the outstar should learn to associate with the command event. An additional event presented at a time well removed from arrival of prediction signals from the command node would be a good way to test interference between outstars in an avalanche. As v was selected to result in well learning in two presentations, this test pattern will be presented twice and then a prediction will be called for to see how well the pattern has been learned.

This gives us two grid nodes. A third grid node is included to study the effects of the non zero initial conditioned z processes. No inputs will be given to this grid node.

We need now to only assign numbers to the parameters in accordance with the above specifications:

Geometric parameters:

N = number of grid nodes = 3

τ = time delay of prediction signal = 0.3 sec.

Input parameters:

Input pulse shape is rectangular

A = input pulse amplitude = 10

δ = input pulse duration = 0.3 sec.

Input pulses will be delivered to the command node, V_c, at times: 0.1 sec., 1.9sec., and 3.7 sec.

No input pulses will be delivered to grid node V_1

Input pulses will be delivered to grid node V_2 at times: 0.4 sec., and 2.2 sec.

Input pulses will be delivered to grid node V_3 at times: 1.0 sec. and 2.8 sec.

Network parameters:

α = time constant of x process = 3.3333 $sec.^{-1}$

β = prediction signal amplification constant = 1.0

u = "forgetting rate" = 0.01 $sec.^{-1}$

v = correlation amplification constant = 1.6 (satisfies well learning in two presentations criteria)

Initial conditions:

$x_c(0) = x_i(0) = 0$ for all i

$z_{c1}(0) = 0.1$

$z_{c2}(0) = z_{c3}(0) = 0$

The above lengthy description of the reasons for selection of the parameters for the experiment to be presented in the next section was provided as an illustration of the decisions that must be made when performing the experiments in this study. Except where noted, in the future the same reasoning will underlie the selection of parameters for experiments.

section 3.2 Experiment I - A Look at a Simple Outstar

Figure 3.2.1 shows the results of the experiment outlined in section 3.1 The inputs to the nodes are plotted on the same trace as the x process response of the nodes.

A striking feature of figure 3.2.1 is that the x process node responses all have amplitudes of significantly less than the amplitudes of the input pulses. It can be seen that this is as it should be if we consider the equation governing the response of a node to an input only:

$$\dot{x}_i(t) = -\alpha x_i(t) + P_i(t)$$

The solution of this equation for a rectangular input pulse of amplitude A and duration δ is:

$$x_i(t) = \begin{cases} (A/\alpha)(1 - e^{-\alpha t}) & \text{for } 0 \leq t \leq \delta \\ (A/\alpha)(1 - e^{-\alpha\delta})e^{-\alpha t} & \text{for } t \geq \delta \end{cases}$$

The maximum of this response occurs at $t = \delta$. For the parameters specified for this experiment, the maximum amplitude of an $x_i(t)$ response to an input pulse only is:

$$\max x_i(t) \cong 1.9$$

which is about 20% of the amplitude of the input pulses.

The pattern we intended to teach to the outstar was to associate the occurance of the command event with event 2. The outstar was instructed in this pattern twice by presenting the command event to it and then presenting event 2 to it τ time units later. This can be seen from the command input trace and grid node V_2's input trace. After the instruction was over, the command event above was presented to see if the outstar had learned the pattern. As can be seen from

Figure 3.2.1. The results of experiment I - an initial look at a simple outstar.

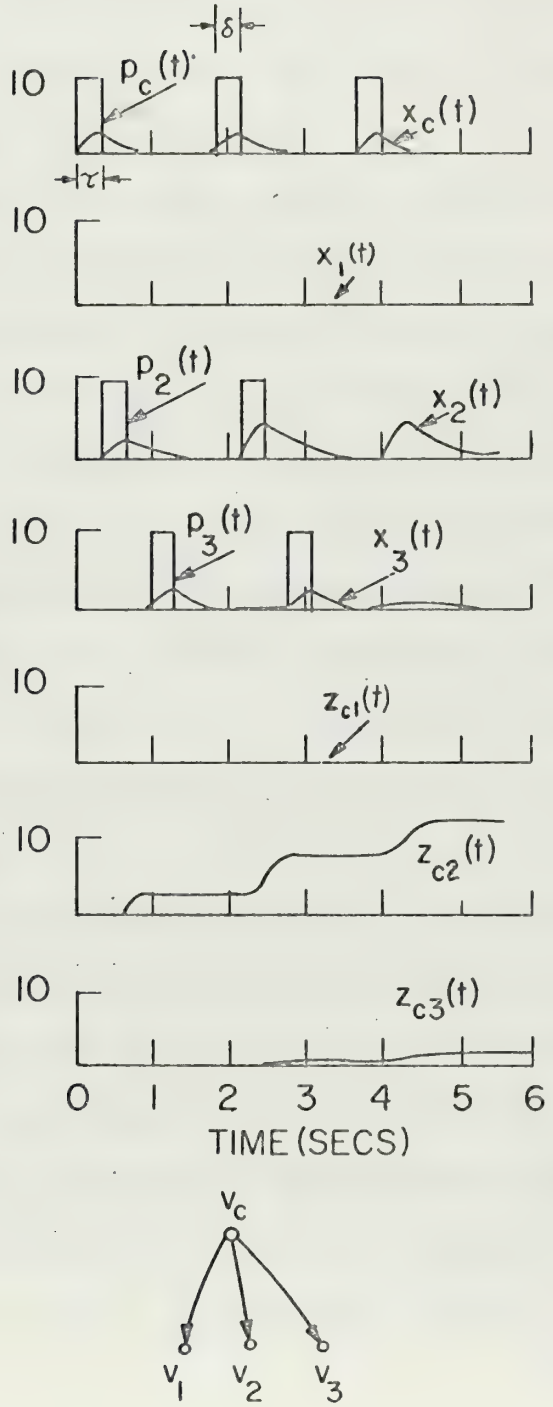

V_2's third response, the outstar did predict event 2 and we can consider that it has learned the pattern.

This experiment was also designed to see what effect a small non zero initial condition on a z would have. Thus z_{c1} was given the initial value of 0.1 while z_{c2} and z_{c3} were given zero initial values. As can be seen from the x_1 response trace, the small non zero initial value for $z_{c1}(0)$ had no perceptible effect. $x_{c1}(t)$ did respond to the prediction signals, but the response was so small that it does not show on the scale shosen for figure 3.2.1.

We gave the input pulses a finite duration to see if there would be any effects associated with this duration. Such a duration effect is the fact that the x responses reach a maximum at the end of the input pulses and then decay exponentially away from this maximum. This effect is entirely due to the shape selected for the input pulses and the exponential response of the x processes. If we accept the sampled data input apparatus described in section 3.1 as the input apparatus for the outstar, then this effect has important consequences. It says that the outstar's response to a sample taken at time t_0 extends, with large amplitude, into the next sampling period starting at $t_0 + \delta$ and beyond. In this experiment, we selected the inputs to V_3 to occur 2δ after the inputs to V_2. As explained above, the inputs to V_2 were selected to result in maximum learning. From the trace for $x_3(t)$ it can be seen that event 3 was also learned to be associated with the command event, although to a much lesser extent. This resulted from the "tail" of the prediction signal still being reasonably large when event 3 occured. The product $x_3(t)x_c(t - \tau)$ was therefore sufficient to cause z_{c3} to grow as can be seen from $z_{c3}(t)$'s trace. Thus when the

outstar was tested to see what it had learned, it predicted event 3 as well as event 2.

Thus the "tail" duration effect will result in the outstar learning not only what happens in the sample in which prediciton signals arrive from the command node, but also in the sample taken after that. By symmetry, it will learn the samples taken before in the same way. We will mark this effect for further study.

Another effect to note in figure 3.2.1 is that $z_{c2}(t)$ grew with each presentation of the pattern and on the recall test. Because u was chosen small, $z_{c2}(t)$ did not decrease and essentially acted as an integrator of $vx_2(t)x_c(t - \tau)$. The effect of the growing $z_{c_2}(t)$ can be seen in the trace for $x_2(t)$ where the x_2 response increases in amplitude on each presentation or prediction. If this growth continues, we could expect x_2 responses to get impractically large. Experiment I was continued and the $x_2(t)$ responses did continue their growth. Figure 3.2.2 shows this continuation and it can be seen from the trace for $x_2(t)$ that the x_2 responses continued to grow on predictions only. Not only are the x_2 responses growing with each prediction, but a quick look at the $z_{c2}(t)$ trace will show that they are growing at an increasing rate.

Experiment I was continued not only to study the growth of x_2 responses but also to test the theoretical prediction that outstars are capable of correcting all mistakes. An attempt was made to correct two types of mistakes in the continuations. It was decided to consider the already learned associations between the command event and event 2 as a mistake and that the correct association should be with event 3.

Figure 3.2.2.

Continuation of experiment I.

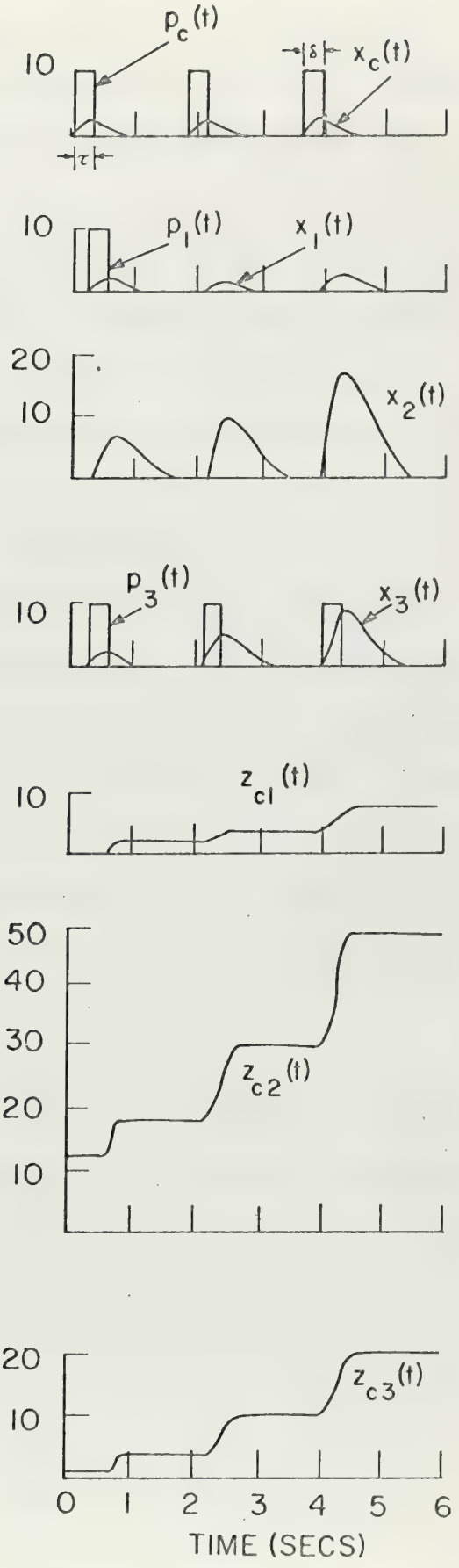

Therefore, event 3 was presented τ time units after presentation of the command event three times. Event 2 was not presented at all.

The second type of mistake was simulation of a "random" mistake by presenting event 1 once τ time units after presentation of the command event.

The results are interesting. Due to their growth, x_2 responses continued to be greater than x_1 and x_3 responses. The x_3 responses were catching up with the x_2 responses, but from the $z_{c3}(t)$ and $z_{c2}(t)$ traces, it can be seen that it will require many presentations of the $V_c \rightarrow V_3$ association before x_3 responses will reach a point where we could say that the $V_c \rightarrow V_2$ mistake is corrected.

From x_1's trace it can be seen that the "random" mistake was remembered by the outstar. It was also predicted with increasing amplitude on subsequent predictions. However, with the results of experiment I plotted as they are in figure 3.2.2 it is difficult to see if any mistakes were corrected. The theoretical prediction that all mistakes could be corrected involved the convergence of the probabilities $X_i(t)$ and $y_i(t)$ to θ_i. Translating the data from figure 3.2.2 to these probabilities, we have the following results:

Table 3.2.1

Translation of data from figure 3.2.2 to probabilities suitable for comparison to theoretical prediciton that an outstar can correct all mistakes.

Table 3.2.1

Response number, M		0	1	2	3
	θ_1	0	0.5	0	0
V_1	X_1	0	0.188	0.083	0.097
	y_1	0.07	0.083	0.091	0.101
	θ_2	1.0	0	0	0
V_2	X_2	0.892	0.563	0.0625	0.612
	y_2	0.886	0.75	0.682	0.632
	θ_3	0	0.5	1.0	1.0
V_3	X_3	0.107	0.249	0.292	0.319
	y_3	0.107	0.167	0.227	0.265

The M = 0 response column is the results from the last response in figure 3.2.1 and is the initial data that the continuation of experiment I began with. The M = 1 response column begins the attempt to correct the mistake $V_c \rightarrow V_2$ to $V_c \rightarrow V_3$ and includes the "random" mistake of presenting event 1. The M = 2 and M = 3 response columns are the continuing effort to correct $V_c \rightarrow V_2$ to $V_c \rightarrow V_3$ without "random" mistakes.

Except when the random mistake occured, X_1 and y_1 remain small and about the same magnitude as the duration effect "error" of event 3 in the first part of experiment I. We conclude that a "random" mistake affects the memory of the outstar to a small extent.

Table 3.2.1 does show that the $V_c \rightarrow V_2$ mistake is being corrected to $V_c \rightarrow V_3$ as X_2 and y_2 are decreasing while X_3 and y_3 are increasing. However, from the numbers we can conclude that it will require many presentations of the $V_c \rightarrow V_3$ pattern before the magnitudes of X_3 and y_3 exceed X_2 and y_2 and many more presentations of $V_c \rightarrow V_3$ before

X_3 and y_3 bear the same relation to X_2 and y_2 as X_2 and y_2 had to X_3 and y_3 an the M = 0 response. In the meantime, it could be expected that the x response will have become unrealistically large.

The uncontrolable growth of the x responses makes this outstar an unattractive device. Although it conforms to the theoretical predictions, the actual means by which we measure its performance is the x response and not the X probabilities. The growing x responses means that in our piano playing example, this outstar will be punching holes through the keyboard of the piano with its fingers when it plays a frequently used chord. Thus, to make this a useful device, we must find some means of limiting the x responses at a practical amplitude. As we pointed out, the growth of the x responses was due to the growth of the z_{ci} process which determines the amplitude of prediction responses. We had chosen the "forgetting rate" u of the z_{ci} processes to be small. At the same time we did so, it seemed reasonable to have the outstar forget slowly. However, non decaying z_{ci} processes have lead us to an undesirable situation. We will therefore try to control the amplitude of the x response by increasing the "forgetting rate".

section 3.3 A Simple Outstar with a "Fast" Forgetting Rate

The forgetting rate of experiment I was selected to be "slow" relative to the time scale of experiment I. In experiment I, the characteristic decay time, 1/u, for the z_{ci} process was 100 seconds which was long compared to the 11 seconds total length of the experiment. In that 11 seconds, the network was asked to learn one pattern and then to correct it. The time between presentation and/or predictions was 1.8 seconds. Thus, when we speak of a "fast" forgetting rate, we must decide "fast relative to what?".

To conserve computation time, we shall make the forgetting rate fast relative to the presentation and/or prediction time interval, i.e. 1/u = 1.8 seconds, or u = 0.556 $sec.^{-1}$. This leads us into another problem. The v of experiment I was selected on the "two presentations mean well learning" criteria. That is, the z_{ci} process would get large enough in two presentations of the pattern so that a prediction following these presentations would drive the amplitudes of the x processes to the same values as the input pulses alone would drive them. If we expect the network to forget in time comparable to the presentation interval, it would be better to change v such that it conformed to a "one presentation means well learning" criteria. We will therefore double v to v = 3.2.

To compare the fast forgetting rate outstar to the slow forgetting rate outstar of experiment I, we shall re-perform the first part of experiment I with all other parameters specified as they are in section 3.1. This experiment will be called experiment II.

Figure 3.3.1. The results of experiment II - a simple outstar with a fast forgetting rate.

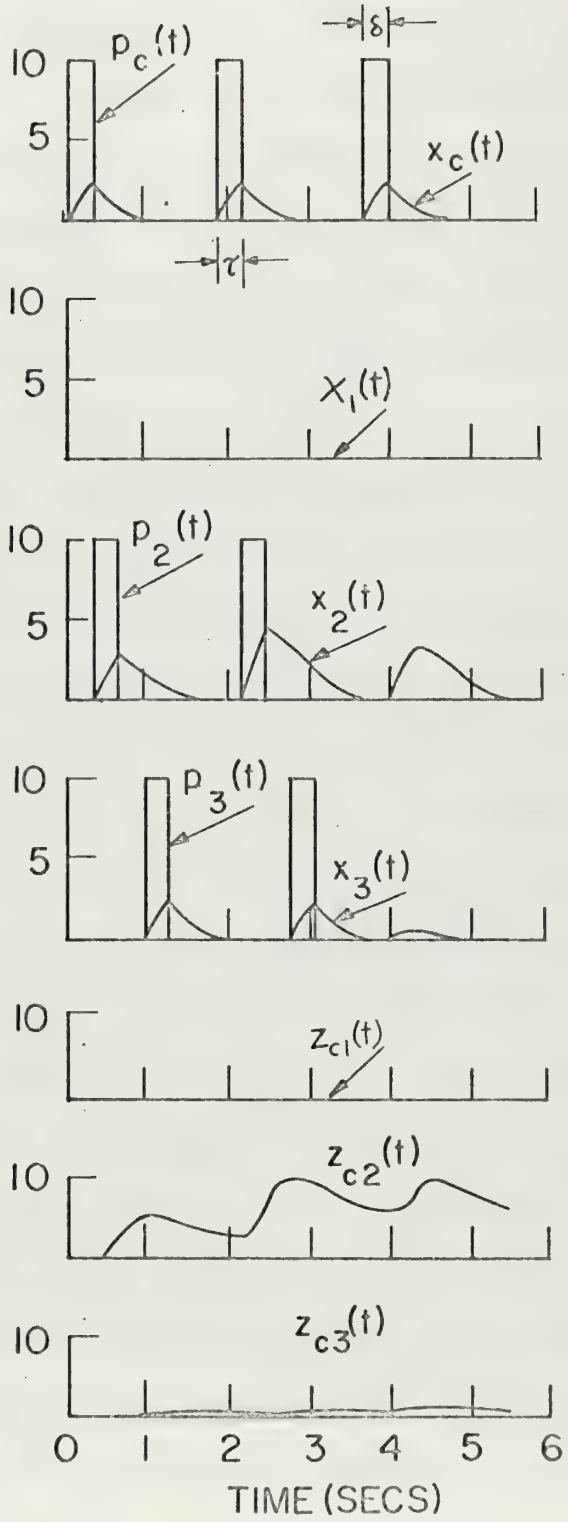

Figure 3.3.1 shows the results of this experiment. Because the responses of this experiment were smaller than in experiment I, the vertical scale for the x traces was doubled in figure 3.3.1.

As can be seen, we have managed to reasonably control the amplitudes of the x responses by allowing the z's to decay between excitements of the command node. At least the z's do not exhibit the monotonic growth they did in experiment I. The intended association $V_c \rightarrow V_3$ was learned well. Again there is some learning of $V_c \rightarrow V_3$ due to the "tails" of the prediction signal. The non zero initial condition on z_{c1} produced no perceptible effect. It can be concluded that the outstar performs very well over short periods of time. However, with its memory decaying rapidly, how long will its memory persist?

This question hits upon one of the key features of an outstar. The mathematical theorem concerning outstars states that the outstar's memory of a pattern remains unimpaired for all time after the last presentation of the pattern, provided no new or random pattern is presented to it subsequently. Of course, in the language of the theorem, this meant that the y_i's would not change even though the z_{ci}'s were decaying exponentially. It looks like a fast forgetting outstar has the opposite problem from the slowly forgetting one. That is, the responses, while retaining the proper x_i probabilities to define the pattern, are so minute that they are meaningless measured against a practical scale. However, the third response on the $z_{c2}(t)$ and $z_{c3}(t)$ traces shows that a prediction will cause the z processes to grow.

Now, suppose that the z processes have all decayed to the point where a prediction by the outstar results in meaninglessly small grid x responses. Then if enough predictions are made rapidly enough, we

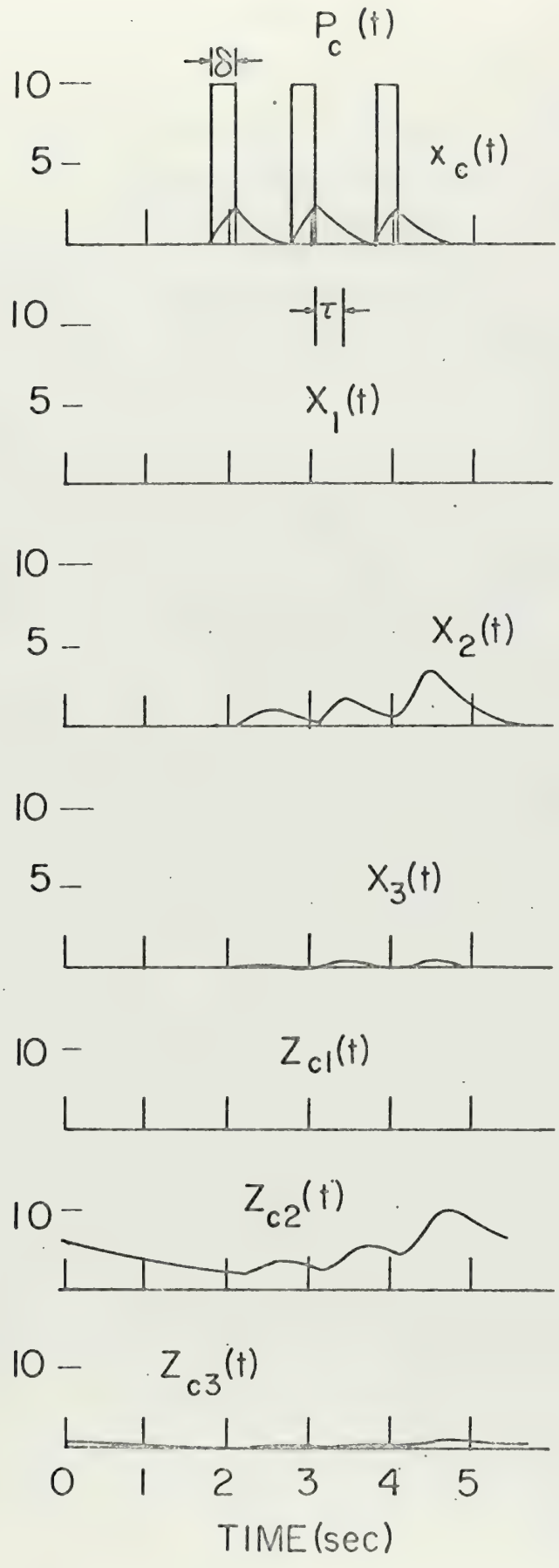

Figure 3.3.2. The results of continuing experiment II. A demonstration of "pumping up" the memory of a simple outstar with a fast forgetting rate.

can "pump up" the z's to the point where the x responses are large enough to mean something. Grossberg's theorem insures that the amplitude of the x process will remain in the proper ratios to one another. Experiment II was continued to demonstrate this memory "pumping up" and the results are shown in figure 3.3.2. As can be seen, the outstar's memory was allowed to decay for awhile and then the command event was presented to the outstar three times in rapid succession. "Pumping up" occured as expected.

A psychological interpretation of memory pumping up would not be tenuous. It is an every day occurance to have a piece of previously learned information, a name say, on the "tip of one's tongue", but not be able to recallit until all the associations connected to it have been recalled. If we consider the name to be inscribed on the grid on an outstar, then recalling things associated with the name would be equivalent to rapid excitements of the command node. After enough such excitements, the name would appear to "pop into one's head". The memory of the name would then be "fresh" for sometime after being resurrected before it again faded into the "preconscious". We will introduce a modification in section 3.5 which will make the idea of a faded memory "popping" into the outstar's "head" more precise.

Of course, a presentation of the pattern after the outstar's z processes have decayed to small values will also refresh its memory.

section 3.4 Resistance to Random Mistakes vs. Correction of Learned Mistakes: A Philosophy for Learning in Outstars

Experiment II was continued to investigate the effects of a simulated random mistake on a simple outstar with a fast forgetting rate. The results are shown in figure 3.4.1. Event 1 was presented at the same time as event 2 to simulate the occurance of a random mistake in the pattern. As can be seen from the x_1 and z_{c1} traces, the random mistake completely confused the outstar. Whereas the outstar had previously learned the association $V_c \rightarrow V_2$, occurance of the random mistake resulted in the outstar remembering $V_c \rightarrow V_2$ and to only a slightly lesser extent, $V_c \rightarrow V_1$. The amplitude of the second and third x_i prediction responses in figure 3.4.1 are significant enough to conclude that the random event resulted in confusion. The memory of a simple outstar with a fast forgetting rate has very little resistance to random mistakes.

To understand the significance of this outstar's low resistance to random mistakes, we must develop an understanding of the outstar's relationship to its external environment. Up to now, we have just been concerned with the interval workings of the outstar. Now consider that the outstar is a machine which includes the outstar network previously described plus an input apparatus. This machine "lives" in an environment in which events occur. The input apparatus filters the events occuring in the environment and delivers an input pulse to the appropriate node in the outstar when one of the events the outstar is capable of recognizing occurs. The outstar is capable

Figure 3.4.1. Continuation of experiment I from Figure 3.3.2. $P_1(t)$ simulates a random mistake in the pattern previously taught to the outstar.

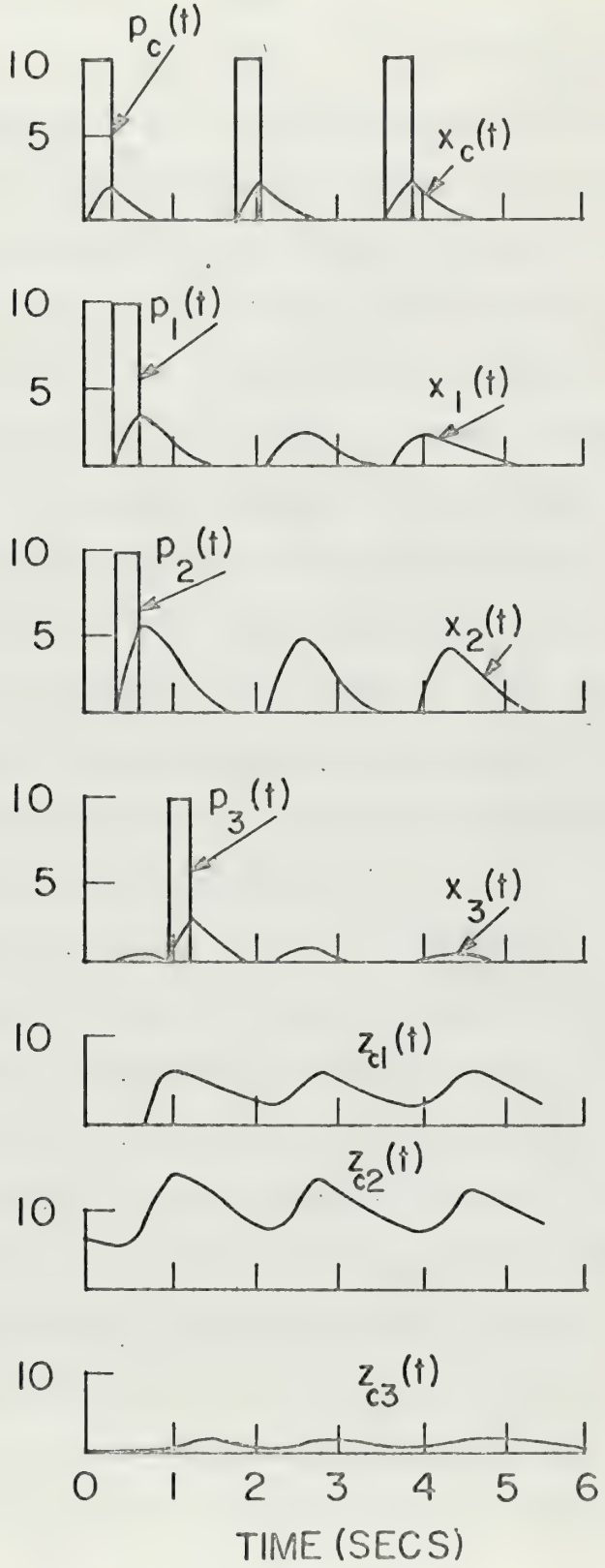

of learning the association between the command event and any events which are represented by grid nodes if they occur approximately τ time units after occurance of the command event.

In order for the outstar's learning ability to conform with intuitive notions about learning, we would want it to learn that the command event is associated with a particular pattern if and only if the occurance of the command event in the environment is usually followed by the occurance of the pattern. Suppose the outstar observed one bowling ball colliding with another with the result that the first ball stopped dead and the second bowling ball rolled away from the collision point with the same velocity that the first bowling ball had before the collision. After the first observation of this event, we would expect the intelligent outstar to suspect that it had observed a law of nature that applied to all bowling ball collisions. We would expect the outstar to go from a state of ignorance about the conservation of momentum to an intuitive understanding of it. Philosophically, we desire the outstar to be an inductive learning machine.

If we described this situation statistically, we may assign probabilities to the occurance of events in the environment. At any given time, t, we may describe the likelihood of the occurance of an event associated with the V_k node in the outstar by the probability PR_k. Additionally, we can describe the relationship between the occurance of events with the conditional probability $PR_{j/k}$ which is the probability of the occurance of event j given that event k occured recently. In the outstar we are particularly concerned with the probabilities $PR_{i/c}$ where c is the command event and the i are the grid events. To make the outstar an inductive learning machine, we want

it to learn $V_c \rightarrow V_i$ if and only if $PR_{i/c}$ is large. If $PR_{j/c}$ is small we would want the outstar definitely not to learn $V_c \rightarrow V_j$.

On the first occurance of a pattern following the command event by approximately τ time units, the outstar can have no idea of how large $PR_{i/c}$ is. Therefore we would want it to only suspect that the command event usually preceeds this pattern. However, if the next time the command event occurs, it is followed by the pattern, then there is good evidence that $PR_{i/c}$ is large and the outstar should draw this conclusion. Now, in the real world, we expect background noise. That is, if event j does not usually follow the occurance of event c, there is nevertheless a small probability that it will occur as a random mistake sometime. In order to protect the outstar's memory, we would want it to be resistant to drawing spurious conclusions about the association of the command event with randomly occuring mistakes. If the outstar observed the collision of bowling balls in which one of the balls was shattered into many pieces, we would not want this random occurance to destroy its confidence in the conservation of momentum.

The memory of a pattern in an outstar is contained in the probabilities:

$$y_i(t) = z_{ci}(t)\left[\sum_{j=1}^{N} z_{cj}(t)\right]^{-1}$$

The equation describing the z's is:

$$\dot{z}_{ci}(t) = -uz_{ci}(t) + vx_i(t)x_c(t - \tau)$$

In the case where u is very small, this is equivalent to:

$$z_{ci}(t) = v \int_{-\infty}^{t} x_i(\xi)x_c(\xi - \tau)d\xi$$

Define $I = v \int_{-\infty}^{\infty} x_i(\xi) x_c(\xi - \tau) d\xi$

where $x_i(t)$ is the response of a grid node to one input pulse in the infinite time period, and $x_c(t - \tau)$ is the prediction signal from the command node τ time units before the grid event. Thus, if in all time predeeding t, the command event has been presented to the outstar M times,

$$z_{ci}(t) \sim M(PR_{i/c})I$$

Thus, if $PR_{i/c}$ is large corresponding to a causal association between event c and i in the environment, $z_{ci}(t)$ will be large. On the other hand, a small $PR_{j/c}$ corresponding to event j occuring randomly and not causally associated with event c in the environment, $z_{cj}(t)$ will be small. Thus the z's can be considered random variables faithfully reflecting the a priori conditional probabilities in the environment. Note that this reflection of the statistical description of the environment is contained in the amplitudes of the z's and is built up by experience with M presentations of the pattern. The resistance of the simple outstar with a slow forgetting rate in experiment I to random mistakes was due to this correspondence between the amplitudes of the z's and the a priori probabilities in the environment. It may be concluded that whereas the outstar's memory of a pattern is contained in the $y_i(t)$'s, its memory of its experience is contained in the amplitudes of the z processes. Thus, when its memory of its past experience is allowed to be forgotten at a fast rate as in experiment II, the occurance of a random mistake has disastrous consequences for its memory of the pattern.

It is not surprising that a machine which forgets its past experience rapidly will be very susceptible to having its mind changed.

We may look at this as both a benefit and a drawback. In the slow forgetting outstar of experiment I, the attempt to change its mind about a previously learned pattern by teaching it a new one was only partially successful. It required only two presentations of the original pattern for the outstar to learn it. However, the evidence of the attempt to correct this pattern indicated that many more presentations of the correcting pattern would be required to change its mind. The outstar's resistance to random mistakes was laudable, but its relative inability to change with changing times could be a serious drawback in its environment. On the other hand, the fast forgetting outstar will have no trouble changing its mind with the times, but its low resistance to random mistakes is also a serious drawback.

We may summarize the above heuristic discussion of the constant u in an outstar:

(a) A small u implies:

(i) past experience is slowly forgotten

(ii) high resistnace to random mistakes

(iii) low correctability of previously learned mistakes.

(b) A large u implies:

(i) past experience is rapidly forgotten

(ii) low resistance to random mistakes

(iii) high correctability of previously learned mistakes.

In addition, we must consider one further effect of the constant u on the performance of an outstar:

(c) A small u results in uncontroled growth of the grid x processes' amplitudes.

Again it is stressed that "large" and "small" u's refer to whether

the characteristic decay time 1/u is long or short relative to the expected time interval between presentations to and/or predictions by the outstar.

Because of condition (c) above, a practical simple outstar requires a large u. Thus design improvements to the fast forgetting outstar which results in greater resistance to random mistakes are desireable. In the next several chapters we shall introduce more complicated outstars which exhibit improved noise resistance without the x process amplitude problems of the simple outstar. However, for the present, we still have an avenue open for increasing the simple outstar's noise resistance.

Part of the reason for the poor noise resistance of the simple outstar in experiment II was due to the fact that v was selected by the "one presentation means well learning" criteria. Thus presentation of a random mistake once resulted in its being well learned. Had we selected a smaller v and required more presentations of the pattern in rapid succession to result in well learning, then the effect of the random mistake would be smaller. At the same time the correctability of previously learned mistakes would decrease. If we wish to make the noise resistance of the outstar very good by this method, then we must be content with an outstar of slow intelligence that requires having a pattern drummed into its head before it learns it; or, we could use the pumping up phenomena of the outstar and have it think about a pattern presented to it many times in rapid succession before it is well learned. Selection of the proper v to be used in an outstar is a design decision which must take into account this trade off.

section 3.5 The Occurence of a Pattern of Events over a Period of Time; Thresholds

In experiments I and II, the grid node events in a pattern were always presented exactly τ time units after the command event. The reason for this is that it takes τ time units for the x response to the command input pulse to travel along the directed edges to the arrowheads impinging on the grid nodes. Until the prediction signal $x_c(t - \tau)$ arrives at the arrowheads there can be no correlation between $x_c(t - \tau)$ and the x process response to a grid input pulse at the adjacent grid node. Thus no learning can occur until the prediction signal begins to arrive at the arrowheads. However, we have seen indications that learning does occur with grid events presented at times other then τ time units after presentation of the command event. In this section we shall examine this phenomena, but first we must develop a notion that will make discussion of this phenomena easier. If we are going to study how well an outstar learns associations between the command event and grid events which may occur more than or less than τ time units after presentation of the command event, we will need a method of describing when these events occur. Measuring the occurance of grid events relative to the occurance of the command event is not a very good idea. No learning can occur until the prediction signal has arrived at the arrowheads. The transmission time delay τ is a rather arbitrary time interval which may be changed from outstar to outstar.

However, once the prediction signal begins to arrive at the arrowheads, the outstar will begin to learn the pattern on the grid nodes

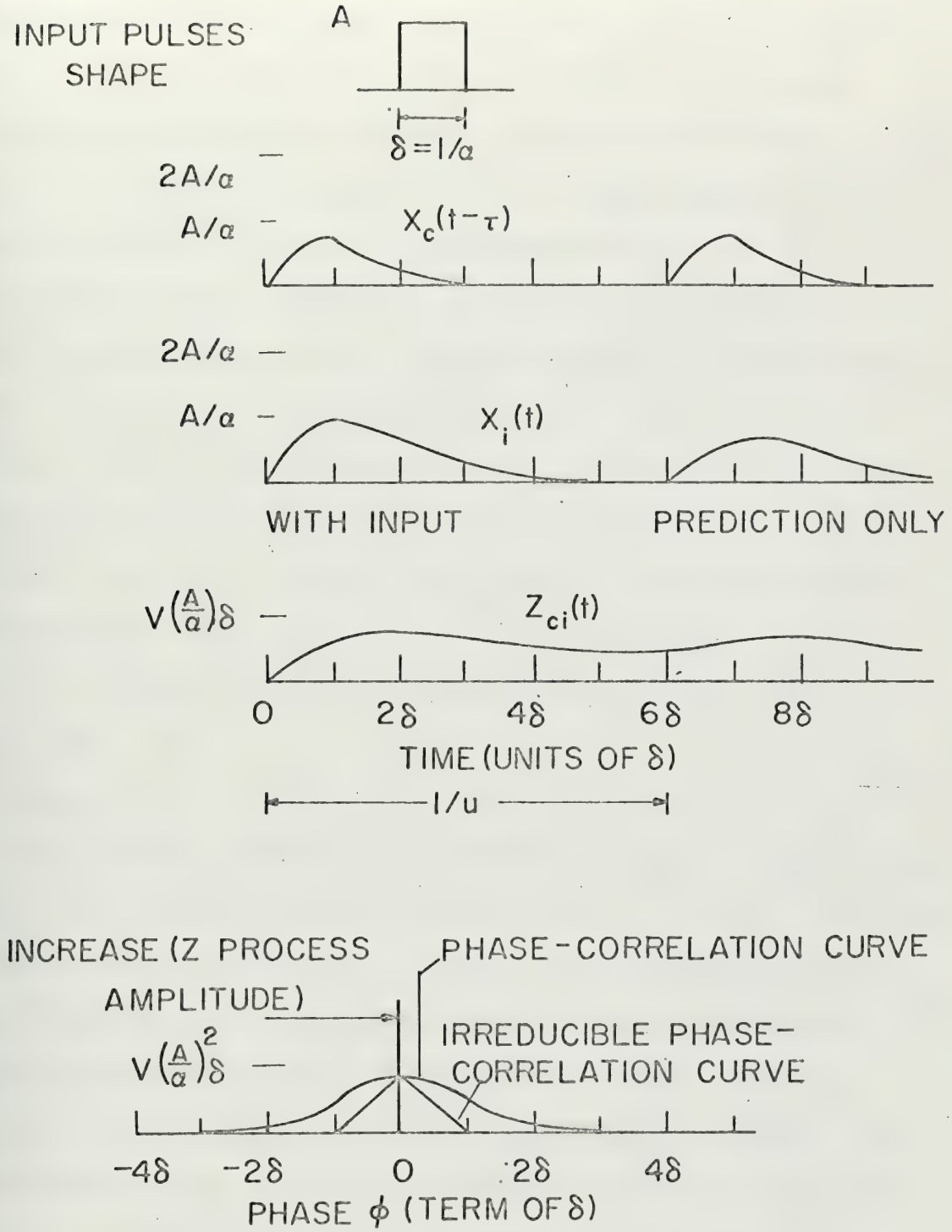

Figure 3.5.1. The upper traces show the input pulse used, the resulting prediction signal, the response of a grid node to an event of $\varphi = 0$ presentation phase, and the response of the $z_{ci}(t)$ process associated with that node. The bottom curve shows the phase-correlation curve and the irreducible phase-correlation curve.

independent of how long it took the prediction signal to travel from the command node. Thus a good reference point for describing the occurance of grid events is the time instant when the prediction signal begins to arrive at the arrowheads. We shall denote this instant in time as $\varphi = 0$ and let φ be the time measured relative to $\varphi = 0$ at which grid events are presented. Grid events which occur before $\varphi = 0$ will be said to occur at negative values of φ and grid events which occur after $\varphi = 0$ will be said to occur at positive values of φ. shall be called the phase of an event with respect to the prediction signal, or simply the presentation phase. To be precise, φ will be defined as follows. Let t_p be the time instant at which the prediction signal begins to arrive at the arrowheads. Let t_e be the time instant at which a grid node input pulse begins to be non zero. Then is:

$$\varphi = t_e - t_p$$

The following experiment was performed. A practical simple outstar with a fast forgetting rate and many grid nodes was set up. The constant v was selected to result in well learning in one presentation of a grid event with $\varphi = 0$ presentation phase. Then each of the grid nodes were excited with events presented with various presentation phases. The z processes were all given zero initial conditions. The maximum amplitude of the z processes attained during the experiment was plotted against the presentation phase φ. Lacking any better name for a curve showing the variation of z process amplitudes with the presentation phase, the curve shall arbitrarily be called a "phase-correlation" curve. A phase-correlation curve is shown at the bottom of figure 3.5.1

Figure 3.5.1 shows a variety of things besides a "phase-correlation" curve. The top trace in figure 3.5.1 shows the shape and dimensions of the input pulse used in the experiment. The $x_c(t - \tau)$ trace shows what the prediction signal looked like as it arrived at the arrowheads. The first response of the $x_i(t)$ trace shows what the x process response looked like for a grid node excited by an event presented with $\varphi = 0$ presentation phase. The second response on the $x_i(t)$ trace shows what a prediction response for this grid looks like. The $z_{ci}(t)$ trace shows what the $z_{ci}(t)$ process in the arrowhead impinging on the above V_i grid looked like. The irreducible phase-correlation curve shown is related to the phase-correlation curve and will be explained shortly.

The additional information shown in figure 3.5.1 is provided as a pictoral look at the various processes going on in an outstar. This information was gathered from a number of experiments and will be compared to the results of the next section in which we study the effects of using other input pulses in an outstar. Thus the actual numerical values for the amplitudes of the processes shown are somewhat meaningless. To allow comparisons to be made, the data in figure 3.5.1 was plotted as functions of various network parameters.

In the preceding experiments we have followed the convention in assigning values to the x process rise rate α and the input pulse duration δ of setting $\delta = 1/\alpha$. The time interval $\delta = 1/\alpha$ describes two important time intervals in the network: The input pulse duration, and the rise time of the x processes. Since this study is limited to input pulses of duration δ and since we have assigned α such that $1/\alpha = \delta$ throughout, a natural selection

for a time unit among the experimental parameters is $\delta = 1/\alpha$. The time axes in figure 3.5.1 are thus in terms of $\delta = 1/\alpha$. Since the time constant associated with the z processes is the decay time 1/u, this period is shown on the z traces.

The analytical solution for a x process responding to a rectangular input pulse presented at time $t = t_0$ of amplitude A and duration is:

$$x(t) = \begin{cases} (A/\alpha)(1 - e^{-\alpha[t-t_0]^+}) & \text{for } t_0 \leq t \leq t_0 + \delta \\ (A/\alpha)(1 - e^{-1})e^{-\alpha[t-(t_0+\delta)]^+} & \text{for } t_0 + \delta \leq t \end{cases}$$

where the notation $[\ ]^+$ is defined by:

$$[y]^+ = \begin{cases} y \text{ for } y > 0 \\ 0 \text{ for } y \leq 0 \end{cases}$$

Note that this solution is valid independent of the numerical values assigned to A, α , and δ as long as $\delta = 1/\alpha$.

Thus the amplitudes for the x processes are always proportional to A/α and this combination of experimental parameters was used as the amplitude axes for the x processes shown in figure 3.5.1.

The equation for the z processes is nonlinear and an analytical solution was not found in this study. A combination of experimental parameters was sought to scale the amplitude axes for the z process traces and the phase-correlation curves. It was desired that a plot of a z process against this scale factor would be the same for all experiments even though the numerical values of the parameters in the experiments were different. At the beginning of the experimental study, the parameter combination $v(A/\alpha)^2\delta$ seemed to work well and was therefore adopted. However later experiments showed that this

scale factor did not work well. Nevertheless, it was retained to allow comparisons. With this explanation of the scales for the axes of the plots in figure 3.5.1 , we may proceed with a discussion of the phase-correlation curve.

The phase-correlation curve in figure 3.5.1 shows the maximum increase in amplitude of a z process due to the correlation between the prediction signal and a grid node x process excited by an event presented with presentation phase φ . As can be seen, the maximum increase in amplitude for a z process occurs when a grid node is excited by an event with $\varphi = 0$ presentation phase. Events presented with $\varphi \neq 0$ indicating that they were presented before or after the arrival of the prediction signal at the arrowheads result in a lesser increase in z process amplitude. For $|\varphi| > 3\delta = 3/\alpha$, there is no appreciable increase in z process amplitude.

The effect of the phenomena revealed by the phase-correlation curve may be interpreted in a number of ways. Suppose that a command event is presented to the outstar at time t_c. Suppose further that a collection of gird events, 1, 2, ..., M, usually accompany the occurance of the command event in the environment. However, suppose that these grid events do not all occur at the same time. Let each one occur at time t_1, t_2, ..., t_M. The prediction signal generated by the command event will arrive at the arrowheads at time $t_c + \tau$. The phase-correlation curve tells us that the outstar will learn to some extent that all the grid events which occur at times t_i such that:

$$|(t_c + \tau) - t_i| < 3\delta = 3/\alpha$$

are associated with the command event. Note that $(t_c + \tau) - t_i$ is the presentation phase φ_i, for the ith event. The phase-correlation

curve tells us further that those events which occur at times t_j such that:

$$|(t_c + \tau) - t_j| < 0.5 \quad = 1/2\alpha$$

will be learned to be associated with the command event very well.

One interpretation of this information is that we now have a means by which we intelligently can specify τ in an outstar. We have said nothing about when a command event occurs relative to a pattern of grid events. In every day experience we are confronted with situations in which the occurance of a "command" event results in the occurance of a "pattern" of events. The time delay between occurance of the command event of switching an electric light switch resulted almost immediately in the pattern of the electric lights in a room going on. We also learned that the command event of putting a seed in the ground resulted days later in the "pattern" of a plant sprouting. In designing an outstar functioning in a "real" environment, specification of τ should be made according to the average time delay between occurance of command events and the associated patterns that the outstar is capable of learning. The phase-correlation curve tells us what the standard deviation of this time delay can be and still result in the outstar being able to learn.

On the other hand, the phenomena shown by the phase-correlation curve is a source for errors in an outstar avalanche. Suppose that the command nodes in an avalanche command node cascade are so arranged that the time interval between excitement of the V_{cj} command node and the V_{cj+1} command node is τ_c. This means that the avalanche takes "pictures" of the time varying pattern of grid events every τ_c time units to make a sampled data approximation of the pattern. From the

phase-correlation curve of figure 3.5.1 we can see that if τ_c is less than $3\delta = 3/\alpha$, the picture taken by the outstars in the avalanche will overlap one another. That is, the V_{cj+1} outstar will learn to some extent the same pattern of events that the V_{cj} outstar learns. In particular, suppose that the pattern of events is varying rapidly enough that the pattern of grid events at time $t + \delta$ is significantly different from that at time t. To get an accurate sampled data approximation in this situation, the avalanche would have to take a "picture" every δ time units and we would set $\tau_c = \delta$. However, the phase-correlation curve shows us that in this case the V_{cj+1} outstar will learn not only the pattern of events on the grid when its prediction signal arrives at the arrowheads, but also the pattern of events that was on the grid when the prediction signal from the V_{cj} outstar arrived at the arrowheads. In this situation, the avalanche's sampled data approximation will be seriously in error.

The phenomena shown by the phase-correlation curve in figure 3.5.1 is due to two things. First, the input pulses used in the experiment were rectangular and of duration δ. Suppose that the equation for the x processes was such that the x processes exactly reproduced the input pulse. That is:

$$x(t) = P(t)$$

Then the prediction signal and the x processes' responses would be rectangular in shape and of duration δ. The z process correlates the prediction signal with the grid node x process. Thus we could expect the z process amplitude increase due to a correlation to be proportional to the correlation between the rectangular prediction signal and the rectangular grid node x process. If the grid node is

excited by an event which occurs with presentation phase φ with respect to the arrival of the prediction signal, we get:

$$z(t) \approx \begin{cases} \left[\int_{\varphi}^{\delta} dt \right]^{+} & \text{for } \varphi > 0 \\ \left[\int_{\varphi}^{\delta - \varphi} dt \right]^{+} & \text{for } \varphi < 0 \end{cases}$$

or

$$z(t) = \begin{cases} [\delta - \varphi]^{+} & \text{for } \varphi > 0 \\ [\delta + \varphi]^{+} & \text{for } \varphi < 0 \end{cases}$$

This is just the correlation between two rectangular pulses of duration δ whose leading edges are separated in time by φ . This function is shown in figure 3.5.1 as the "irreducible phase-correlation" curve. This curve is called irreducible because it shows what the phase-correlation curve would look like if the x processes exactly reproduced the input pulse.

As we have seen, the x processes do not exactly reporduce the input pulses. This is because embedding field network nodes are low pass filters. We have seen, and our analytical solution shows, that the x processes' response decays exponentially away from the maximum value it obtained during the presentation of the input pulse. This exponentially decaying portion of an x process response will be called a "tail". These tails account for the difference between the irreducible phase-correlation curve and the phase-correlation curve. Because of the tails, events presented with presentation phase φ such that $\varphi << 0$ still have non zero amplitudes to correlate with the prediction signal when it arrives at the arrowheads. Prediction signals also have tails which correlate with grid node x process responses to events presented with presentation phase $\varphi >> 0$. As can be seen,

this effect begins to become important for events presented with presentation phase $|\varphi| < 3\delta$.

In an avalanche with a fast sampling rate, modifications of the component outstars that result in a phase-correlation curve which more closely resembles the irreducible phase-correlation curve are important. One modification would be to increase the x process rise rate α . Making α very large will result in x process response that will very closely follow the shape of the input pulses. Thus the phase-correlation curve should be very close to the irreducible phase-correlation curve.

However, increasing α is not always possible. In this study, increasing α either resulted in intolerable errors or extremely lengthy computer runs to perform an expreiment. Appendix A explains the error-computation time trade off in selection of α for the digital simulations of this study.

If α can not be increased enough to make the phase-correlation curve sufficiently close to the irreducible phase-correlation curve, there are other methods which will accomplish this. Grossberg has proposed the use of thresholds. The equations for a simple outstar with thresholds are:

3.5.1 $$\dot{x}_c(t) = -\alpha x_c(t) + P_c(t)$$

3.5.2 $$\dot{x}_i(t) = -\alpha x_i(t) + \beta z_{ci}(t)\left[x_c(t-\tau) - \Gamma_c\right]^+ + P_i(t)$$

3.5.3 $$\dot{z}_{ci}(t) = -uz_{ci}(t) + v\left[x_c(t-\tau) - \Gamma_c\right]^+ \left[x_i(t) - \Gamma_x\right]^+$$

where:

$$[y]^+ = \begin{cases} y \text{ for } y > 0 \\ 0 \text{ for } y \leq 0 \end{cases}$$

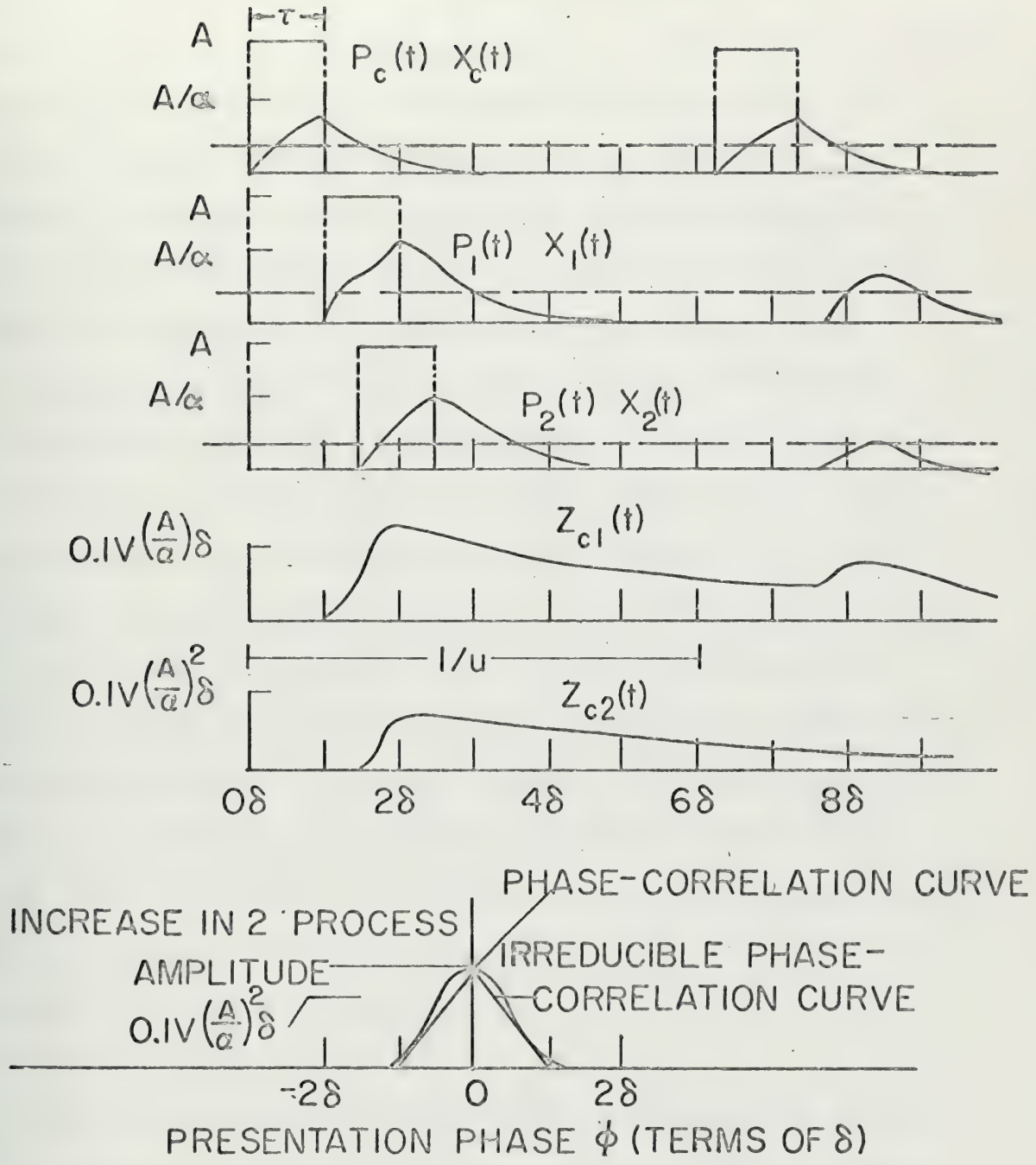

Figure 3.5.2. Illustration of the effects of thresholds on a simple outstar. Equivalent thresholds are placed on both the command node and the grid nodes. Note how close the phase-correlation curve is to the irreducible phase-correlation curve.

Γ_c is the command node threshold. As can be seen, it prevents the prediction signal $x_c(t - \tau)$ from exciting a grid x process until $x_c(t - \tau) > \Gamma_c$. Additionally, it prevents the prediction signal from being correlated with the grid nodes' x processes until $x_c(t - \tau)$ is suprathreshold. The grid node threshold, Γ_x, performs the same function. In effect, these thresholds will cut off the "tails" of the x processes and thus should result in a phase-correlation curve which closely resembles the irreducible phase-correlation curve.

Figure 3.5.2 shows the results of an experiment conducted with an outstar with thresholds. The command node threshold Γ_c used in this experiment was selected to make the time interval during which the prediction signal is suprathreshold approximately δ time units in duration as can be seen from the $x_c(t)$ trace. The grid node threshold Γ_x was selected to be the same, $\Gamma_x = \Gamma_c$. As can be seen, the phase-correlation curve very closely approximates the irreducible phase-correlation curve. Using thresholds, we could make an avalanche which could accurately sample a time varying pattern every 2δ time units. Without thresholds, the shortest the accurate sampling interval could be is about 6δ time units as shown in figure 3.5.1. Thus the addition of thresholds has increased the accurate sampling rate for an avalanche by a factor of three.

However, this possible increase in the accurate sampling rate for an avalanche has not been obtained without a cost. The $x_2(t)$ traces and the $z_{c2}(t)$ traces in figure 3.5.2 are for a grid node excited by an event with presentation phase $\varphi = 0.5\,\delta$. Looking closely at the $x_2(t)$ trace, one can see that in the first response, $P_2(t)$ drove $x_2(t)$ above threshold and thus $z_{c2}(t)$ grew. However, on the second

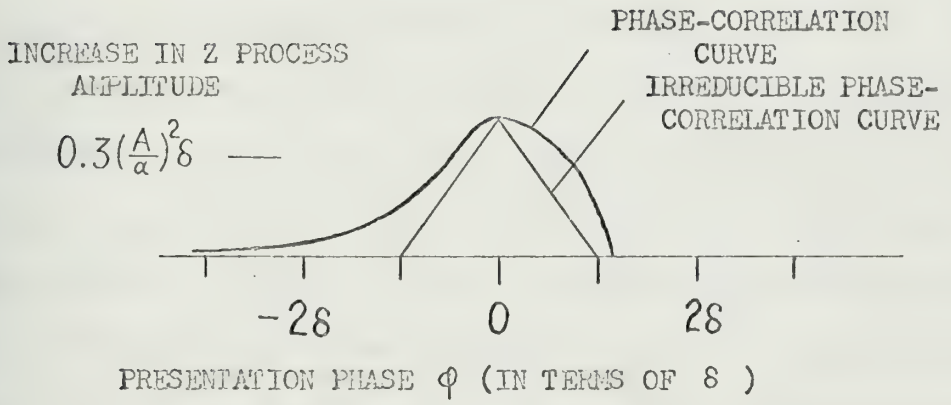

FIGURE 3.5.3. Effect on the phase-correlation curve of a threshold placed on the command node only.

response, the excitement of $x_2(t)$ was insufficient to drive it suprathreshold and thus $z_{c2}(t)$ continued its exponential decay. Lacking the ability to drive $x_2(t)$ suprathreshold, the outstar can not "pump up" the $z_{c2}(t)$ process and we must conclude that the memory $z_{c2}(t)$ is bound for extinction. In the same way, if the $z_{c1}(t)$ is allowed to decay further, prediction excitement of $x_1(t)$ will also be unable to drive $x_1(t)$ suprathreshold and all memory of the pattern would be bound for extinction. In the simple outstar without thresholds, we saw that no matter how much the z processes decayed, we could still recover the information stored in them by "pumping up". Thus, although a memory could fade due to forgetting, it could not be absolutely forgotten. An outstar with grid node thresholds can absolutely forget a pattern it has learned.

To prevent a memory from being absolutely forgotten, we must set $\Gamma_x = 0$. This was done and a series of experiments were performed to determine the phase-correlation curve. Figure 3.5.3 shows the results. The only x process "tail: that was cut off by a threshold was the prediction signal's. Thus, the phase-correlation curve for $\varphi > 0$ is very close to the irreducible phase-correlation curve. This is because events with presentation phase $\varphi > 0$ occur after the prediction signal has arrived at the arrowheads. Cutting the prediction signal's tail off prevents it from correlating with x process responses to events presented with presentation phases greater than the time interval during which the prediction signal is suprathreshold. In this case, this meant no correlation with x processes responding to events presented with presentation phase $\varphi > \delta$. On the other hand, the x processes retained their "tails" because $\Gamma_x = 0$. Thus the "tails"

of grid node responses to events occuring before the prediction signal arrived at the arrowheads ($\varphi < 0$) were available for correlation. This explains why the phase-correlation curve for $\varphi<0$ in figure 3.5.3 is similar to the phase-correlation curve for an outstar without thresholds.

In addition to making the phase-correlation curve for an outstar closer to the irreducible phase-correlation curve, thresholds may be used for an interprative purpose. Since the prediction signal $[x_c(t - \tau) - \Gamma_c]^+$ could not effect the grid nodes until $x_c(t - \tau)$ was suprathreshold, we could follow the convention of saying that an x process at a node does not indicate a response by that node until it is suprathreshold. We could still set $\Gamma_x = 0$ in equation 3.5.3 and place an imaginary threshold on the grid nodes. With this interpratative convention, we have a concrete relationship between the amplitudes of the x processes and the psychological idea of a response from a subject. Additionally, the phenomena of a faded memory popping up into the outstar's consciousness during "pumping up" is given a concrete interpretation.

section 3.6 Other Input Pulse Shapes

A short study was made of the effects on a simple outstar of using input pulses with shapes other than rectangular. The results were that there appear to be no qualitative differences in the performance of an outstar using any input pulse of duration less than or equal to $1/\alpha$. The sole exception to this qualitative finding was that the choice of input pulses does affect the shape of the phase-correlation curve.

Quantitatively, the input pulse did affect the maximum amplitude of the x responses. Additionally, the magnitude of v to meet a specific well learning criteria was affected.

One important result of this study was that the maximum amplitude of a grid node x process responding to a prediction signal alone was at approximately $1/\alpha$ time units after arrival of the prediction signal for all input pulses. If we consider the input apparatus of the outstar to be a data sampler which samples the environment at time t_0 and delivers appropriate input pulses to the outstar's nodes, then this effect can be considered to be an inherent time delay in the outstar's prediction. That is, an event which occurs in the environment at time t_0 is predicted by the outstar to occur at time $t_0 + 1/\alpha$.

Figures 3.6.1, 3.6.2, and 3.6.3 show the results for the pulses used in this study. They should be compared to figure 3.5.1 which shows similar results for a rectangular pulse. The irreducible phase-correlation curves in these figures were computed by analytically correlating the input pulses.

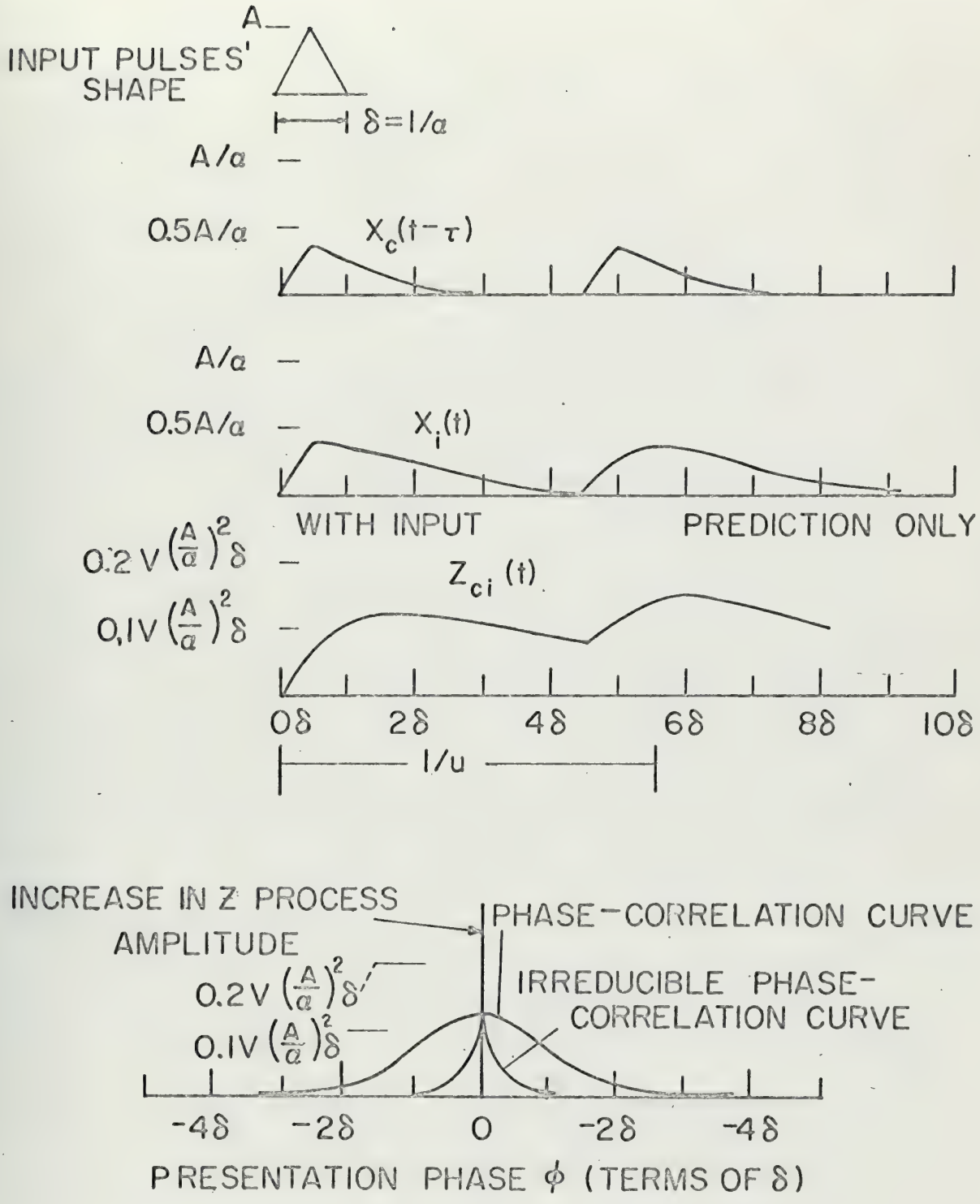

Figure 3.6.1. The response of an outstar to a triangular input pulse.

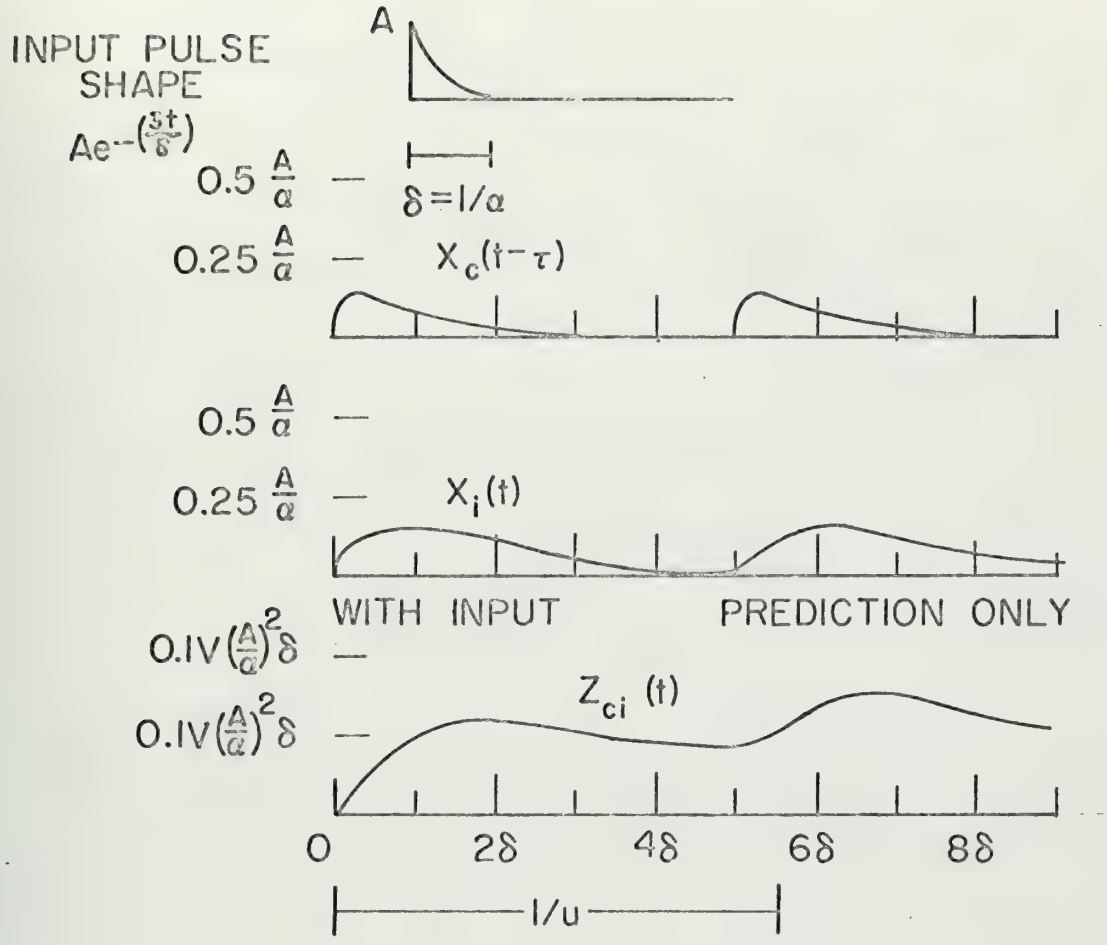

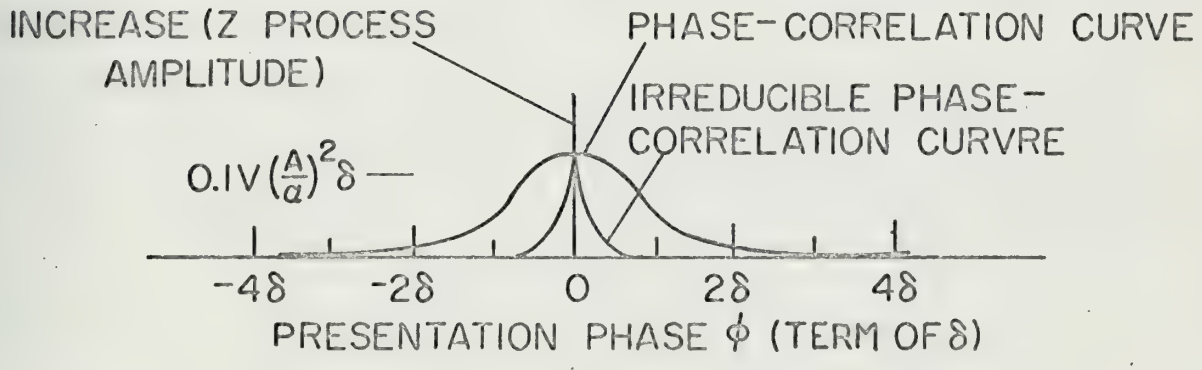

Figure 3.6.2. The response of an outstar to an exponential input pulse.

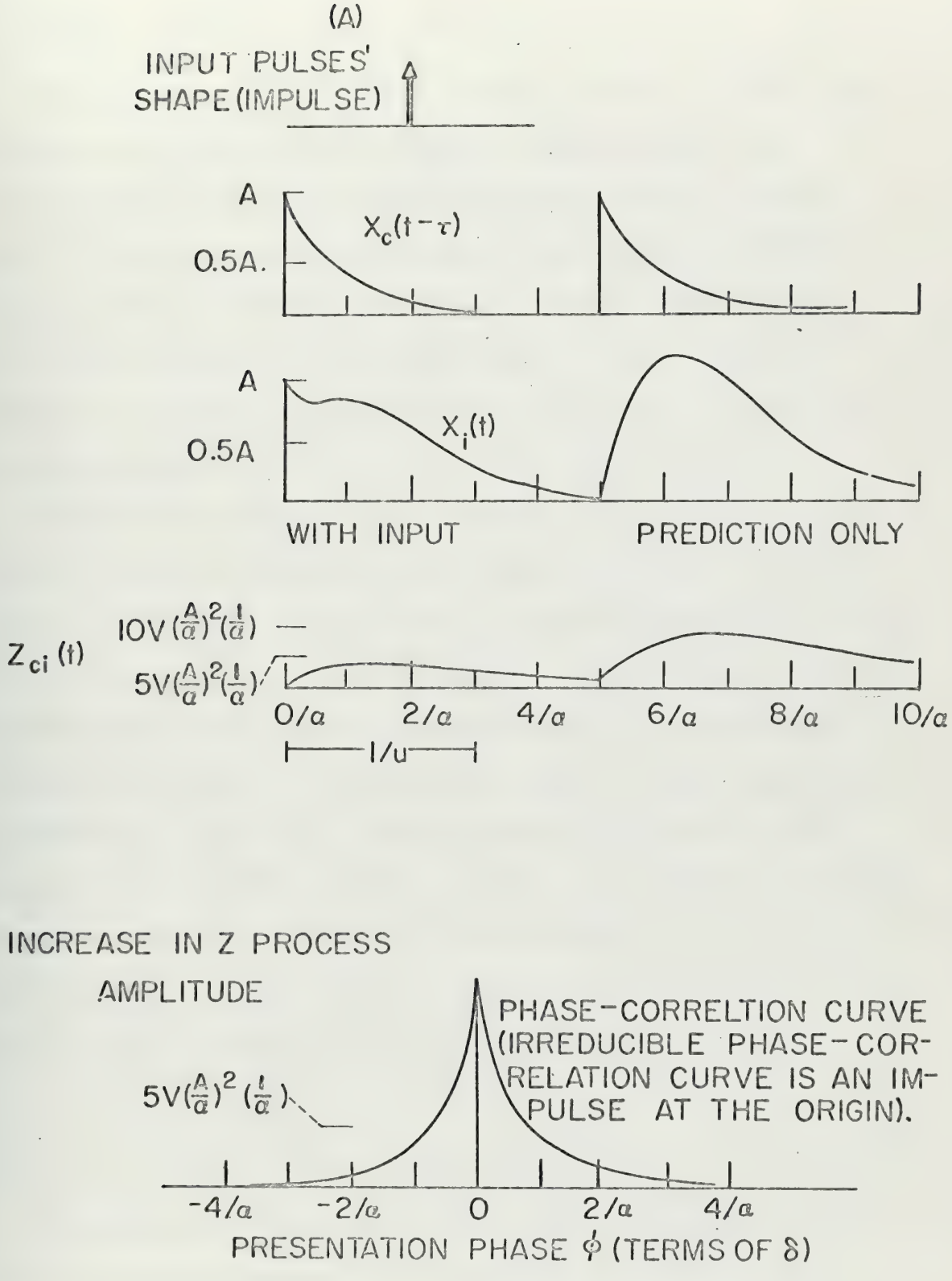

Figure 3.6.3. The response of an outstar to an impulse input pulse.

CHAPTER 4 LATERAL INHIBITION

section 4.1 Introduction to Lateral Inhibition

The last chapter showed that a practical outstar (one with a fast forgetting rate) had the major drawback of either being a slow learner or having very low resistance to random mistakes. This was due to its inability to additively sum its past experience in the z processes because of the large decay rate. In this chapter we will study a more complicated outstar which retains all the desirable qualities of the simple outstar with a fast forgetting rate and has the further property that it is resistant to random mistakes.

The additive summing of past experience in the slowly forgetting outstar of chapter 3 resulted in good resistance to random mistakes because this outstar's experience with the correct pattern was so great that it could absorb mistakes. The opposite of this passive absorption of mistakes would be to use the past experience to actively supress a mistake when it occurs. The psychological term for active suppression is inhibition. Figure 4.1.1 shows the geometric schematic and the equations for a laterally inhibiting outstar. The equations governing its performance are here repeated for convenience:

4.1.1 $$\dot{x}_c(t) = -\alpha x_c(t) + P_c(t)$$

4.1.2 $$\dot{x}_i(t) = -\alpha x_i(t) + P_i(t) + \beta x_c(t-\tau) z_{ci}(t) - \beta^- \sum_{\substack{j=1 \\ j \neq i}}^{N} \left[x_j(t-\tau^-) \right]^+$$

4.1.3 $$\dot{z}_{ci}(t) = -uz_{ci}(t) + v\left[x_c(t-\tau) x_i(t) \right]^+$$

The notation $[y]^+$ means the maximum of the variable y, or 0, as in the case with thresholds. A short discussion of the significant differences between equations 4.1 and those for a simple outstar follows.

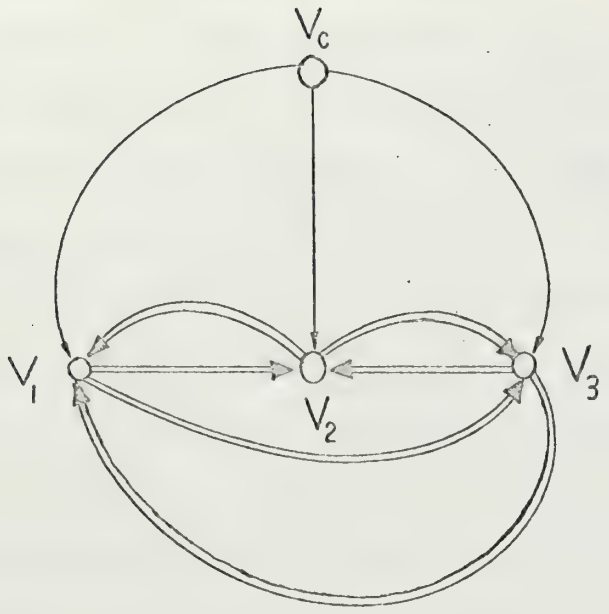

EQUATIONS GOVERNING NETWORK PERFORMANCE

4.1.1 $$\dot{X}_c(t) = -\alpha X_c(t) + P_c(t)$$

4.1.2 $$\dot{X}_i(t) = -\alpha X_i(t) + P_i(t) + \beta Z_{ci}(t) X_c(t-\tau) - \beta \sum_{\substack{j=1 \\ j \neq i}}^{N} [X_j(t-\tau)]^+$$

4.1.3 $$\dot{Z}_{ci}(t) = -u Z_{ci}(t) + V[X_c(t-\tau) X_i(t)]^+$$

Figure 4.1.1. An outstar with lateral inhibition. The double lined directed edges transmit inhibitory signals. Only three grid nodes are shown (N = 3).

A negative prediction signal $-\beta^{-} \sum_{j=1, j\neq i}^{N} \left[x_j(t - \tau^{-}) \right]^{+}$ has been added to the equation for the grid nodes' x processes. This is the net inhibitory signal sent to grid node i from all the other nodes in the grid. These inhibitory signals are sent along the double lined directed edges in figure 4.1.1. The transmission delay from the originating node to the receiving node is τ^{-}. Note that a grid node sends an inhibitory signal only if its x process is positive. With inhibition, it is possible for an x process to have negative amplitudes. We shall adhere to the convention of considering that a node is responding only if its x process is positive. Although we will be able to measure the negative excursions of the x processes they shall be considered equivalent to zero amplitudes in the simple outstar.

In the simple outstar, zero or small amplitudes were interpreted as no response. In the laterally inhibiting outstar, negative amplitudes mean that node is in an inhibited state. Using the above convention for interpreting the response of a node implies that an inhibited node is in a super non responding state. Limiting a node's ability to affect other nodes via the inhibitory signals to only those times when its x process is positive is consistent with the above convention.

No learning occurs in the arrowheads of the inhibitory directed edges. The z process in those arrowheads can be considered to always have a value of unity.

Equation 4.1.3 for the z processes located in the arrowheads of the directed edges from the command node is the same as that for a simple outstar. Again, a node's inhibited state is ignored by the correlation driving function $v\left[x_c(t - \tau) x_i(t) \right]^{+}$. Thus the

z processes can only have non negative values. For this reason this outstar is an excitory biased machine. We will have occasion in a later chapter to investigate outstars which allow negative z processes and are more neutrally biased.

The rationale for lateral inhibition is to have a responding grid node inhibit all the other grid nodes. When several grid nodes are responding at the same time, we expect the node responding with the greatest amplitude to inhibit the other nodes the most while suffering the least inhibition itself. When a random mistake occurs in a previously learned pattern, the prediction signal inputs to the grid nodes will cause the nodes corresponding to events in the pattern to respond with greater amplitude than the nodes corresponding to the mistake. This will result in inhibition of the response to the mistake.

section 4.2 Experimental Study of an Outstar with Lateral Inhibition

To test the claim that the laterally inhibiting outstar has good noise resistances, we shall repeat experiment II which was performed with the simple outstar. All the parameter specifications for that experiment will be retained. However, we have two new parameters to specify, β^- and τ^-.

If it takes too long for inhibitory signals to travel along their directed edges, then we shall have defeated the purpose of lateral inhibition by having inhibiting signals arrive after the damage has been done. Thus τ^- should be small. Lateral inhibition would be most effective if $\tau^- = 0$, but we shall observe the constraints on transmissions along directed edges set up in chapter 1. With these arguments in mind, τ^- is selected to be:

$$\tau^- = \frac{1}{3a} = \frac{1}{3}\delta = \frac{\tau}{3}$$

A rational guess for β^- is difficult. In order to specify it most efficiently we would need some idea of the average number of grid events composing a pattern and the average number of events that compose a random mistake. The reason for desiring this information when selecting β^- is obvious: Suppose that we had two patterns we wished to teach to two outstars sharing the same grid. Pattern $\vec{\theta}_1$ is composed of one event. Pattern $\vec{\theta}_2$ is composed of n events where $1 < n < N$ and N is the number of grid nodes. Then the node corresponding to the event in pattern $\vec{\theta}_1$ will not be inhibited at all. However, each of the nodes corresponding to events in $\vec{\theta}_2$ will inhibit each other and the node responses to $\vec{\theta}_2$ will have a diminished amplitude. Thus the

z correlations for $\vec{\theta}_2$ will be smaller and it will require many more instructions to learn $\vec{\theta}_2$ than it will require to learn $\vec{\theta}_1$. Any selection for β^- will work well in learning $\vec{\theta}_1$. On the other hand an excessively large β^- will result in very inefficient learning of $\vec{\theta}_2$.

However, we want β^- large enough to inhibit random mistakes. Thus we are faced with a trade off between inefficient learning and the proper degree of inhibition to counter mistakes. A fore-knowledge of the average situation to expect would greatly aide in the proper selection of β^-. Of course, if we wanted our outstars to be completely unbiased at the beginning of the experiment, we could make a large number of them with various β^- and turn them lose in the environment. Survival of the fittest would soon select the optimal β^-.

For the purposes of this study, it was decided to select β^- on the idea that at most two events would compose a pattern and a random mistake on the average would consist of one event. β^- was chosen to allow the inhibitory signal from excited nodes to drive an unexcited node to approximately one-half the amplitude of the excited node. A brief analysis was made to meet this criteria as follows:

Maximum amplitude of an x process excited by a rectangular pulse of amplitude A and duration $\delta = 1/\alpha$ was $\max(x_i(t)) = (A/\alpha)(1 - e^{-1}) \cong 0.63\ A/\alpha$.

Amplitude of such an input resulting in $(1/2)\max(x_i(t))$ is $(1/2)A$.

$$\beta^-(0.63)(A/\alpha) = (1/2)\ A$$

or $\beta^- = \alpha/1.26$

for $\alpha = 3.333$, $\beta^- = 2.64$

An experimental check of this resulted in $\beta^- = 2.38$. The 11% error is due both to the naiveté of the analysis and errors inherent to the digital simulation.

Inadvertently, v was changed to 2.4 resulting in a well learning in one and one-half presentations criteria. This minor descrepancy is not sufficient to prevent comparison with experiment II. For convenience the major parameters used are listed here:

Network parameters:

$\alpha = 3.3333$ sec.$^{-1} = 1/\delta$

$\beta = 1.0$

$u = 0.556$ sec.$^{-1}$

$v = 2.4$

$\tau = 0.3$ sec.

$\tau^- = 0.1$ sec.

$\beta^- = 2.38$

Input pulse parameters:

$A = 10$

$\delta = 0.3$ sec. $= 1/\alpha$

The equations governing the performance of the laterally inhibiting outstar are:

$$\dot{x}_c(t) = -\alpha x_c(t) + P_c(t)$$

$$\dot{x}_i(t) = -\alpha x_i(t) + P_i(t) + \beta z_{ci}(t)x_c(t - \tau) - \beta^- \sum_{\substack{j=1 \\ j \neq i}}^{N} \left[x_j(t - \tau^-)\right]^+$$

$$\dot{z}_{ci}(t) = -uz_{ci}(t) + v\left[x_c(t - \tau)x_i(t)\right]^+$$

Experiment III was begun by teaching the outstar the pattern $V_c \rightarrow V_2$ by two presentations of event 2, τ time units after presentation of the command event. Figure 4.2.1 shows the result. Thr prediction

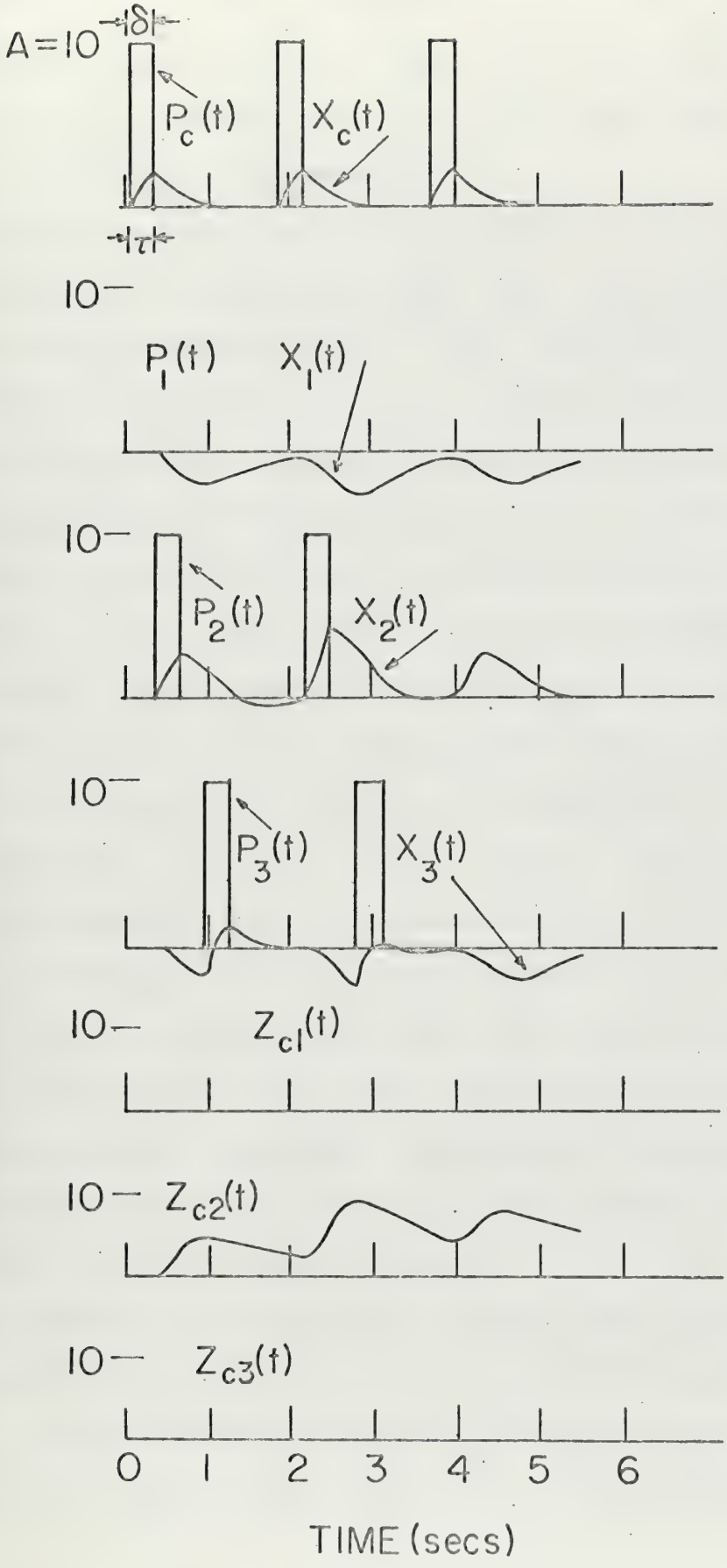

Figure 4.2.1. Teaching a laterally inhibiting outstar the pattern $V_c \rightarrow V_2$. Note that $V_c \rightarrow V_3$ is not learned.

response on the $x_2(t)$ trace shows that $V_c \rightarrow V_2$ was well learned as is indicated by the $z_{c2}(t)$ trace. Figure 4.2.1 should be compared with figure 3.3.1 which shows the result of the same pattern being taught to a practical simple outstar.

Of interest in figure 4.2.1 is the fact that a minor association of V_c with V_3 did not occur to any significant extent. Event 1 was presented with presentation phase $\varphi = 0$ with respect to arrival of the prediction signal at the arrowheads. That is, event 1 was presented at the exact time instant that the prediction signal arrived at the arrowheads. In the discussion of the phase-correlation curves of section 3.5, we saw that presenting an event with presentation phase $\varphi = 0$ results in the greatest increase in the amplitudes of the z process. In this sense, an event presented with presentation phase $\varphi = 0$ is learned best. Events presented with presentation phase $\varphi \neq 0$ are learned to a lesser extent. In figure 4.2.1, event 3 was presented 0.6 seconds after event 1. That is, event 3 was presented with presentation phase $\varphi = +0.6$ seconds $= 2\delta = 2/\alpha$. From the phase-correlation curve for a simple outstar without thresholds in section 3.5, we saw that presenting an event with presentation phase $\varphi = +2\delta = +2/\alpha$ resulted in a significant increase in the associated z process's amplitude. The addition of thresholds to the simple outstar prevented any increase in the associated z process by cutting off the "tails" of the x processes.

The laterally inhibiting outstar currently under study does not have thresholds. However, from the fact that only a very minor association $V_c \rightarrow V_3$ was learned in figure 4.2.1, it appears that lateral inhibition has some of the same effects that thresholds have on the

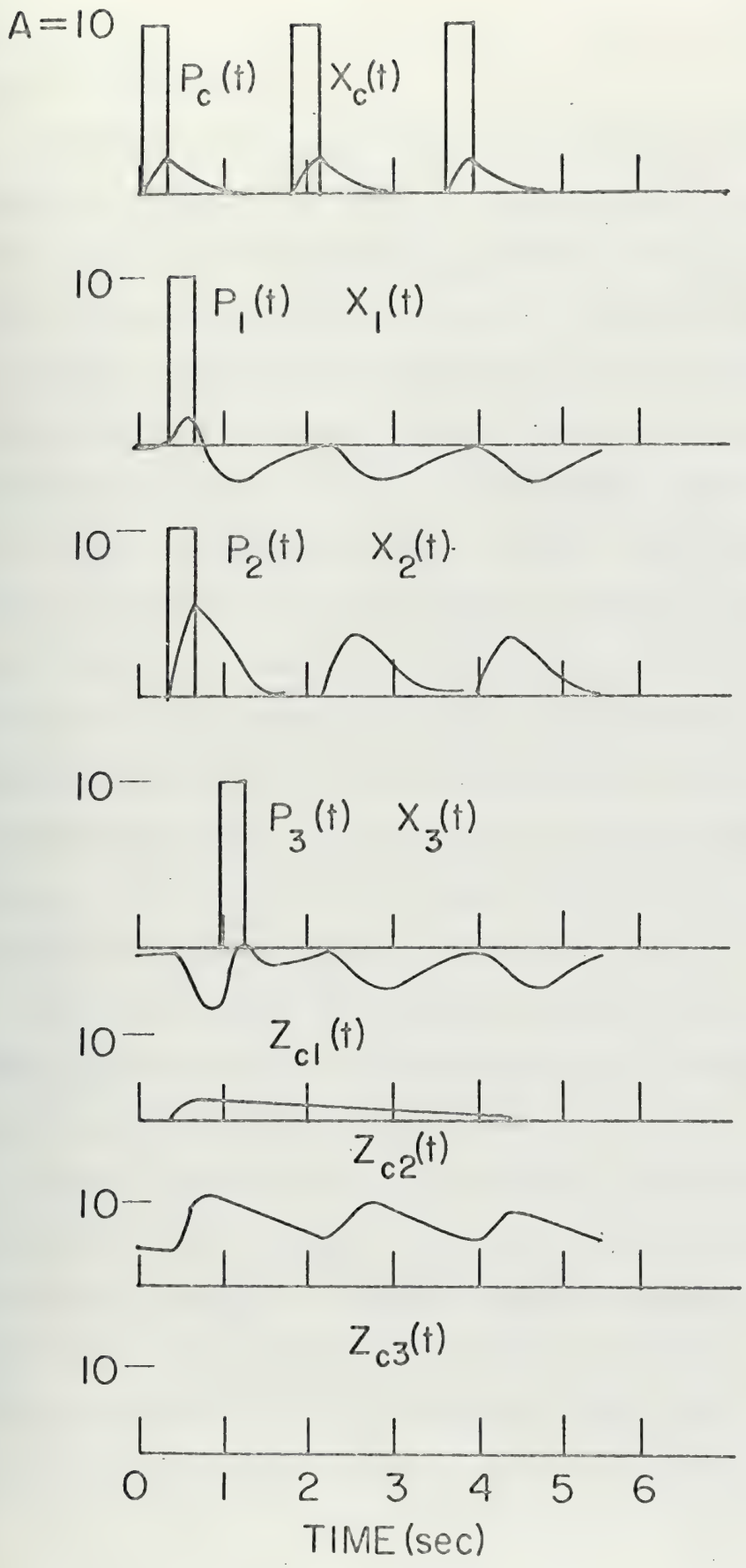

Figure 4.2.2. Resistance to random mistakes offered by a laterally inhibiting outstar. $P_1(t)$ simulates a random mistake in the pattern $V_c \rightarrow V_2$ learned previously. Note inhibited response of $x_1(t)$ and extinction of memory of mistake revealed by $z_{c1}(t)$.

performance of an outstar. We will investigate this performance in detail in section 4.4.

Experiment III was continued to check the claim that lateral inhibition increases resistance to random mistakes. Figure 4.2.2 shows the result of presenting the previously learned pattern $V_c \rightarrow V_2$ with a simulated random mistake, event 1. As the $x_1(t)$ and $z_{c1}(t)$ traces show, the mistake was inhibited to the point where $V_c \rightarrow V_1$ was learned to only a minor extent. (Compare to figure 3.2.3.) Additionally, predictions following the mistake presentation resulted in the $x_1(t)$ process being totally inhibited. This resulted in the memory of the mistake decaying towards extinction, as shown by the $z_{c1}(t)$ trace. Of course the dramatic results shown in figure 4.2.2 were due to the comparative freshness of the pattern $V_c \rightarrow V_2$ in the outstar's memory as shown by the large amplitude for $z_{c2}(t)$ when the mistake was presented. The memory of $V_c \rightarrow V_2$ will fade as $z_{c2}(t)$ decays. If the memory is sufficiently faded, we will not expect the resistance to random mistakes to be as good.

This has parallels in every day experience. Students are less likely to be deceived by a tricky question in an examination when the subject matter is fresh in their minds.

Lateral inhibition does not prevent the outstar from correcting a previously learned pattern which is in error. Experiment III was continued to convert the previously learned pattern $V_c \rightarrow V_2$ with a new pattern $V_c \rightarrow V_1$. Figure 4.2.3 shows the results. As can be seen, two presentations of the new pattern were sufficient to totally inhibit the old pattern and insure extinction of its memory.

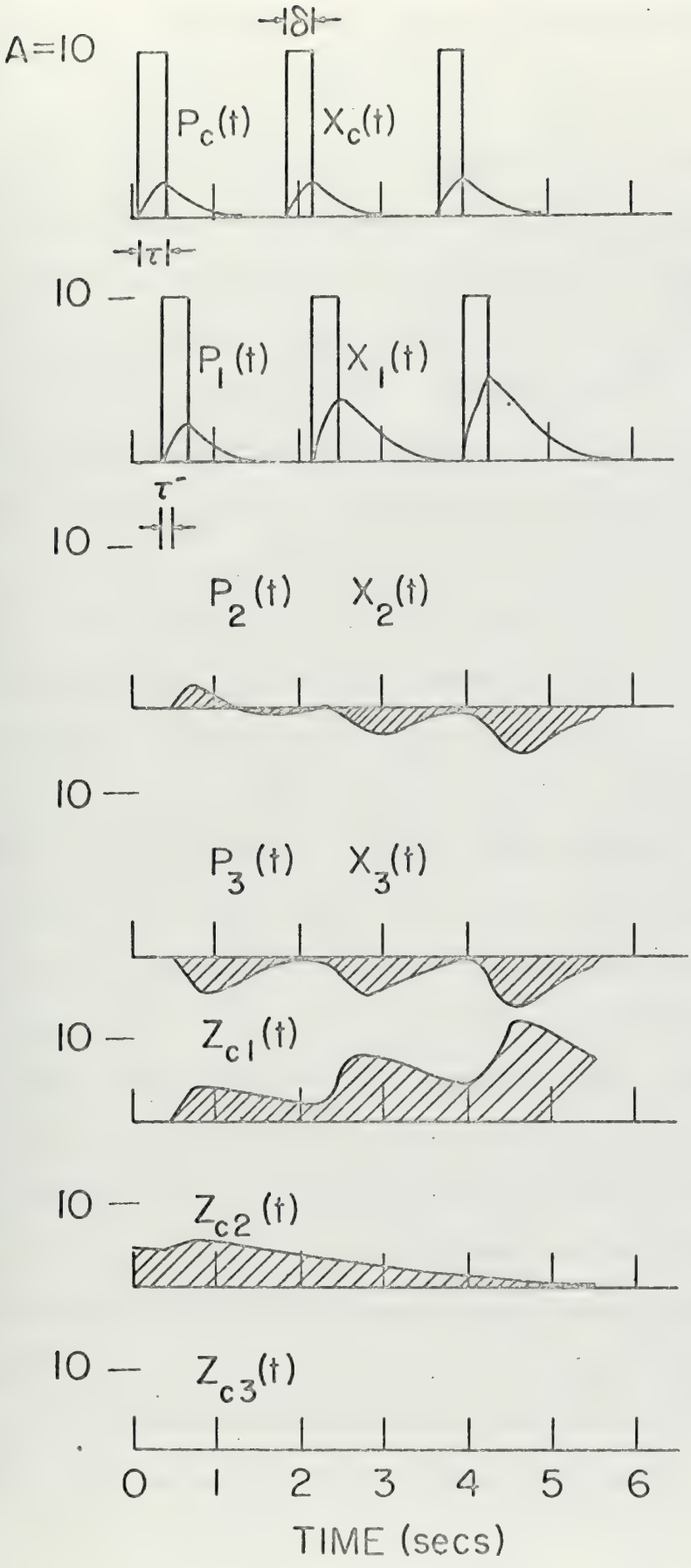

Figure 4.2.3. Correcting the previously learned pattern $V_c \rightarrow V_1$ in a laterally inhibiting outstar. Note the extinction of $z_{c2}(t)$ due to the inhibited state of $x_2(t)$.

section 4.3 Advantage of Correcting a Learned Mistake with Lateral Inhibition

In section 3.4 we discussed the effects of the forgetting rate u on a simple outstar's resistance to random mistakes and on its ability to correct learned mistakes. The conclusion was that a small u resulted in good random mistake resistance, but very low correctability. A large u had the opposite effect. From the outstar's point of view, the only difference between a random mistake and a correction to a previously learned pattern is that the random mistake occurs infrequently with the command event whereas the correcting pattern usually occurs with the command event. It was shown in section 3.4 that the outstar remembered the difference between an event which infrequently occurs with the command event and one which usually occurs with the command event in the accumulated past experience contained in the amplitude of its z processes. With a small u the past experience was not forgotten rapidly and resulted in a great accumulation of experience. It was not surprising that an infrequent variation in the pattern had a small effect on the accumulated experience. On the other hand, a great accumulation of past experience with a pattern makes it very difficult to convince the outstar that the pattern was an error. Due to the fast rate of forgetting past experience in the large u outstar, little accumulation of experience occured resulting in its random mistake resistance and correctability properties. Thus by interpreting the amplitudes of the z processes as accumulated past experience it seemed very reasonable to conclude that good random mistake resistance and correctability were incompatible.

Figure 4.2.2 and 4.2.3 show that this need not be the case. The laterally inhibiting outstar has both good resistance to random mistakes and good correctability. Lateral inhibition was introduced to make an outstar with a fast forgetting rate more resistant to random mistakes. It might have been expected that this would decrease its correctability. We shall inquire why it did not.

In the slowly forgetting simple outstar the only way a pattern can be corrected is by brute force. The amplitude of grid node x process responses is a linear function of the sum of the event input pulses and prediction signal inputs:

$$\dot{x}_i(t) = -\alpha x_i(t) + \beta z_{ci}(t) x_c(t - \tau) + P_i(t)$$

Thus the amplitude of a grid node x process response is greater when there is an event input pulse than when there is only a prediction signal input alone. Therefore the correlating signal $vx_c(t - \tau)x_i(t)$ is greater when there is an event input pulse and the z process grows faster. In correcting a pattern in a slowly forgetting simple outstar, we simply stop presenting the events of the erroneous pattern and start presenting the events of the correcting pattern. As was shown in figure 3.2.2, the additional amplitude of the grid node x processes due to the correcting event input pulses results in the z processes associated with the correcting pattern events growing faster than the z process associated with the erroneous pattern. By the outstar theorem we are assured that eventually the probabilities $X_i(t)$ and $y_i(t)$ will go from values describing the erroneous pattern to values describing the correcting pattern. However, we have seen that in the slowly forgetting outstar, the x process amplitudes will have become impractically large long before this happens.

In the rapidly forgetting outstar, we do not have the problem of impractically large amplitude x processes. Further, in trying to correct a previously learned pattern we are aided by the rapid forgetting rate. In addition to the effects of the brute force correcting process, the rapidly forgetting outstar forgets the erroneous pattern while it is learning the correcting pattern. (Provided of course, the excitations of the command node are spaced far enough apart not to result in significant pumping up of the erroneous pattern.) Thus in addition to the active process of forcing the z process associated with the correcting pattern to grow larger than those associated with the erroneous pattern, there is the passive process of forgetting the old pattern. As has been emphasized this passive forgotting process results in the better correctability of the rapidly forgetting simple outstar as well as its low resistance to random mistakes.

In the laterally inhibiting outstar, we retained the fast forgetting rate to control grid node x process amplitudes. Thus we have both the active brute force correcting process and the passive forgetting process working to correct an erroneous pattern. If we look closely at figures 4.2.2 and 4.2.3, we can see the effect of lateral inhibition in both random mistake correction and pattern correction. In figure 4.2.2, presentation of the previously learned pattern $V_c \longrightarrow V_2$ with the simulated random mistake $V_c \longrightarrow V_1$ resulted in growth of both $z_{c2}(t)$ and $z_{c1}(t)$. However, the sum of the input pulse $P_2(t)$ and the input prediction signal $\beta z_{c2}(t)x_c(t - \tau)$ drove $x_2(t)$ to a greater amplitude than $x_1(t)$ was driven by $P_1(t)$ alone. Therefore $x_1(t)$ was diminished by the inhibiting signal from $x_2(t)$

and $z_{c1}(t)$ did not grow to a very large amplitude. Both $z_{c1}(t)$ and $z_{c2}(t)$ decayed. On subsequent predictions the prediction input signal for V_1 was not sufficient to overcome the inhibitory signal from V_2 and the correlating signal $v[x_c(t-\tau)x_1(t)]^+$ was zero. Thus $z_{c1}(t)$ was unable to grow on subsequent predictions and the fast forgetting rate insured that the random mistake would be totally forgotten.

We have said that a random mistake occurs infrequently. Thus we can expect that the fast forgetting rate will insure that the random mistake will be forgotten before it occurs again during presentation of the pattern and there will be no accumulation of experience with the mistake in $z_{c1}(t)$. Now, look at the successful correction of the previously learned pattern $V_c \rightarrow V_2$ with $V_c \rightarrow V_1$ in figure 4.2.3. It is seen that on the first presentation of the correcting pattern, the accumulated experience with the erroneous pattern was still greater than the experience accumulated on the first presentation of the correcting pattern. At this point the outstar could not be aware that $V_c \rightarrow V_1$ is a correcting pattern and not a random mistake. However, on the next presentation of $V_c \rightarrow V_1$, the experience now accumulated with $V_c \rightarrow V_1$, coupled with the event input pulse, is sufficient to drive $x_1(t)$ to a greater amplitude than prediction alone can drive $x_2(t)$. Consequently, $x_2(t)$ is inhibited and $z_{c2}(t)$ grows very little. The fast forgetting rate now insures that $z_{c2}(t)$ will decay to a point where a third presentation of the correcting pattern will completely inhibit prediction of $V_c \rightarrow V_2$ and it is impossible thereafter to accumulate any more experience with $V_c \rightarrow V_1$ by prediction. At this point we can say that the pattern has been corrected.

It is a combination of brute force correcting resulting in accumulation of experience with the correcting pattern, rapid forgetting of the erroneous pattern, and use of accumulating experience to inhibit the erroneous pattern which accounts for the correctability property of a laterally inhibiting outstar. The same combination of processes results in its random mistake resistance. It is the inability of a simple outstar to couple accumulation of experience with forgetting that results in the incompatibility of random mistake resistance with correctability.

Because of the inability to control the amplitudes of grid node responses with small u's we will not undertake to study the variation of these properties in a laterally inhibiting outstar with a fast forgetting rate. In chapter six, we will present a different formulation of the outstar equations which control the amplitudes of the grid node responses independent of the amplitudes of the z processes and incorporate a form of lateral inhibition. At that time we will consider the effect of decreasing the forgetting rate on the properties of a laterally inhibiting outstar.

In the first part of experiment III, figure 4.2.1, it was noted that lateral inhibition appears to have some of the same effects that thresholds have on the performance of outstars. The evidence was that presentation of event 3, 0.6 seconds = $2\delta = 2/\alpha$, after arrival of the prediction signal at the arrowheads did not result in any learning of $V_c \rightarrow V_3$. Further investigation shows that this result is of dubious value.

The $x_3(t)$ trace in figure 4.2.3 shows the inhibitory response of a node to a single input pulse at another node in the grid. The maximum of this inhibitory response occurs approximately $2\delta = 2/\alpha$ time units after arrival of the inhibitory signal at the node. Thus the maximum inhibitory response occurs at approximately $\tau^- + 2/\alpha$ time units after beginning excitement of the other node. The result is maximum inhibition of events presented a little less than $\tau^- + 2\delta$ after beginning excitation of a grid node. Now, if an event has been presented $\tau^- + 2\delta$ before arrival of the prediction signal, the event presented with $\varphi = 0$ presentation phase relative to the arrival of the prediction signal at the arrowheads would have been most inhibited and little learning of this event would have resulted. In effect, this means that to avoid inhibiting an event to be associated with the command event of one outstar sharing the grid with other outstars, the interval between event presentations must be greater than approximately $\tau^- + 4/\alpha$ time units.

The reason for the maximum of an inhibitory response occuring so long after excitation of a node can be seen analytically. If the

total input signal, $I_i(t)$, to an embedding field network node, V_i, is a linear, time invariant function of time, then the node's x process has a transfer function $1/(s+\alpha)$, such that:

$$x_i(s) = (I_i(s))/(s+\alpha).$$

A cascade of n nodes has a transfer function of $(1/(s+\alpha))^n$. Due to the short duration of our input pulses, we are dealing essentially with the transient response of the x process. Thus the transform of $1/(s+\alpha)^n$ is a good indication of what our pulse should look like after having traveled through n nodes.

$$\frac{1}{(s+\alpha)^n} \leftrightarrow \frac{(-1)^n}{(n-1)!}\frac{\partial^{n-1}}{\partial\alpha^{n-1}}\left(e^{-\alpha t}\right) = \frac{1}{(n-1)!}\left(t^{n-1}\ e^{-\alpha t}\right) = x_n(t)$$

The maximum of this occurs at:

$$\frac{dx_n(t)}{dt} = 0$$

or $$\frac{\alpha}{(n-1)!}\left(t^{n-1}\ e^{-\alpha t}\right)$$

Thus the more nodes a pulse travels through, the later its maximum occurs. Of course, the input signal to a grid node in a laterally inhibiting outstar is partially non linear. However, if we consider that the z process vary slowly enough so that we can consider them to be approximately constant, then the above analysis approximately holds. Thus in the case where an input is given to one node which inhibits another, we have a n = 2 node cascade, and:

$$x_2(t) = +te^{-\alpha t}$$

with maximum at:

$t = 1/\alpha$ after arrival of the inhibitory signal.

Now, if we add a prediction signal from the command node also, we have

Figure 4.3.1. Result of choosing β too large for the number of events to be learned in a pattern. v was selected to result in well learning in one presentation for a pattern composed of one event. The inhibitory effect here is too large to learn a three event pattern efficiently.

a n = 3 node cascade and:

$$x_3(t) = +(1/2)t^2e^{-\alpha t}$$

with maximum at :

$t = 2/\alpha$ after arrival of the inhibitory signal.

Thus the occurance of the maximum inhibitory response between $\tau^- + 1/\alpha$ and $\tau^- + 2/\alpha$ is inherent to the network according to the approximate analysis. The experimental evidence shows that this approximate analysis is reasonably correct. We will have further occasion to consider this "lengthening" of pulses as they go through successive nodes when we study outstar avalanches.

The earlier prediction that a β^- suitable for learning a pattern of one event results in inefficient learning of patterns with more than one event was tested. A N = 4 grid node laterally inhibiting outstar was used. v = 3.2 was selected to result in well learning of one event in one presentation and this was experimentally verified. All other parameters were the same as in experiment III. The initial conditions on the z processes were reset to zero. Three events were presented to the grid τ time units after excitation of the command node. A prediction was requested 1/u time units later. The results are shown in figure 4.3.1. The pattern $V_c \rightarrow (V_1, V_2, V_3)$ was learned very poorly. From this evidence it can be concluded that it would require many more rapid presentations of this pattern to result in well learning.

Of course with lateral inhibition any $\beta^- > 0$ will result in faster learning of a pattern with fewer events. If we consider the number of elemental events as a measure of the complexity of a pattern, then this

effect translates into the statement that a complicated pattern is harder to learn. A laterally inhibiting outstar has some of the same drawbacks as the human mental process.

CHAPTER 5 THE OUTSTAR AVALANCHE

section 5.1 Introduction

In section 2.1 the outstar avalanche was briefly introduced. Its geometric schematic and equation were shown in figure 2.1.2 which is here repeated for convenience. The basic idea behind the avalanche is to arrange the command nodes of many outstars in a linear cascade. Excitement of the first node in the cascade results in a prediction signal arriving at the jth command node of the cascade $j\tau$ time units later. Thus each outstar in the avalanche takes a picture of the time varying pattern on the grid at integer multiples of τ. The result is that the avalanche can learn and reproduce a sampled data approximation of a time varying pattern of events. The starting command node in the cascade represents an event which is associated with the start of the time varying pattern.

The linear command node cascade essentially acts as a clock to determine when the data samples are taken. In order to perform the function we would want thr response of each node in the cascade to the prediction signal from the node immediately before it to be approximately the same as every other node. This is, however, not the case with the outstar avalanche arrangement shown in figure 2.1.1. The reason was discussed in section 4.4 where we noticed that the response of nodes in a cascade got longer the more nodes a signal passed through. Based on the transient response of such a linear cascade, we analytically computed that the maximum of the nth node's response occured at $(n - 1)/\alpha$. A short experiment was conducted to test this result. Figure 5.1.1 shows a linear cascade of four nodes

STARTING NODE

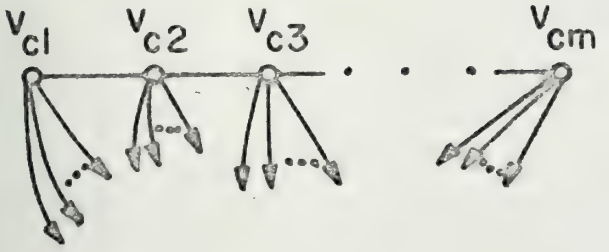

COMMAND NODE CASCADE

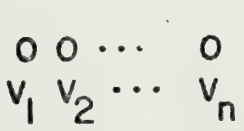

} GRID NODES

EQUATIONS GOVERNING NETWORK PERFORMANCE

2.1.4 $\dot{x}_{c1}(t) = -\alpha x_{c1}(t) + P_{c1}(t)$

2.1.5 $\dot{x}_{ci}(t) = -\alpha x_{ci}(t) + \beta x_{ci-1}(t-\tau)$ for $1 < i \leq M$

2.1.6 $\dot{x}_j(t) = -\alpha x_j(t) + \beta \sum_{i=1}^{M} z_{ci,j}(t) x_{ci}(t-\tau) + P_j(t)$ for $1 \leq j \leq N$

2.1.7 $\dot{z}_{ci,j}(t) = -uz_{ci,j}(t) + vx_{ci}(t-\tau)x_j(t)$

Figure 2.1.2. An outstar avalanche and the equations governing its performance.

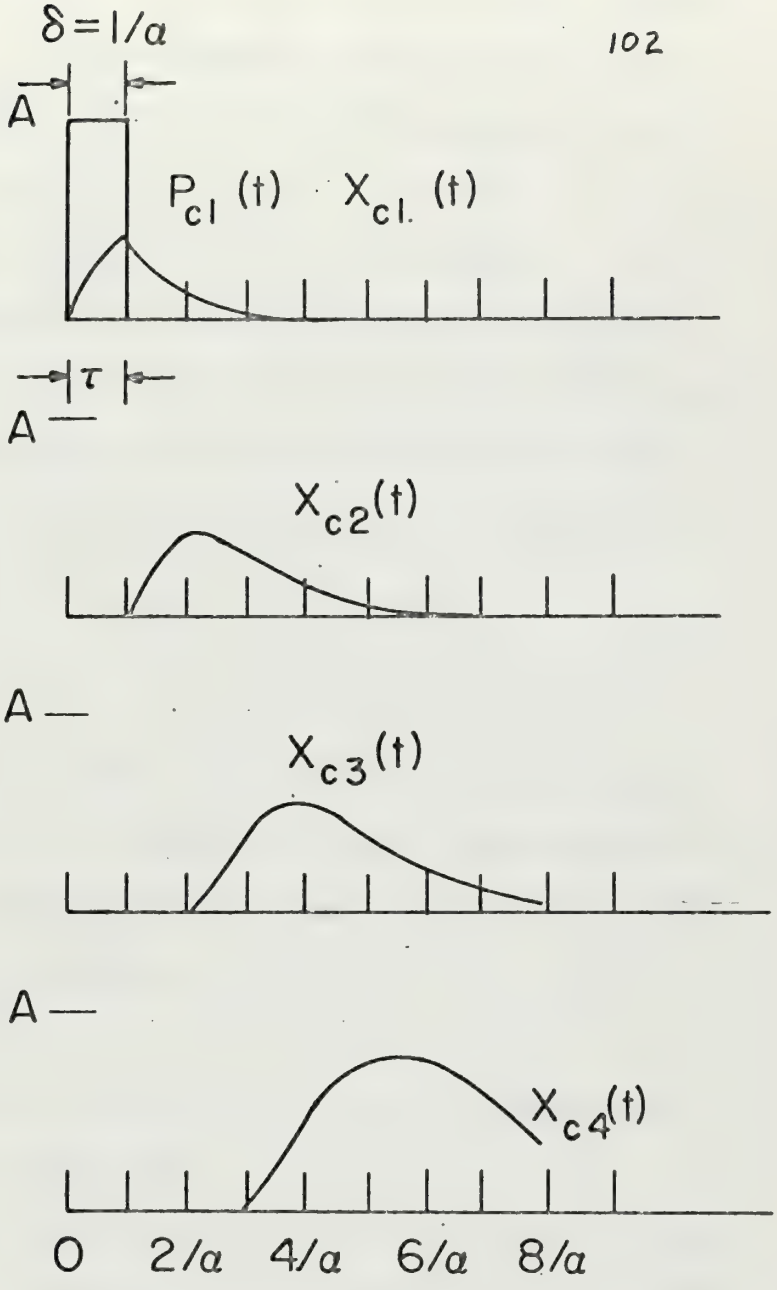

Figure 5.1.1. Response of an outstar avalanche command node cascade. Note the lengthening of the pulse as it travels through sucessive nodes.

SCHEMATIC

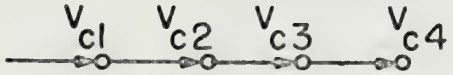

EQUATIONS

$$\dot{x}_{c1}(t) = -\alpha x_{c1}(t) + P_{c1}(t)$$

$$\dot{x}_{ci}(t) = -\alpha x_{ci}(t) + \beta x_{ci-1}(t - \tau) \qquad \text{for } i \geq 2$$

excited by a rectangular pulse at node V_{c1}. As can be seen from the traces $x_{c1}(t)$ through $x_{c4}(t)$, the responses did lengthen by approximately $(n - 1)/\alpha$. The equations used in this experiment were;

$$\dot{x}_{c1}(t) = -\alpha x_{c1}(t) + P_c(t)$$

$$\dot{x}_{ci}(t) = -\alpha x_{ci}(t) + \beta x_{ci-1}(t - \tau) \quad \text{for } i \geq 2$$

The growing amplitude of successive node responses in figure 5.1.1 is due to the fact that β was selected to result in the $x_{c2}(t)$ response being of approximately the same maximum amplitude as the $x_{c1}(t)$ response. For the parameter selection shown in figure 5.1.1, this resulted in a β of:

$$\beta = \frac{\alpha}{(1 - e^{-1})}$$

However, the steady state response of a node with transfer function $1/(s + \alpha)$ to a step input is to amplify the step's amplitude by $1/\alpha$. Thus, in order to maintain approximately equal amplitude responses in a cascade, should be selected to be

$$\beta = \alpha$$

The β in the experiment shown in figure 5.1.1 was too large and resulted in the amplitude growth shown.

The inadvertant amplitude growth in figure 5.1.1 does not detract from the basic result. A linear cascade of command nodes for an avalanche is unsatisfactory due to the progressive lengthening of command node responses. In fact, this effect renders a complex network of embedding field elements requiring transmission of signals through many nodes rather impractical. In a later chapter we shall address this problem directly, but for the time being we shall side step it by introducing a differently configured avalanche.

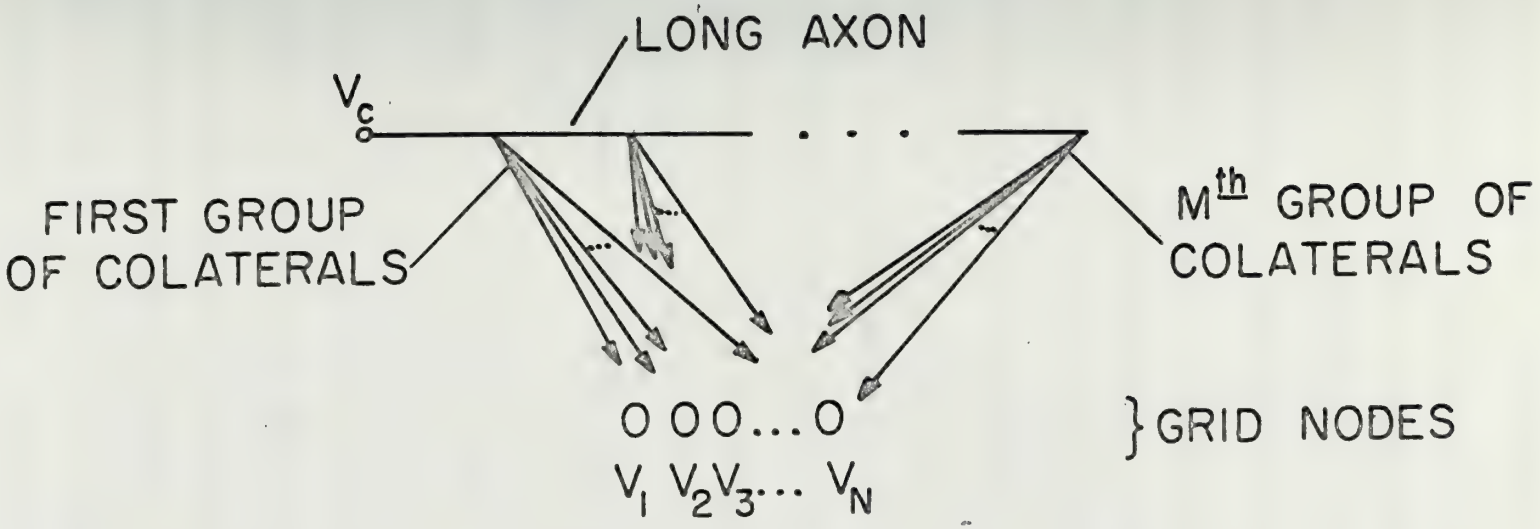

EQUATIONS GOVERNING NETWORK PERFORMANCE ARE:

$$5.1.1. \quad \dot{x}_c(t) = -\alpha x_c(t) + P_c(t)$$

$$5.1.2. \quad \dot{x}_i(t) = -\alpha x_i(t) + P_i(t) + \beta \sum_{j=1}^{M} z_{ji}(t) x_c(t - j\tau)$$

$$5.1.3. \quad \dot{z}_{ji}(t) = -u z_{ji}(t) + v x_i(t) x_c(t - j\tau)$$

Figure 5.1.2. An outstar avalanche using a single starting command node, V_c, a long axon, and colaterals. Note that $j\tau$ is the time ellapsed from excitement of the starting command node V_c to arrival of the prediction signal $x_c(t - j\tau)$ at the arrowheads of the j^{th} colateral group.

Figure 5.1.2 shows an avalanche which performs the same theoretical function as that pictured in figure 2.1.2 without the pulse lengthening effects. The neurophysiological names given to the new elements of figure 5.1.2 were suggested by the geometric arrangement of the nervous system in the cerebellum of vertebrates. The long axon is a long directed edge. At periodic points along the long axon, the directed edge splits into a continuation of the long axon and a group of N branches of the directed edge called a collateral group. Each of the collaterals has an arrowhead impinging on a grid node. The distance from the starting command node, V_c, to the arrowheads of the jth collateral group are so arranged that the time elapsed from excitement of the starting command node to arrival of the prediction signal at these arrowheads is $j\tau$ time units. In each collateral arrowhead is located a z process for correlating the prediction signal $x_c(t - j\tau)$ with the grid node responses. This long axon and collateral geometry performs the clock function of the avalanche.

For ease of reference, the equations for this avalanche are given here:

5.1.1 $$\dot{x}_c(t) = -\alpha x_c(t) + P_c(t)$$

5.1.2 $$\dot{x}_i(t) = -\alpha x_i(t) + P_i(t) + \beta \sum_{j=1}^{N} z_{ji}(t) x_c(t - j\tau)$$

5.1.3 $$\dot{z}_{ji}(t) = -uz_{ji}(t) + vx_i(t)x_c(t - j\tau)$$

Equation 5.1.2 is for the response of a grid node in a simple outstar. We will perform a simple experiment on an avalanche with this formulation and then change equation 5.1.2 to incorporate lateral inhibition in our avalanche. The two avalanches thus formed will be called a simple avalanche and a laterally inhibiting avalanche.

Time does not permit an exhaustive study of avalanches. This chapter on avalanches is an illustration of the results and problems of using the outstars studied previously in an avalanche.

section 5.2 A Simple Avalanche

In this section we will use a simple avalanche to learn a time varying pattern of events. In designing a simple avalanche to do this, we must first ask what sort of time varying pattern are we going to have it learn. If we have M collateral groups in our avalanche and N grid nodes, we must keep track of M x N z processes during the experiment. To conserve computation time, M x N should be small. An avalanche with M = 3 collateral groups and N = 2 grid nodes is chosen. It would be rather unrealistic to expect an avalanche which takes only three sample data points to approximate a continuous time varying pattern. Thus we will try to learn a series of time discrete events. That is, we allow the possibility of the occurance of the two events associated with the grid nodes in the environment. We assume that the events represent time discrete events such as depressing the key of a piano. We further assume that there is a minimum time between occurance of separate patterns of these events and we synchronize the avalanche's sampling interval τ with this minimum interval. To simplify the experiment still further, we shall indicate the occurance of these events with equal amplitude rectangular input pulses to the appropriate grid node and follow the convention of the past chapters by making the pulse duration δ equal to the rise time of a node's response:

$$\delta = 1/\alpha$$

With this specification of the allowable input patterns, we have made the results of the previous chapters applicable to the avalanche. The other parameters will be specified accordingly:

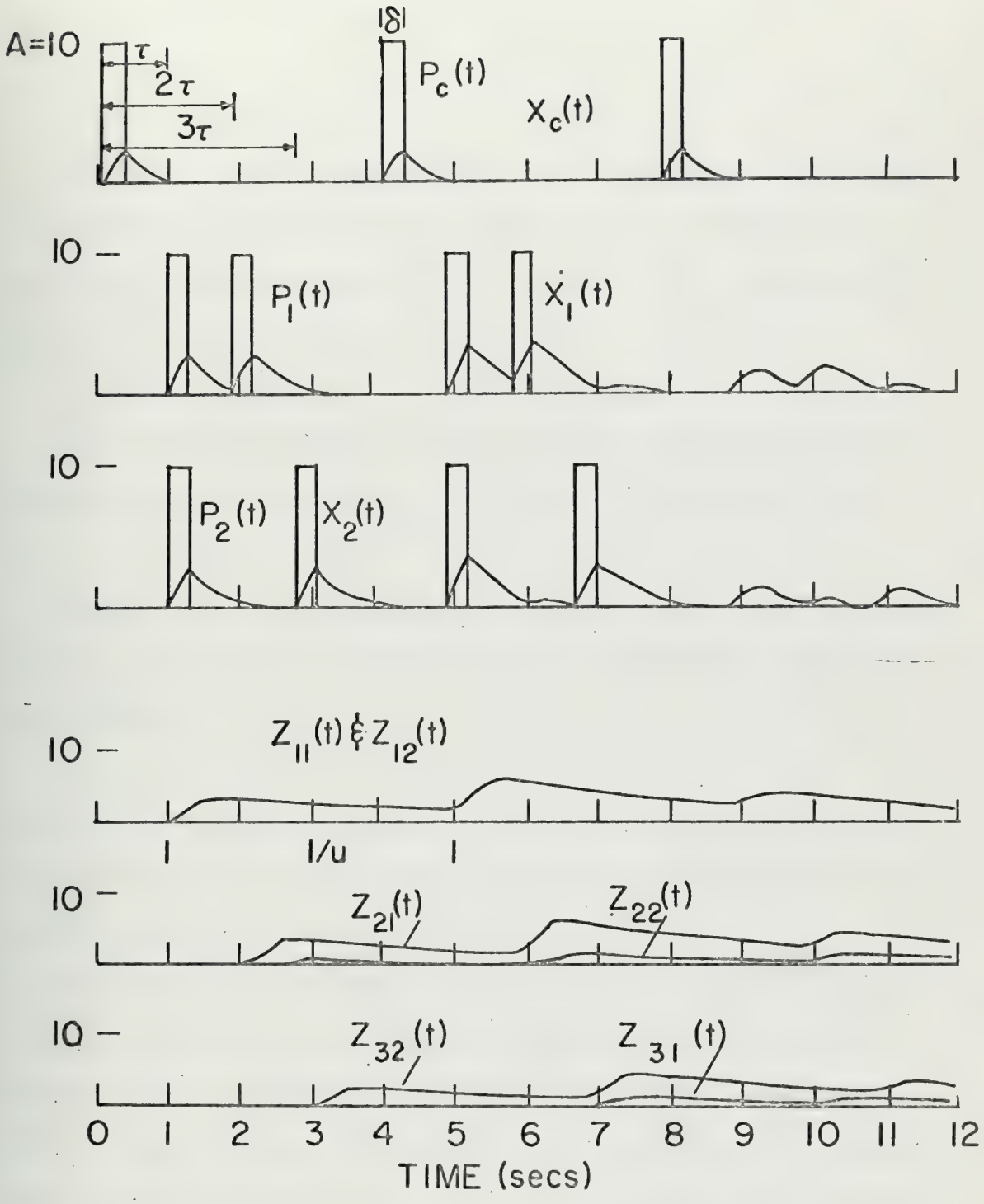

Figure 5.2.1. Results of an experiment with a simple outstar avalanche.

$\alpha = 3.3333 \text{ sec.}^{-1}$

$\beta = 1$

$v = 1.6$ (two presentations for well learning criteria)

$A = 10$

$\delta = 1/\alpha = 0.3$ sec.

We want τ to be large enough to avoid significant over lapping of the "pictures" taken by each collateral group. From the phase-correlation curves of section 3.5, $\tau = 3/\alpha = 3\delta$, should work. Thus τ is selected to be:

$\tau = 3/\alpha = 0.9$ sec.

The memory decay time 1/u is specified to be the time between successive presentations and/or predictions of the pattern. Thus:

$u = 1/4 \text{ sec.} = 0.25 \text{ sec.}^{-1}$

Figure 5.2.1 shows the pattern presented to the avalanche and the results. The pattern was presented twice. Symbolically, the pattern presented was:

$V_c \rightarrow (V_1, V_2), (V_1, 0), (V_2, 0)$

The grid node responses following t = 8.8 seconds are the avalanche's learned prediction of the pattern ellicited by the excitement of the starting command node alone at t = 7.9 seconds.

As can be seen, the avalanche's prediction is not an unqualified success. Of course α is too small to approximate the input pulses with any degree of accuracy. Nonetheless, grid node V_1 did respond with two large amplitude responses in a row and grid node V_2 responded with large responses spaced 2τ apart as in the input pattern. However, the third response of $x_1(t)$ and the second response of $x_2(t)$ show

that the avalanche has noticable "picture over lapping" error problems. Increasing α and/or using thresholds would result in a better approximation.

section 5.3 A Laterally Inhibiting Avalanche

Although the results with a simple avalanche were not encouraging, equations 5.1 were modified to produce a laterally inhibiting avalanche for comparison. To convert a simple avalanche to a laterally inhibiting one, inhibiting directed edges between the grid nodes must be added and equation 5.1 changed to:

5.3.1 $$\dot{x}_c(t) = -\alpha x_c(t) + P_c(t)$$

5.3.2 $$\dot{x}_i(t) = -\alpha x_i(t) + P_i(t) + \beta \sum_{j=1}^{N} z_{ji}(t) x_c(t - j\tau) - \beta^- \sum_{j=1, j\neq i}^{N} [x_k(t - \tau^-)]^+$$

5.3.3 $$\dot{z}_{ji}(t) = -u z_{ji}(t) + v [x_i(t) x_c(t - j\tau)]^+$$

where:

$$[y]^+ = \begin{cases} y \text{ if } y > 0 \\ 0 \text{ if } y \leq 0 \end{cases}$$

Figure 5.3.1 shows the results of performing the experiment of section 5.2 on a laterally inhibiting avalanche. The parameters used in this experiment were the same as those in section 5.2 except that $v = 2.4$ as in the study of the laterally inhibiting outstar. τ^- and β^- are the same as in that study:

$\tau^- = 0.1$ sec.

$\beta^- = 2.38$

The prediction response of the grid nodes following $t = 8.8$ seconds in figure 5.3.1 shows that the pattern learned by the avalanche is definitely not the pattern taught to it. Briefly analyzing the reasons for this failure, we can see that the deleterious effects of lateral inhibition all acted in concert. Firstly, the fact that lateral inhibition diminishes the amplitude of a node's response

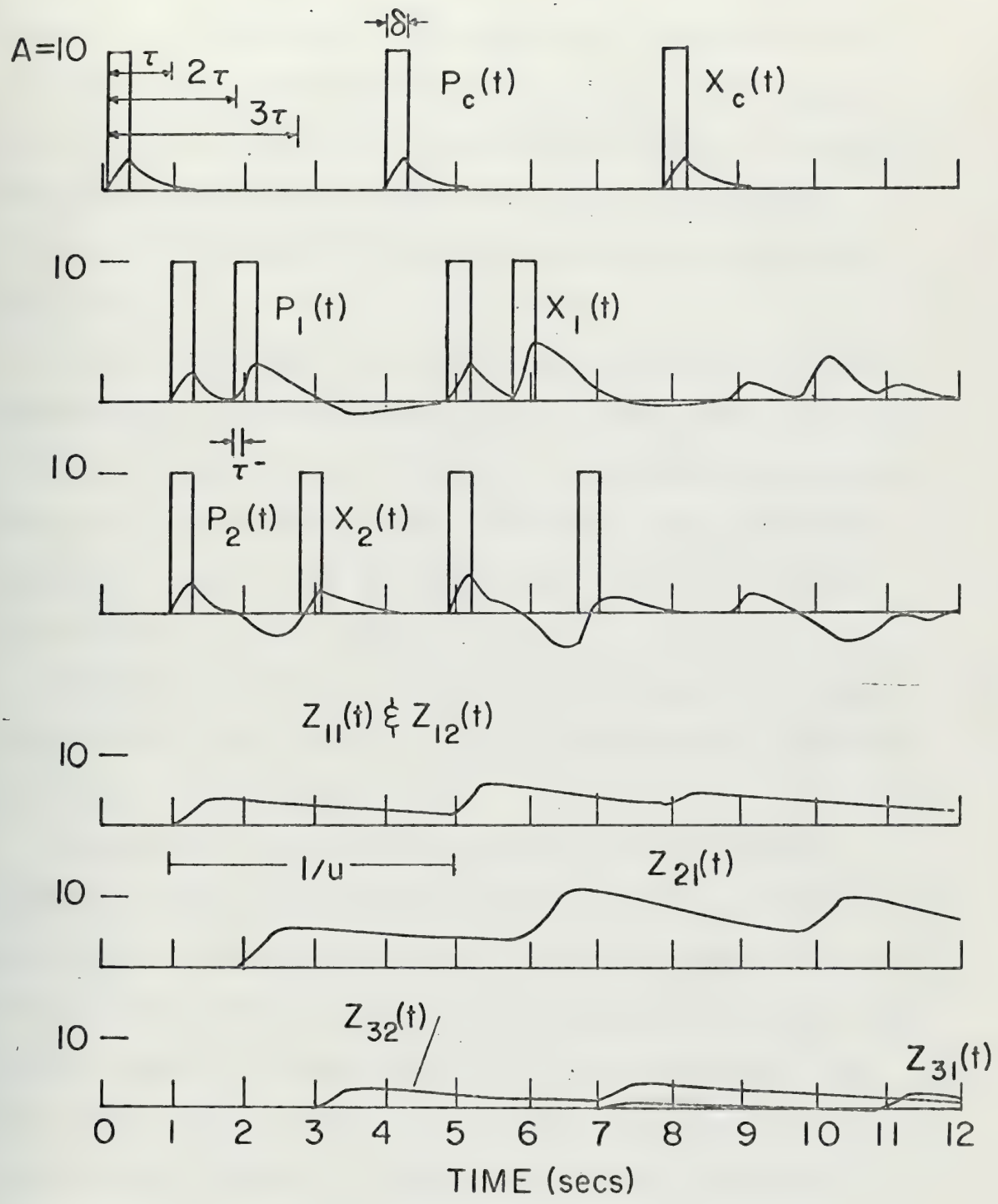

Figure 5.3.1. Results of an experiment with a laterally inhibiting outstar avalanche.

when more than one node is excited at the same time resulted in responses to presentation of both of the events at the same time at the beginning of the pattern being diminished. This resulted in a smaller correlation amplitude for $z_{11}(t)$ and $z_{12}(t)$ when compared to $z_{21}(t)$ which was the result of the uninhibited response to the presentation of event 1 alone as the second event of the pattern. The first two responses of the prediction response of $x_1(t)$ show this effect.

Secondly, the lengthening of the negative amplitude inhibitions responses due to transmittal through several nodes resulted in a large inhibitory response in $x_2(t)$ when event 2 was presented alone as the third event of the pattern. This resulted in a small correlation amplitude for $z_{32}(t)$ which was insufficient to drive $x_2(t)$ positive in the prediction at the appropriate time.

Additionally, the errors associated with "picture over lapping" combined with the above resulted in $x_1(t)$ responding to a third event that was not in the pattern.

If an attempt were made to improve the laterally inhibiting avalanche's performance, β^- should be reduced. It is noted that if the pattern had been composed on the average of a large number of events at each sampling with only a few events changing between samples, the amplitude diminishing effect would not have been as serious. Due to the large number of nodes in such a pattern, the resistance to random mistakes composed of a small number of events would not be compromised with a smaller β^-.

Both to avoid the inhibitory response lengthening and "picture over lapping" errors, the interval between samples, τ , should be

increased. Of course this last suggestion seriously compromises the ability of a laterally inhibiting outstar to accurately approximate a rapidly varying pattern. Thus solution of the response lengthening problem of a signal that must be transmitted through several nodes is important. A solution will be proposed in a later chapter.

The avalanches presented in this chapter were for illustrative purposes to show some of the problems encountered when outstars are combined into an avalanche. Rather than dwelling upon the design improvements which could be made to the avalanches, we will go on to consider other formulations of outstars which are the basic components of an avalanche.

CHAPTER 6 THE VIRTUAL LATERALLY INHIBITING OUTSTAR

section 6.1 Other Outstars Which Control the Maximum Amplitudes of Grid Node Responses

Lateral inhibition was added to the simple outstar as a means of using past experience to suppress random mistakes in a pattern. Its addition was necessitated by the rapid forgetting rate required to control the amplitudes of prediction responses. There are methods by which the amplitudes of prediction responses can be controled other than by allowing a fast forgetting rate. We will review a few of them as illustrations of different formulations of the equations for an outstar and then investigate one of them.

One method of controling the amplitudes of prediction responses would be to place an upper bound on the z processes:

6.1.1 $$\dot{x}_c(t) = -\alpha x_c(t) + P_x(t)$$

6.1.2 $$\dot{x}_i(t) = -\alpha x_i(t) + P_i(t) + \beta z_{ci}(t)x_c(t - \tau)$$

6.1.3 $$\dot{z}_{ci}(t) = -uz_{ci}(t) + [M_z - z_{ci}(t)]^+ vx_i(t)x_c(t - \tau)$$

where: $$[y]^+ = \begin{cases} y \text{ if } y > 0 \\ 0 \text{ if } y \leq 0 \end{cases}$$

Equation 6.1.3 limits $z_{ci}(t)$ to values between 0 and M_z. M_z is specified such that $\beta M_z x_c(t - \tau)$ produces the maximum grid response amplitude we are willing to tolerate. This method has limited random mistake resistance. However, if we specify v such that it requires several presentations of a pattern to drive a z process to M_z, then the occurance of one random mistake will result in a relatively small z amplitude. If u is specified to result in a memory decay time 1/u

approximately equal to the average time interval between consecutive occurances of the same random mistake, then equations 6.1.1 through 6.1.3 describe an outstar which has a relatively slow forgetting rate and amplitude control of the grid node responses. However, if an outstar governed by this set of equations is confronted with a random mistake and is then asked to predict the pattern rapidly for a prolonged period, we can expect the pumping up process to saturate all the z process at value M_z, including the z process associated with the mistake. Thus upper bounding the z processes to insure that the amplitudes of prediction responses remain tolerable is not very useful for an outstar functioning in a noisy environment. Additionally, we could expect that use of a small u would result in poor correctability as in the simple outstar.

A more direct method of controling the amplitudes of predictions responses would be to upper bound the grid x processes:

6.1.4 $$\dot{x}_c(t) = -\alpha x_c(t) + P_c(t)$$

6.1.5 $$\dot{x}_i(t) = -\alpha x_i(t) + \left[M_x - x_i(t)\right]^+ (P_i(t) + \beta z_{ci}(t) x_c(t - \tau))$$

6.1.6 $$\dot{z}_{ci}(t) = -u z_{ci}(t) + v x_c(t - \tau) x_i(t)$$

By specifying u in equation 6.1.6 to be small, the outstar governed by equations 6.1.4 through 6.1.6 would be able to absorb random mistakes in its experience as did the simple outstar with a slow forgetting rate in chapter three. The bound on the grid node's x processes in equation 6.1.5 insures that this outstar will not have the uncontroled growth of prediction responses that the slowly forgetting simple outstar did. However, in this outstar, a large $z_{ci}(t)$ would result in a maximum prediction input signal to a grid node of magnitude M_z for as long as $z_{ci}(t)x_c(t - \tau) \geq M_z$. Because

the prediction signals have exponentially decaying tails, this would result in the effective duration of the maximum prediction signal input getting longer as the $z_{ci}(t)$ process got longer. Thus while being able to control the amplitude of grid node prediction responses, we would not be able to control the duration of the responses. In an outstar, we have absolute control over the shape and amplitude of the prediction signal $x_c(t - \tau)$ by control of the input pulse to the command node. Thus by specifying the input pulses we can analytically compute what the prediction signal looks like. With this knowledge, a threshold Γ_c could be placed on the command node to guarantee that the prediction signal $[x_c(t - \tau) - \Gamma_c]^+$ is non zero only over a specified interval of time. By so restricting the duration of the prediction signal we could also limit the duration of the grid node's prediction responses. Again the small u resulting in good random mistake resistance could be expected to result in poor correctability. The properties of such an outstar would be interesting to investigate but time did not allow an investigation in this study.

Another method of controling the grid node prediction response amplitude which we will study would be to make the prediction input signal to the grid nodes linearly proportional to the probabilities $y_i(t)$ which define the outstar's memory of a pattern. By the outstar theorem, the $y_i(t)$ converge to the pattern probabilities θ_i which are constant. Thus when the $y_i(t)$ have converged sufficiently close to the θ_i we could expect the prediction signal inputs to the grid nodes $\beta y_i(t) x_c(t - \tau)$ to be the same independent of the amplitudes of the $z_{ci}(t)$ processes. As $y_i(t) \leq 1$, specifying β would determine the maximum possible prediction amplitude of the grid node's responses.

Additionally specifying the u of the z processes to be small would allow absorption of random miatakes in accumulated past experience. The equations for such an outstar are:

6.1.7 $\dot{x}_c(t) = -\alpha x_c(t) + P_c(t)$

6.1.8 $\dot{x}_i(t) = -\alpha x_i(t) + P_i(t) + \beta y_i(t) x_c(t - \tau)$

6.1.9 $\dot{z}_{ci}(t) = -u z_{ci}(t) + v x_c(t - \tau) x_i(t)$

6.1.10 $y_i(t) = z_{ci}(t) \Big/ \left(\sum_{j=1}^{N} z_{cj}(t) \right)$

Another attractive property of an outstar governed by these equations is that equal prediction signals will result in equal grid node responses independent of the amplitudes of the z processes. Thus we could say that the memory of a pattern is always fresh in such an outstar's memory and pumping up is not required.

A close examination of equations 6.1.7 through 6.1.10 shows that an outstar governed by these equations is a laterally inhibiting outstar. By lateral inhibition we mean the ability of a grid node responding with large amplitude to diminish the amplitude of grid nodes responding with lesser amplitudes. From equation 6.1.9, a grid node responding with a large amplitude will result in a large correlating amplitude for the associated $z_{ci}(t)$ process. This will result in a large probability $y_i(t)$ from equation 6.1.10 which in turn will allow a larger prediction signal input in equation 6.1.8. At the same time a large $z_{ci}(t)$ will result in a smaller $y_j(t)$ for nodes not responding with large amplitudes by the inclusion of $z_{ci}(t)$ in the denominator of equation 6.1.10 for $y_j(t)$. This in turn will result in a smaller input prediction signal in equation 6.1.8 for $x_j(t)$. As can be seen from equation 6.1.10, the accumulated past experience of the outstar in the $z_{ci}(t)$ processes plays a major part in this

lateral inhibition and thus the past experience can be counted upon to inhibit the effects of a random mistake. An outstar governed by these equations combines absorption of random mistakes and active inhibition of them.

The major drawback of such an outstar is that it is not consistent with the elements of embedding field theory presented in chapter one. Their neat geometric elements performing one function each were presented. Because the $y_i(t)$'s perform the prediction signal amplification function for this outstar, they should be located in the arrowheads of the directed edges with the z processes. This raises the problem of how the $z_{ci}(t)$'s from each of the arrowheads of directed edges from the command node are made simultaneously available at all the arrowheads to form the $y_i(t)$'s. We have constrained all other information transmissions in the outstar to finite velocities along directed edges. Because the $z_{ci}(t)$'s are instantaneously available at all the arrowheads without any apparent means of traveling between the arrowheads, the $y_i(t)$ is a virtual process. The outstar described by equations 6.1.7 through 6.1.10 is there fore called a virtual laterally inhibiting outstar.

Although the virtual $y_i(t)$ process is not consistent with the elements of embedding field networks presented in chapter one, we will study the performance of a virtual laterally inhibiting outstar. Grossberg has done considerable theoretical work with it. (Ref. 7) In the realm of theory, there is no reason why a virtual process should be excluded from consideration. A virtual process does not present any difficulties to a digital simulation either. Moreover, if we were to build electrical devices to make an outstar with, we would

have more trouble engineering the transmission delays for prediction signals than engineering the virtual $y_i(t)$ processes. The only place where the virtual processes are clearly inapplicable is in the nervous system of living organisms where all information transmissions from one point in the system to another are at a finite velocity. Whereas a virtual laterally inhibiting outstar is not useful as a model for nervous systems, it is a legitimate device for study.

section 6.2 Specifying the Parameters in a Virtual Laterally Inhibiting Outstar

We will perform the same experiment on a virtual laterally inhibiting outstar as has already been performed on the simple and laterally inhibiting outstars. Therefore the parameters of the virtual laterally inhibiting outstar are specified to be the same as in the other outstars except where there are special considerations to be made:

Input parameters:

$A = 10$

$\delta = 1/\alpha = 0.3$ sec.

Network parameters:

$\alpha = 3.3333$ sec.$^{-1}$

$\tau = 0.3$ sec.

$N = 3$

Initial conditions on x_c and all x_i are zero.

Selection of β, u, v, and the initial conditions on the z processes will require some discussion.

As the $y_i(t)$ are ratios of $z_{ci}(t)$ to the sum of all $z_{ci}(t)$, we want at least one of the z_{ci} to have a non zero initial condition to avoid the problem of dividing by zero. The initial value should not be too large to avoid biasing the network at the beginning of the experiment. Therefore at least one z_{ci} will be specified to have an initial condition of 0.1. Again, to prevent biasing of the network in favor of predicting any one grid event, all the $y_i(t)$ should be approximately equal. This accomplished if the initial conditions on all the z_{ci} are equal.

Therefore:

$$z_{ci}(0) = 0.1 \quad \text{for } i = 1, 2, 3$$

Notice that this means that there is a non zero initial condition on the $y_i(t)$'s:

$$y_i(0) = 0.3333 \quad \text{for } i = 1, 2, 3$$

This means that the precidtion signal at the beginning of the experiment is split up evenly between all the nodes in the grid. A prediction made in the initial state of the experiment will result in all grid nodes responding equally. We must accordingly modify our interpretation of what grid node responses mean. Heretofore we have considered the outstar to be in a state of complete ignorance at the beginning of an experiment. In the simple and laterally inhibiting outstars this state of initial ignorance was specified by making the initial conditions on the z processes zero. A prediction by one of those outstars while it was in its initial state resulted in no response of the grid nodes. Thus we were able to re-enforce our interpretation of initial ignorance by saying that there was nothing in the outstar's memory and the outstar could predict nothing. The virtual laterally inhibiting outstar does not have this nicety.

We will interpret the prediction responses of a laterally inhibiting outstar to indicate total ignorance if all grid nodes respond with the same amplitude. Equivalently, total ignorance is the state in which all $y_i(t)$ are equal. Note that this interpretation means that the pattern composed of all the events represented by nodes in the grid is not perceivable by the outstar. Excitation of all grid nodes will result in the same values of the $y_i(t)$ as they have initially. This is equivalent to saying that white light is the same as complete

darkness in this outstar. Thus an intelligible pattern must be composed of fewer than N events. In our experiment the pattern is composed of one event out of three and thus is intelligible.

In previous outstars, v has been selected on a so many presentations mean well learning criteria. This was due to the fact that the prediction signal amplification process, the $z_{ci}(t)$, had to grow to a certain amplitude before a prediction would drive the grid nodes to the same amplitudes as presentation of the pattern externally would drive them. In the virtual laterally inhibiting outstar, this criteria for v is meaningless. The prediction signal amplification processes are the $y_i(t)$ which by the outstar theorem are always less than or equal to unity no matter what the amplitudes of the z processes are. Thus small amplitude z processes will result in the same amplitude grid node responses as large amplitude z processes as long as the ratios $z_{ci}(t) \left[\sum_{j=1}^{N} z_{cj}(t) \right]^{-1}$ remain the same. Thus specification of v has nothing to do with the amplitude of grid node responses.

β, on the other hand, has a great deal to do with the amplitude of the grid node responses. In previous outstars we have tried to control the grid node responses so that their amplitudes during a prediction were approximately equivalent to those attained by excitement by an event. As v can not be used for that purpose in this outstar, we will use β. With this intention, we run into the usual problem with our outstar possessing some form of lateral inhibition. That is, we would like to know how many events on the average compose a pattern. In a laterally inhibiting outstar we saw that a β selected for an average of a small number of events in a pattern resulted in inefficient

learning of a pattern composed of many more events. Nevertheless, with sufficient instruction and/or predictions, the laterally inhibiting outstar is able to "well learn" a pattern more complicated than it was designed to learn.

In the virtual laterally inhibiting outstar, we do not have this possibility for well learning a pattern more complicated than ones the network is designed to learn. If we have $M < N$ events on the average in a pattern, then the expected value for the $y_i(t)$ corresponding to events in a pattern is $y_i(t) = 1/M$ after learning has occured. The $y_i(t)$ for events not in the learned pattern are small. Now, we can specify β such that:

$$\beta = bM$$

where b is a constant necessary to result in a well learned grid prediction response for a pattern composed of one event. With this β, the input prediction signal to a node representing an event in the learned pattern is:

$$y_i(t)\beta x_c(t - \tau) = (1/M)bMx_c(t - \tau) = bx_c(t - \tau)$$

and thus we get well learned responses.

However, if there are fewer than M events in the pattern learned, the prediction responses will be larger. If there are more than M events in the pattern learned, the prediction responses will be smaller. Because the $y_i(t)$ do not change once the pattern is learned, there is no possibility of changing this situation.

Thus the well learning criteria is an unrealistic requirement for a virtual lateraly inhibiting outstar that is confronted with the possibility of learning a wide variety of patterns. The well learning criteria was originally introduced because we adopted the convention

of reading the amplitudes of the x processes at the nodes as the response of a node. As the measurement of very small or very large amplitudes was improctical, the well learning criteria was adopted as a measurement standard. For the virtual laterally inhibiting outstar we could devise another virtual process to interpret grid node responses. For instance, the probabilities:

$$X_i(t) = x_i(t)\Big[\sum_{j=1}^{N} x_j(t)\Big]^{-1}$$

would be suitable. However, as the pattern we will teach the outstar in this experiment is simple and we know that it will be composed of at most one event, we can retain the well learning criteria for interpretation. In a more general situation the above discussion must be considered.

Since we are going to teach the outstar a pattern composed of at most one event, and we are going to specify β according to the well learning criteria, we can make a quick estimation of what β should be:

The input prediction signal to the grid node corresponding to the event in the pattern should have a maximum amplitude equivalent to the maximum amplitude of an input pulse:

$$\beta y_i(t)(\max x_c(t - \tau)) = A$$

For one event in the pattern, $y_i(t) = 1.0$ after learning. Therefore we want:

$$\beta(\max x_c(t - \tau)) = (A/\alpha)(1 - e^{-\alpha\delta}) = (A/\alpha)(1 - e^{-1}) \cong 0.63(A/\alpha)$$

or:

$$\beta = \alpha/.063 = 5.28$$

Experimentally the appropriate value of β was found to be:

$$\beta = 4.77$$

The 11% error is due to both the naiveté of the estimation and the error inherent in the digital simulation.

Having specified β, we will specify v to be equal to β arbitrarily:

$v = \beta = 4.77$

Only u remains to be specified. Since it is claimed that a virtual laterally inhibiting outstar can use the large z's resulting from a small u to absorb random mistakes, we will specify u to be small.

$u = 0.01 \text{ sec.}^{-1}$

Note again that a small u means that the decay time of the z process 1/u is large compared to the presentation and/or prediction interval to be used in the experiment.

section 6.3 Results of the Experiments with a Virtual Laterally Inhibiting Outstar

Figure 6.3.1 shows the results of presenting the pattern $V_c \rightarrow V_2$ to the virtual laterally inhibiting outstar twice and then asking for a prediction of the pattern. As can be seen from the $x_2(t)$ trace, $V_c \rightarrow V_2$ was well learned. $V_c \rightarrow V_3$ was learned slightly due to the prediction signal's "tail". (Event 3 was presented with presentation phase $\varphi = +2\delta$ with respect to the prediction signal.) Also note that $x_1(t)$ responds to prediction slightly although event 1 has not been presented to the outstar.

Looking at the $y_i(t)$ traces in figure 6.3.1 we can see why. All three $y_i(t)$ started with the same initial values $y_i(t) = 0.3333$ for $i = 1, 2, 3$. The first presentation of the pattern resulted in $y_2(t)$ rising to a maximum value of nearly 0.8 while $y_1(t)$ and $y_3(t)$ decreased to about 0.1 each. When event 3 was presented 2δ after event 1, the $y_i(t)$ changed slightly due to correlation between the prediction signal's tail and $x_3(t)$. Note that on the second presentation of the pattern, $y_1(t)$ decreased again and $y_2(t)$ increased. According to the outstar theorem, more presentations of the pattern because of correlation between the tail of the prediction signal and $x_3(t)$. However, in the two presentations in figure 6.3.1 $y_i(t)$ is still large enough to allow some prediction signal through to excite $x_1(t)$.

If we remember that it was agreed to interpret an equal response from each of the grid nodes as no response, then we can place imaginary thresholds, Γ_x, on the $x_i(t)$ traces. Γ_x shown in way of the third response on the $x_i(t)$ trace was chosen such that if $y_i(t) = 0.3333$ for

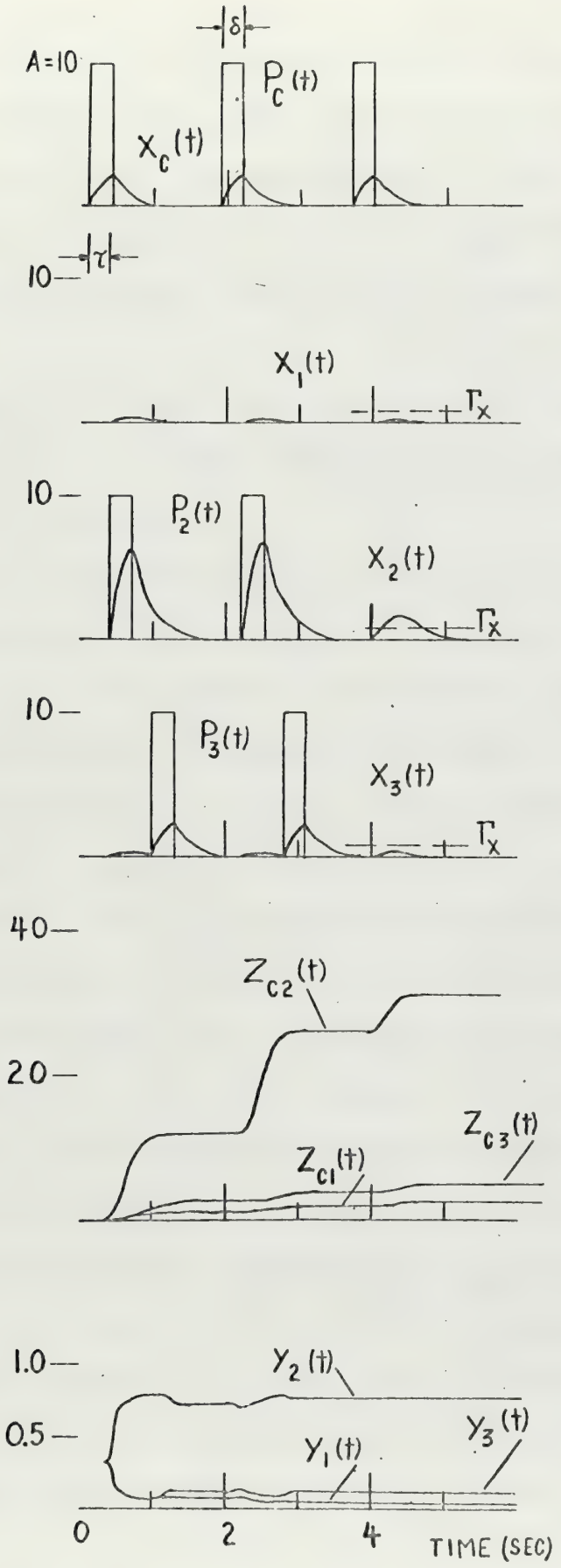

Figure 6.3.1. Results of teaching a virtual laterally inhibiting outstar a pattern.

i = 1, 2, 3 in the outstar, all grid node prediction responses would be subthreshold. Thus, by interpreting a node as not responding until it is suprathreshold, we can interpret the results in figure 6.3.1 as saying that only $V_c \rightarrow V_2$ was learned by the outstar. The results of performing an experiment on a virtual laterally inhibiting outstar with real, versus imaginary, thresholds will be reported later in this chapter.

Of interest is the fact that the $y_i(t)$ did not change during the prediction. This was an outstar theorem guarantee which is now experimentally verified.

Figure 6.3.2 shows the results of continuing the experiment. A simulated random mistake was presented with the pattern by presenting event 1 at the same time as event 2 was presented. Note that on subsequent predictions, $x_1(t)$ remained subthreshold. It can be concluded that this virtual laterally inhibiting outstar is resistant to random mistakes. However, looking at the $y_i(t)$ traces, it can be seen that the random mistake did reduce $y_2(t)$ and this effect persisted through subsequent predictions. Thus, even though the prediction responses of $x_1(t)$ are subthreshold, the $y_i(t)$ remember the mistake. It will take several presentations of the correct pattern to undo the effect of the random mistake. In the discussion of using large amplitude z processes to absorb mistakes in section 3.4 it was shown that the z processes would reflect the conditional probabilities $PR_{i/c}$. Up to the end of the experiment in figure 6.3.2, the c event has been presented 6 times. Event 2 has been presented 3 times and event 1 has been presented 1 time. Using the past history of the occurance of the events in the environment to estimate the conditional probabilities $pR_{1/c}$ and $pR_{2/c}$ we get:

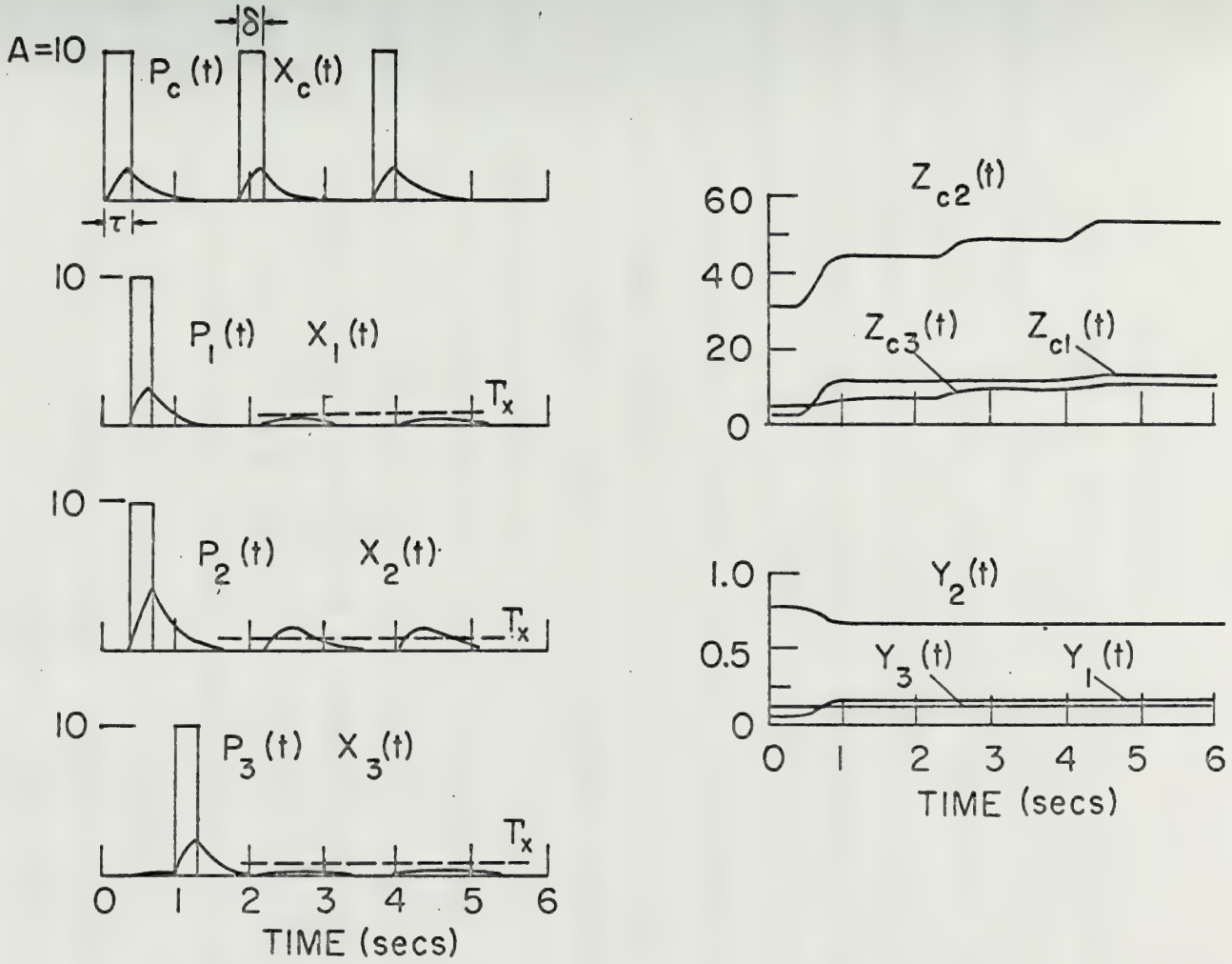

Figure 6.3.2. Effect of a simulated random mistake on a virtual laterally inhibiting outstar which has previously learned $V_c \rightarrow V_2$. $P_1(t)$ simulates the random mistake.

$pR_{1/c} = 1/6 = 0.1666$

$pR_{2/c} = 3/6 = 0.5$

The ratio $pR_{1/c} / pR_{2/c} = 0.3333$. At the end of the experiment in figure 6.3.2, $y_1(t) = 0.15$ and $y_2(t) = 0.6666$. The ratio $y_1(t)/y_2(t)$ is:

$$y_1(t) / y_2(t) = (0.15)/(0.6666) = 0.225$$

As the $y_i(t)$ are directly proportional to the $z_{ci}(t)$, the above calculations show that the virtual laterally inhibiting outstar is more resistant to random mistakes than would be expected if it were just using large amplitude z processes to absorb mistakes. On the other hand, we can show expect the large z's to reflect the statistics of the environment some what and the inhibitory mechanism of the outstar is not sufficient to completely overcome this. Thus some effect on the $y_i(t)$'s must be expected from the statistics of the environment.

Figure 6.3.3 shows the results of continuing the experiment and trying to correct the learned pattern $V_c \rightarrow V_2$ with the pattern $V_c \rightarrow V_1$ by presenting event 1 three times in a row. As can be seen, the correction attempt was not successful. Looking at the $z_{ci}(t)$ traces, it can be seen that the past accumulated experience of $V_c \rightarrow V_1$ in the large $z_{c2}(t)$ is so great that although the accumulated experience of $V_c \rightarrow V_1$ in $z_{c1}(t)$ is increasing, it will require many more presentations of $V_c \rightarrow V_1$ to say that the outstar has corrected the mistake. This was a phenomena noticed in the slowly forgetting simple outstar also. Even though this outstar does laterally inhibit, it is not surprising that a large amount of experience with a pattern will make it difficult to convince the outstar that the pattern is a mistake. In order to

Figure 6.3.3. Attempt to correct a previously learned pattern in a virtual laterally inhibiting outstar. The previously learned pattern $V_c \rightarrow V_2$ is being corrected with the pattern $V_c \rightarrow V_1$.

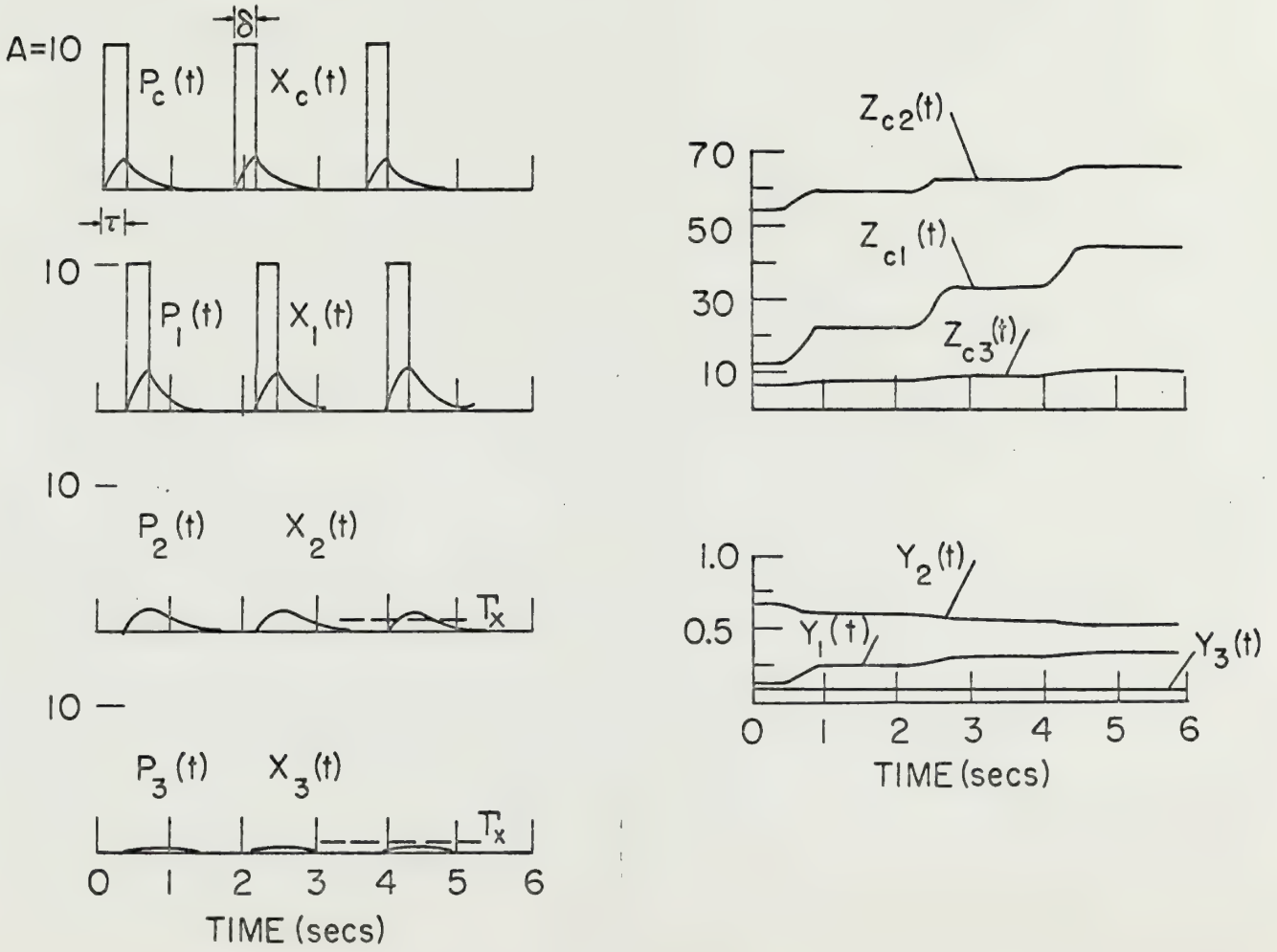

improve the virtual laterally inhibiting outstar's correctability, the forgetting rate u will have to be decreased.

section 6.4 A Virtual Laterally Inhibiting Outstar with Thresholds and an Intermediate Forgetting Rate Designed to Learn Patterns of More than One Event

In the previous section, it was concluded that the addition of thresholds to a virtual laterally inhibiting outstar would be an aide to the interpretation of responses. It was also concluded that a faster forgetting rate would increase correctability. In this section ,we will test these conclusions. Additionally, it would be instructive to see what happens when the pattern being taught to the outstar is composed of more than one event.

In order to have sufficient possibilities available to study teaching an outstar a pattern composed of more than one event, the number of grid nodes, N, will be increased to N = 5. We will specify β to result in a well learned response for patterns composed of an average $\bar{M} = 2.5$ events. The input pulse parameters; the x process rise rate, α , and the transmission delay, τ , will be kept the same as in section 6.2. The following parameters are therefore specified:

Rectangularly shaped input pulses:

$A = 10$

$\delta = 0.3$ sec.

$\alpha = 3.3333$ sec.$^{-1} = 1/\delta$

$\tau = 0.3$ sec.

Since thresholds are to be added to the outstar, the equations governing its performance will have to be changed:

6.4.1 $\dot{x}_c(t) = -\alpha x_c(t) + P_c(t)$

6.4.2 $\dot{x}_i(t) = -\alpha x_i(t) + P_i(t) + y_i(t)\beta[x_c(t-\tau) - \Gamma_c]^+$

6.4.3 $\dot{z}_{ci}(t) = -uz_{ci}(t) + v[x_c(t-\tau) - \Gamma_c]^+ [x_i(t) - \Gamma_x]^+$

6.4.4 $y_i(t) = z_{ci}(t)\left[\sum_{j=1}^{N} z_{cj}(t)\right]^{-1}$

Now we are faced with the problem of assigning values to the thresholds Γ_c and Γ_x. In section 3.5 it was concluded that putting thresholds on the grid node x processes of a simple outstar was inadvisable because this would result in eventual extinction of all memory. This was due to the fact that the z processes decayed exponentially at the rate u. It was quite possible for the z's to decay until the predictions input signal $\beta z_{ci}(t)\ [x_c(t - \ ) - \Gamma_c]^+$ to the grid nodes is unable to drive the grid node x process suprathreshold. In this situation the outstar could no longer "pump up" the z process because the correlating signal $v[x_c(t-\tau) - \Gamma_c]^+ [x_i(t) - \Gamma_x]^+$ would be zero. However, in the virtual laterally inhibiting outstar, we do not have this problem. The prediction signal amplification processes are the $y_i(t)$ which do not decay. Thus we may specify a non zero Γ_x in equation 6.4.3.

In fact, use of a grid node threshold is advantageous in a virtual laterally inhibiting outstar. Beside the interpretive advantage discussed in section 6.3, there is a real improvement of performance. Since the convention for interpreting the responses of a virtual laterally inhibiting outstar says that equal responses by all the nodes in the grid is a state of total ignorance, we have specified equal initial conditions on the $y_i(t)$'s. That is, $y_i(t) = (1/N)$ for all i. Now suppose that we have have a virtual laterally inhibiting outstar in a state of total ignorance. This means that we have not presented

an intelligible pattern of grid events with the command event. However it does not mean that the command event alone has not been presented to the outstar. In fact, until we decide to teach the outstar that the command event is associated with an intelligible pattern, we may excite the command node as many times as we like. Because the prediction signal so generated is being split up evenly between the grid nodes, the $y_i(t)$ will not deviate from a state indicative of total ignorance. However, the correlating signal $vx_c(t - \tau)x_i(t)$ will become positive on each such ignorant prediction and the $z_{ci}(t)$ will grow. We had great difficulty correcting a learned mistake in section 6.3 because the esperience with the erroneous pattern was great. If the outstar is allowed to accumulate experience with the ignorant pattern by spurious excitements of the command node, then it will be equally difficult to correct the ignorant pattern with an intelligible one.

Of course, increasing the forgetting rate should partially alleviate this problem. However, it would be better to prevent the outstar from accumulating experience with the ignorant pattern altogether. A properly selected grid node threshold Γ_x would achieve this result. In the state of initial ignorance, the amplitude of prediction signal inputs to the grid nodes is:

$$(\beta/N)x_c(t - \tau)$$

as $y_i(t) = 1/N$ for all i. Suppose β has been specified to result in a well learned response for an average of $M < N$ events to a pattern. Then the ignorant state input prediction signal is:

$$(bM)/(N)\, x_c(t - \tau)$$

where b is a constant which results in a well learned response from a grid node when $bx_c(t - \tau)$ is the prediction input signal. Now a well

learned prediction response is one in which the maximum amplitude of the response is equal to the maximum amplitude of a response elicited by an event input pulse alone. Knowing the shape, amplitude, and duration of the input pulses, the maximum amplitude of a well learned response can be analytically calculated. For the input pulses of this experiment, it is:

x = max amplitude of well learned response = $(A/\alpha)(1 - e^{-1}) =$

$0.63(A/\alpha)$

Thus the proper Γ_x to prevent accumulation of experience with the ignorant pattern may be analytically specified by:

Γ_x = max amplitude of prediction of the ignorant pattern response =

$(M/N)(0.63\ A/\alpha)$

Knowing that $M = 2.5$, $N = 5$, $A = 10$, $\alpha = 3.333$:

$\Gamma_x = 0.945$

Note that this Γ_x will work only for the input pulses specified. Outstars are capable of learning patterns independent of the vigor which with they are presented. They are also capable of learning patterns composed of events presented at different strengths. Of course, in a threshold outstar, there is a minimum pulse amplitude A which will result in superthreshold responses and thus learning. In this study it was decided to maintain the specifications on the input pulses constant because a large number of outstars are being studied. A detailed study of varying the input pulse specifications in each outstar requires a prohibitive amount of time. In an outstar functioning in an environment in which events occur with varied amplitudes, a statistically average well learned response could be used to specify a Γ_x sufficient to prevent accumulation of experience with the

ignorant pattern on the average. However, this is not a study that will be undertaken in this paper. In this study we are able to completely know ahead of time the exact specifications of our input pulses and are consequently able to specify the parameters of the outstars to result in the preformance we want.

Unfortunately, the above analytic method was not completely understood at the time the experiment being reported was performed. $\Gamma_x = 0.45$ was used and consequently the outstar was able to accumulate experience with the ignorant pattern. Rather than re-perform the experiment with the "correct" Γ_x, it was decided to present the data collected with the "wrong" Γ_x. It illustrates the problem of accumulating experience with the ignorant pattern. Additionally, examination of the data will reveal that there are other properties associated with any non zero Γ_x which are of more consequence than the property of preventing accumulation of experience with the ignorant pattern.

It was decided to specify the command node threshold, Γ_c, such that there would be no correlation with events presented with presentation phase φ greater than $\varphi = \delta = 0.3$ seconds. From previous experimental data, $\Gamma_c = 1.0$ will satisfy this criteria.

Addition of a non zero Γ_c made the analytical specification of β too difficult. Thus a β resulting in a well learned response for a pattern composed of $M = 2.5$ events was experimentally determined. The value so determined was:

$$\beta = 27.9$$

u was increased to test the conclusion that a faster forgetting rate would result in improved correctability. The interval between presentations and/or predictions is 1.8 seconds which is the same

as in previous experiments. Part of the reason for introducing the virtual laterally inhibiting outstar was to use the accumulation of experience with a small u to aide in resisting random mistakes by absorption. Therefore we will not make u so small as to completely destroy this effect. A decay time of twice the interval between successive predictions and/or presentations was selected:

$u = 0.278 \text{ sec.}^{-1} = 1/(2 \times 1.8 \text{ sec.})$

v was arbitrarily specified to be $v = 10$.

Since a pattern composed of $M = 2.5$ events is impossible, it was decided to teach the outstar a pattern composed of 3 events and then test its random mistake resistance. An additional event presented with presentation phase $\varphi = +2\delta = 0.6$ seconds was included with this pattern to illustrate the effect of the command node threshold. After this part of the experiment it was decided to attempt correction of the pattern with a pattern composed of $M = 2$ events. It was decided to make the correcting pattern to consist of an event not included in the original pattern and an event that was included in the original pattern. The reason for this selection of correcting events was to see if there is any difficulty in learning that only part of a previously learned pattern is in error.

Before beginning to teach the outstar an intelligible pattern, a prediction of the ignorant pattern was gotten by excitement of the command node alone. This was initially done to demonstrate that a properly selected Γ_x would prevent accumulation of experience with the ignorant pattern. Because of the error in specifying Γ_x, it serves as a demonstration that accumulation of experience with the ignorant pattern is a factor to be considered.

The foregoing discussion is summarized in the box below:

Equations governing performance of the outstar:

$$\dot{x}_c(t) = -\alpha x_c(t) + P_c(t)$$

$$\dot{x}_i(t) = -\alpha x_i(t) + \beta y_i(t)\left[x_c(t-\tau) - \Gamma_c\right]^+ + P_i(t)$$

$$\dot{z}_{ci}(t) = -u z_{ci}(t) + v\left[x_c(t-\tau) - \Gamma_c\right]^+ \left[x_i(t) - \Gamma_x\right]^+$$

$$y_i(t) = z_{ci}(t)\left[\sum_{j=1}^{N} z_{cj}(t)\right]^{-1}$$

where:

$$[y]^+ = \begin{cases} y \text{ for } y > 0 \\ 0 \text{ for } y \leq 0 \end{cases}$$

Input parameters:

pulse shape is rectangular

$A = 10$

$\delta = 0.3$ seconds

Network parameters:

$\alpha = 3.3333 \text{ sec.}^{-1} = 1/\delta$

$\beta = 27.9$

$\tau = 0.3$ seconds

$\Gamma_c = 1.0$

$\Gamma_x = 0.45$

$u = 0.278 \text{ sec.}^{-1} = 1/(2 \times 1.8 \text{ sec.})$

$v = 10$

Initial conditions:

$x_c(0) = 0$

$x_i(0) = 0$ for all i

$z_{ci}(0) = 0.1$ for all i

and: $y_i(0) = 0.2$ for all i

section 6.5 An Experiment with a Virtual Laterally Inhibiting Outstar with Thresholds and an Intermediate Forgetting Rate Designed to Learn Patterns of More than One Event

Figure 6.5.1 shows the first phase of the experiment described in the previous section. The first response on the five grid node x process traces is a prediction of the ignorant pattern elicited by excitement of the command node alone. The z trace for all five $z_{ci}(t)$ shows the experience accumulated by this prediction. Although increase in amplitude of the z processes due to this single prediction is small, many such predictions would result in an accumulation. Even this small accumulation of experience with the ignorant pattern affects the performance of the outstar when the pattern $V_c \rightarrow (V_1, V_2, V_3)$ is presented to the outstar as is shown by the $y_i(t)$ traces. One presentation of the pattern is insufficient to result in convergence of the $y_i(t)$ to values describing the pattern and a second presentation is required.

Even though the grid node threshold Γ_x is too small to prevent accumulation of experience with the ignorant pattern it does improve the learning performance of the outstar. Looking at the $x_5(t)$ trace it can be seen that the first presentation of the pattern resulted in a redistribution of the values for the $y_i(t)$. This redistribution was sufficient to prevent $x_5(t)$ from going suprathreshold long enough to add any appreciable amplitude to $z_{c5}(t)$ on the second presentation of the pattern. Due to the reasonably rapid forgetting rate u, $z_{c5}(t)$ continued its decay during the second presentation. With $y_5(t)$ so small that $x_5(t)$ can not be driven suprathreshold, future presentations

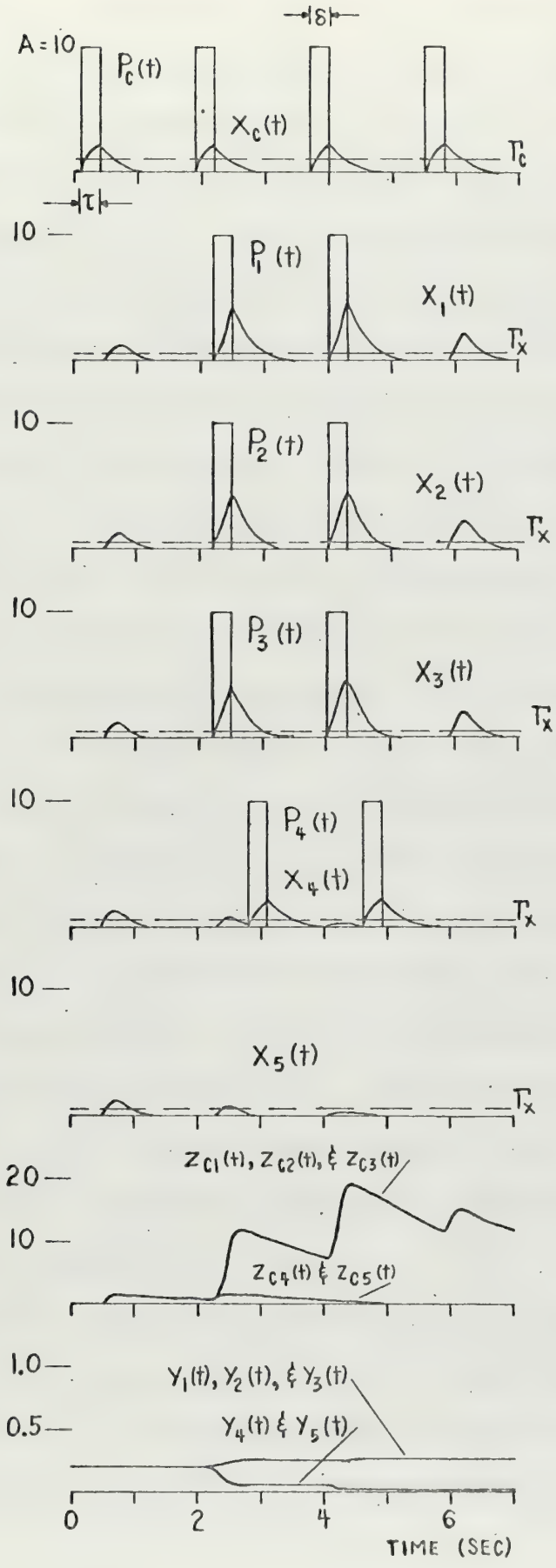

Figure 6.5.1. Result of teaching a virtual laterally inhibiting outstar with thresholds the pattern $V_c \rightarrow (V_1, V_2, V_3)$.

and/or predictions will result in no further increases in the amplitude of $z_{c5}(t)$. This would be of particular importance if in the first two presentations of the pattern $y_1(t)$, $y_2(t)$, and $y_3(t)$ had not converged so closely to the final values describing the pattern of $y_i(t) = 0.3333$ for $i = 1, 2, 3$. For, if the $y_i(t)$ were not so close to their final values, then the prediction of the learned pattern would have resulted in furthur convergence of the $y_i(t)$'s to this final value. The prediction of the learned pattern shown in the fourth response of the grid node x processes shows why. The prediction response for the nodes V_1, V_2, and V_3 included in the pattern are all suprathreshold and result in an increase in amplitude for the corresponding $z_{ci}(t)$'s. The prediction response for the nodes V_4 and V_5 not included in the pattern are subthreshold and therefore do not result in increases in the amplitudes of $z_{c4}(t)$ and $z_{c5}(t)$. Thus the $y_i(t)$ continue to converge during predictions. However, the $y_i(t)$ converged so close to their final values in the two presentations of the pattern shown, that this effect can not be seen in figure 6.5.1. A higher resolution look at the $y_i(t)$ showed that $y_1(t)$, $y_2(t)$, and $y_3(t)$ increased from 0.3096 to 0.3225 on this prediction. This phenomena is not in contradiction to the outstar theorem which guarantees only that the $y_i(t)$ will not diverge during a prediction. Convergence is therefore theoretically permissible and grid node thresholds result in convergence during predictions.

In figure 6.5.1, event 4 was presented $2\delta = 0.6$ seconds after events 1, 2, and 3 in the pattern. The command node threshold Γ_c was chosen to prevent any correlation with events presented more than $\delta = 0.3$ seconds after arrival of the prediction signal at the arrowheads.

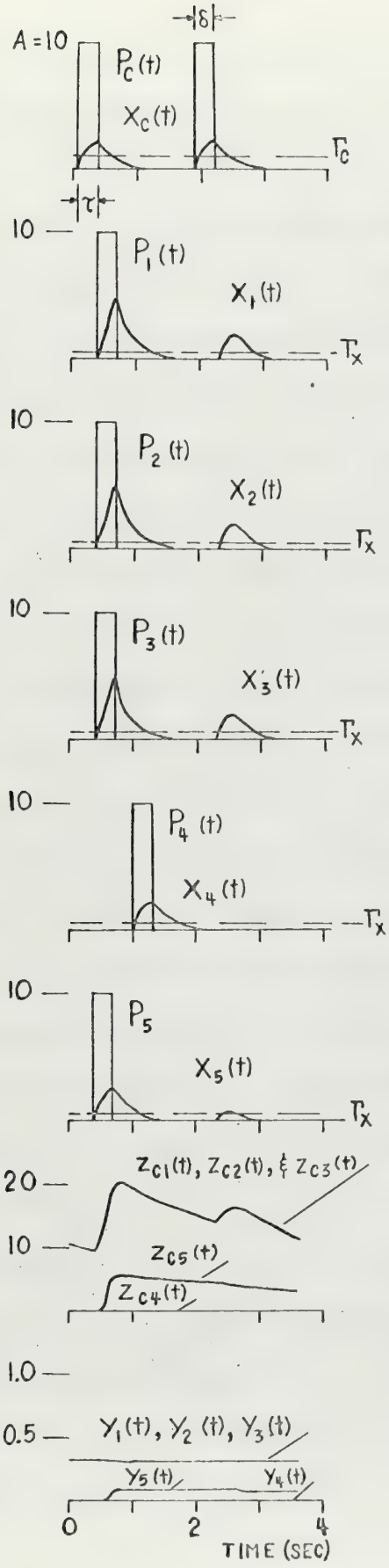

Figure 6.5.2. Results of presenting a random mistake in the previously learned pattern $V_c \rightarrow (V_1, V_2, V_3)$. Event 5 is the mistake. Note that $x_5(t)$ does not go suprathreshold on the following prediction response. Also note that $z_{c5}(t)$ does not grow and that $y_5(t)$ decreases.

The fact that $y_4(t)$ and $z_{c4}(t)$ are identical to $y_5(t)$ and $z_{c5}(t)$ shows that the command node threshold was successful. Presentation of event 4 resulted in a correlation equivalent to no presentation at all.

As can be seen, the β selected resulted in learned prediction responses for the three events in the pattern of approximately the same amplitudes as the response elicited by an input pulse alone. (Compare the maximum amplitudes of the prediction responses of $x_1(t)$, $x_2(t)$, and $x_3(t)$ with the maximum amplitude of $x_c(t)$.)

Figure 6.5.2 shows the continuation of the experiment. The pattern $V_c \rightarrow (V_1, V_2, V_3)$ is presented with a simulated random mistake. Event 5 is this mistake. As can be seen the presentation of the random mistake resulted in a healthy increase in $z_{c5}(t)$. However, this was insufficient to drive $y_5(t)$ large enough to result in a suprathreshold $x_5(t)$ on prediction. Therefore $z_{c5}(t)$ continues to decay on subsequent predictions and is bound for extinction. A slight decrease in $y_5(t)$ can be seen during the prediction response in figure 6.5.2. This is due to the prediction convergence phenomena described above. Thus we can conclude that more predictions will result in the $y_i(t)$ converging back to the values they had before the occurance of the random mistake.

Figure 6.5.3 shows the results of continuing the experiment. The previously learned pattern $V_c \rightarrow (V_1, V_2, V_3)$ is corrected by the pattern $V_c \rightarrow (V_1, V_4)$. The difficulty with this correcting pattern is that event 1 is included in both the original pattern and the correcting pattern. As can be seen, it only required four presentations of the correcting pattern to result in subthreshold $x_2(t)$ and $x_3(t)$ responses. V_2 and V_3 represent the events 2 and 3 which were part of the old

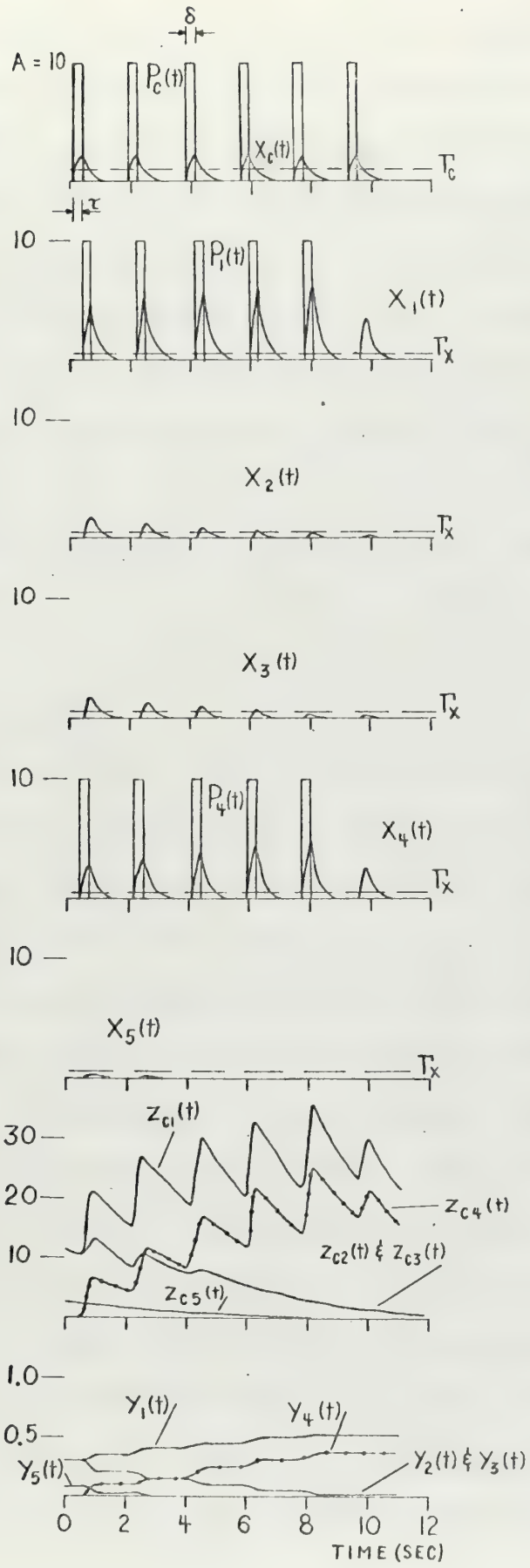

Figure 6.5.3. Correcting a previously learned mistake. The previously learned pattern is $V_c \rightarrow (V_1, V_2, V_3)$. The correcting pattern is $V_c \rightarrow (V_1, V_2)$.

pattern, but are not included in the new pattern. Additionally, $y_2(t)$ and $y_3(t)$ have decreased in these four presentations to the point where it can be safely concluded that the dominant pattern is $V_c \rightarrow (V_1, V_4)$. This situation should be compared to the unsuccessful attempt to correct a pattern by three presentations of the correcting pattern in the virtual laterally inhibiting outstar with a slow forgetting rate shown in figure 6.3.3. It can be concluded that increasing the forgetting rate does improve the correctability of a virtual laterally inhibiting outstar.

The final values for the $y_i(t)$'s to describe the correcting pattern are:

$$y_1(t) = y_4(t) = 0.5$$
$$y_2(t) = y_3(t) = y_5(t) = 0$$

As can be seen, $y_1(t)$ has slightly overshot its final value and $y_4(t)$ has only reached a value of $y_4(t) = 0.38$. However $y_1(t)$ and $y_4(t)$ are converging toward each other. We may conclude that the previously accumulated experience with event 1, which is common to both patterns, is great enough to make convergence to the new pattern difficult.

It should be noticed that the prediction responses of $x_1(t)$ and $x_4(t)$ at the end of the experiment are both of greater amplitude than a response to an input pulse alone. This is an effect of lateral inhibition. In the old pattern of $M = 3$ events, the prediction response amplitudes of grid nodes associated with the pattern was slightly less than the amplitude of a response to an input pulse alone. β had been specified to result in a well learned response for a pattern consisting on the average of $M = 2.5$ events. Thus the 3 event pattern results in smaller than well learned grid node responses and the 2 event pattern results

in larger than well learned grid node responses.

CHAPTER 7 OTHER FORMULATIONS FOR THE z PROCESS

section 7.1 Introduction

In the discussion of the laterally inhibiting outstar it was memtioned that the outstar was excitory biased. The equation for the z processes in the laterally inhibiting outstar was:

6.1.1 $\dot{z}_{ci}(t) = -uz_{ci}(t) + v[x_c(t-\tau)x_i(t)]^+$

where:

$$[y]^+ = \begin{cases} y \text{ if } y > 0 \\ 0 \text{ if } y \leq 0 \end{cases}$$

By excitory biasing, it was meant that the learning z processes could only assume non negative values. Thus the input prediction signal to a grid node, $\beta z_{ci}(t)x_c(t-\tau)$ is always non negative and can not drive the grid node's x process to negative amplitudes. In this way, the z processes are biased against learning to inhibit grid nodes and are biased in favor of learning to excite them.

In this chapter we shall drop the excitory biasing restriction and conduct an investigation to see if there is any value in outstars which can learn to inhibit grid nodes as well as excite them by prediction signals from the command node. One reason for conducting this study is that in the laterally inhibiting outstar we had to introduce a new element in the embedding field network elements. The inhibitory directed edges' arrowheads contained z processes which were assigned the permanent value of -1. These z processes did not learn their values as do the z processes in the other arrowheads in the network and we must consider a non learning z process to be a new feature. In the avalanche using a long axon and collaterals we avoided the use of z processes with permanent values of +1. If we solve the pulse lengthening problems of

the outstar avalanche, then we will have to use another new element. Development of a general formulation for z processes to cover all z processes would eliminate the need for making exceptions for special design feature in a network. We will attempt to formulate more general z processes in this chapter. Throughout, we shall be speaking of embedding field networks which do not have any virtual processes associated with them. The networks we shall discuss conform to the embedding field elements of chapter one.

section 7.2 A Description of the States of the Processes in an Outstar

A z process at an arrowhead correlates the prediction signals arriving at the arrowhead and the x process at the node upon which the arrowhead impinges; and it remembers what the correlations in the past have been. The z process can therefore be considered to be a function of the past and current states of the adjacent node and the prediction signals. The z process itself can be thought of as being in various states. For instance, we can think of a large amplitude z process as being in an excitory state as it allows largw prediction signals through to excite the adjacent node. Small amplitude z processes could be thought of as being in an unlearned or ignorant state.

In this chapter we shall use this idea that z processes are in states which may be completely determined by the past history of the states of the prediction signal and the grid node x processes. We shall develop a state function $\mathcal{L}(\bar{x}_c, \bar{x}_i)$ which maps the states of the prediction signal $\bar{x}_c$ and the grid node x process $\bar{x}_i$ into a z process state $\bar{z}_{ci}$:

$$\mathcal{L}(\bar{x}_c, \bar{x}_i) = \bar{z}_{ci}$$

It will be found that this function $\mathcal{L}$ is a handy way to describe the logic behind the learning process in an outstar and for this reason we shall call the state function $\mathcal{L}$ a "logic". However, before the usefulness of such a "logic" can be demonstrated, we must build up a description of the states of the various processes in an outstar.

In outstars without virtual processes, we are concerned with four processes:

1. Inputs, $P_c(t)$ and $P_i(t)$

2. Node x processes, $x_c(t)$ and $x_i(t)$

3. The prediction signal from the command node, $[x_c(t - \tau) - \Gamma_c]^+$

   where Γ_c may be zero

4. The z processes, $z_{ci}(t)$

Input pulses, $P_c(t)$ and $P_i(t)$ have been used to indicate the occurance of events in the environment. There are two possible states for an event. Either it is occuring, or it is not. We have transmitted information about whether an event is occuring or not to the outstar by the input pulse. A positive amplitude has been used to signify that an event is occuring. A zero amplitude has been used to signify that an event is not occuring. The following code can therefore describe the state of inputs and the state of the events they describe:

(a) $\bar{P} = +1$ indicates that an event is occuring and that the associated input has a positive amplitude.

(b) $\bar{P} = 0$ indicates that an event is not occuring and that the associated input has a zero amplitude.

Node x processes have been used to signify the recent presentation of an event and/or a recent prediction of an event. A large positive amplitude has been interpreted as indicating that the outstar "thinks" that the event represented by the node in question has occured recently or at least, should have occured recently. Small positive amplitudes, or zero amplitudes have been interpreted as indicating that the outstar is not "thinking" anything about the event represented by a node. Negative amplitudes have been interpreted as indicating the same state as small or zero amplitudes.

By placing thresholds on the nodes, we were able to precisely determine when an x process was of large enough positive amplitude to indicate that the outstar is "thinking" an event. With thresholds we may replace the word "large" in the preceding paragraph with the word "suprathreshold". In the same manner "small", "zero", and "negative" may be replaced with "subthreshold".

Thus we have two states for a node x process:

(1) $\bar{x}_i = 1$ indicates a state where the x process at a node is of sufficiently large positive amplitude, or is suprathreshold. This state corresponds to the interpretation that the outstar is "thinking" about the event represented by the node.

(2) $\bar{x}_i = 0$ indicates a state where the x process at a node is of small or zero positive amplitude, or is subthreshold. This state corresponds to the interpretation that the outstar is not "thinking" about the event represented by the node.

Although the notion "thinking" about corresponds to the psychological interpretation of x processes' amplitudes, it is clumsy. In the outstar, the only way an x process can get into the state $\bar{x}_i = 1$ is to respond to an input. That is, it must respond to excitement by an input pulse or an input prediction signal, or both. Thus we could describe the state $\bar{x}_i = 1$ as "responding" or "excited". To avoid semantic difficulties, the state $\bar{x}_i = 1$ will be called the "excited" state.

For semantic reasons also, the state $\bar{x}_i = 0$ will not be called "not thinking" about. Although "not excited" would apply well to $\bar{x}_i = 0$, it will not be used either. Instead the state $\bar{x}_i = 0$ will be called "ambient". "Ambient" is used because it refers to a state

which is the usual state of an x process. The ambient state $\bar{x}_i = 0$ is also the passive state to which an x process always returns. Further, it is the state of an x process when it is not being actively driven by signals from outside the node. Thus it was felt that "ambient" accurately describes the state $\bar{x}_i = 0$.

In the above listing of states for x processes, an x process responding with a negative amplitude was not included. Although we have followed the convention of interpreting negative amplitudes as being the same as ambient amplitudes, the inhibitory process that results in negative amplitudes is not an ambient process. A negative amplitude can be achieved only if the x process is being actively driven in the negative direction by signals from outside the node. It is therefore definitely not "ambient". There is no reason why our description of the states of x processes should have to conform with our interpretation of what those states mean. We will refer to an x process of negative amplitude as being in the inhibited state and indicate this state by $\bar{x}_i = -1$. We will continue to interpret the state $\bar{x}_i = -1$ as indicating the same interpretive state as $\bar{x}_i = 0$.

The difficulty with the inhibited state is that it is a subjective state within the outstar. In the environment the state of an event can be described as actively occuring or passively not occuring. There is no such thing as an event that actively does not occur. However, we saw that a practical simple outstar with only the two x process states of being excited or being ambient had very little resistance to random mistakes. We added lateral inhibition to allow the outstar an active process whereby it could subjectively prevent events from occuring. Particularly, lateral inhibition was added to subjectively prevent

random mistakes from occuring in a previously learned pattern. Suppose we had a black box that was claimed to be a learning machine. The only way we could determine if it was a learning machine is to teach it something and then see if it could reproduce what we taught it. We would only be able to observe the events we were teaching it and the box's response. Now, the box's response would be events to us. Thus from our point of view the only states the box could communicate to us would be the state of a response occuring or the state of a response not occuring. The state of a response somehow being able to not occur with greater vigor than simply not occuring is meaningless. Thus, our interpretation of what an outstar is doing is limited to what we could observe if the outstar were a black box.

We have used this interpretive convention and will continue to do so. However, an outstar is not a black box to us. We can observe all the processes occuring inside it. Thus we are confronted with the inhibited x process state which we can observe inside the outstar, but which is meaningless when observed outside the outstar. Inside the outstar the inhibited state is meaningful and definitely corresponds to something other than ambient. Thus we have assigned a separate state to describe the state of an x process which is being actively driven to negative amplitudes by signals from outside the node.

There is some difficulty in saying when an x process is in the inhibited state in an outstar with thresholds. An x process can be actively driven subthreshold by inhibitory processes and still have a non negative amplitude. For simplicity this situation will be considered to be ambient. The inhibitory state is therefore only the state in which an x process has a negative amplitude. In case of

a negative amplitude, there is no confusion about the x process at a node being actively driven toward negative values by signals from outside the node.

In summary, the states of an x process at a node are:

(1) The excited state, $\bar{x}_i = +1$. The amplitude of the x process is large or suprathreshold.

(2) The ambient state, $\bar{x}_i = 0$. The amplitude of the x process is small, zero, or subthreshold.

(3) The inhibited state, $\bar{x}_i = -1$. The amplitude of the x process is negative.

A prediction signal at an arrowhead is the originating node's method of influencing the other nodes in the network. In order to define our logic $\mathcal{L}(\bar{x}_c, \bar{x}_i)$, we will have to assign states to prediction signals at an arrowhead. We could assign the same states to prediction signals as we have assigned to x processes. This would mean that the prediction signal is conveying the state of its originating node to the arrowhead. However, prediction signals do more than convey the state of the originating node to the arrowheads. They also influence the state of the x process at the node upon which the arrowhead impinges. There is no difficulty in allowing a prediction signal to have a large or suprathreshold amplitude and describing this state as the excited state with state value $\bar{x}_c = +1$. However, the other states we may allow a prediction signal to be in require some discussion.

First, consider the case of a prediction signal coming from a node with a threshold on it. In the past we have used both "real" thresholds and "imaginary" thresholds. The imaginary thresholds were placed on a node for precision in interpreting when the node was

responding. The 'real' thresholds were placed on a node to prevent the z processes from learning spurious associations when the x process was of small amplitude. In the case of the command node, thresholds were used to prevent the command prediction signal from causing spurious associations from being learned when it was of small amplitude. This was accomplished by restricting the command prediction signal to be zero until it was suprathreshold, i.e. $[x_c(t-\tau) - \Gamma_c]^+$. In this case, we also prevented thr prediction signal from influencing the state of the grid node upon which it was impinging until it was suprathreshold. This was accomplished by making the input prediction signal to the grid node to be $\beta z_{ci}(t)\,[x_c(t-\tau) - \Gamma_c]^+$.

There is a reason behind this. Suppose we have an outstar grid which is shared by many command nodes representing separate and distinct command events. In the environment, a distinct pattern of grid events usually occurs with each of the command events. If the outstar is to function properly, it must be able to learn that a certain command event, c_1, is associated only with the pattern, $\vec{\theta}_1$, which occurs with it in the environment. It must be prevented from learning that the patterns occuring with the other command nodes in the environment are associated with c_1.

A subthreshold command node x process only occurs when the command event has not occured recently in the environment. Thus we can expect that a pattern not corresponding to this command event is on the grid when the command node is subthreshold. By making the prediction signal coming from a subthreshold command x process identically zero, we prevent the outstar from building up a wrong association. Additionally, by making the prediction signal identically zero, we prevent it from

exciting the grid nodes which are included in the pattern associated with this particular command node. This is important. Consider two command nodes V_{c1} and V_{c2} which represent events c_1 and c_2 which occur in the environment with patterns $\vec{\theta}_1$ and $\vec{\theta}_2$ respectively. Suppose $x_{c1}(t)$ is subthreshold and $x_{c2}(t)$ is suprathreshold. Then we can expect that the grid node x processes indicate that the pattern $\vec{\theta}_2$ is on the grid. We have already agreed to make the prediction signal $[x_{c1}(t-\tau) - \Gamma_c]^+$ identically zero to prevent $V_{c1} \rightarrow \vec{\theta}_2$ from being learned. Suppose however that we allow the prediction input signal from V_{c1} to the grid nodes representing $\vec{\theta}_1$ to become excited. The pattern on the grid would therefore be the algebraic sum $\vec{\theta}_1 + \vec{\theta}_2$. The prediction signal coming from the suprathreshold node V_{c2} will therefore cause the association $V_{c2} \rightarrow \vec{\theta}_1 + \vec{\theta}_2$ to be learned. To prevent this possibility we have made the prediction signal input from a subthreshold command node identically zero.

Thus the prediction signal from a subthreshold command node is identically zero. We may as well drop the fiction of assuming that a prediction signal was sent from the command node in the first place and say that a prediction signal is sent out along the directed edges only if the x process at the originating node is suprathreshold.

We also used "real" thresholds interpretively. We now have the case that a subthreshold x process at a node is interpreted as no response. Further, it is unable to influence other nodes in the network because no prediction signal is sent from this node. Thus a certain amount of consistency is added to our interpretation of the amplitudes of the x processes. An x process which indicates no response also has no effect on the other nodes and processes in the network. If we were unable

to measure the amplitude of an x process at its node, we would have no way of knowing what amplitude it had as long as it was subthreshold. From the point of view of an external observer or any of the other processes in the outstar, a subthreshold x process is indeed ambient.

Thus we have an "ambient" state for prediction signals at an arrowhead. It is indicated by a zero amplitude and is assigned the state value $\bar{x}_c = 0$. It must be remembered that this state arises from an originating node that was subthreshold τ time units before.

In the case of an outstar without thresholds, we lose the precision in defining when a prediction signal is ambient. We will therefore describe a small amplitude on a prediction signal to be ambient. As previously, "small" will mean small relative to the maximum amplitude of a well learned response.

Having made the prediction signal coming from a subthreshold x process identically zero, it would be silly to allow prediction signals coming from an inhibited x process to be non zero. In this study we will not consider prediction signals of negative amplitude. Part of the reason is that allowing an inhibited x process to send out prediction signals would violate the consistency we have just developed. An x process state which is interpreted as no response should not be able to influence the other processes and nodes in the network. Another reason is that prediction signals of negative amplitude are not required. We have seen that the negative amplitude of inhibitory input prediction signals in lateral inhibition can be accounted for by allowing z processes with negative values. In fact, lateral inhibition has been the only case in which we have used inhibition. The whole function of lateral inhibition was for an excited grid node x

process to inhibit the other nodes in the grid. Thus the emission of inhibitory prediction signals from a node was only useful when that node was in the excited state.

In summary, the states of a prediction signal at an arrowhead are:

(1) The excited state, $\overline{x}_c = +1$. The amplitude of the prediction signal at the arrowhead is large and positive. This results from a large or suprathreshold x process at the originating node τ time units previously.

(2) The ambient state, $\overline{x}_c = 0$. The amplitude of the prediction signal at the arrowhead is small or zero. This results from a small, zero, subthreshold, or negative x process at the originating node τ time units previously.

We will assign the following states to a z process based upon its amplitude:

(1) The excitory state, $\overline{z}_{ci} = +1$. A z process is in this state when its amplitude is large and positive.

(2) The ambient state, $\overline{z}_{ci} = 0$. A z process is in this state when its amplitude is small or zero.

(3) The inhibitory state, $\overline{z}_{ci} = -1$. A z process is in this state when its amplitude is negative.

The states for z processes at an arrowhead were assigned according to what effect a prediction signal modified by the z process would have on the node upon which the arrowhead impinged. Clearly, a z process with a large positive amplitude would result in prediction excitement of the impinged upon node. A z process with a negative amplitude would result in prediction inhibition of the node. A z

process with a small or zero amplitude would result in very little disturbance of the impinged upon node. The ambient state for a z process is also the passive state for a z process. With a non zero forgetting rate, it is the state to which a z process passively returns, and it is the state which a z process assumes when it has not been perturbed by signals from outside the arrowhead.

Up to now, the only way a z process could assume the inhibitory state z_- was by permanent assignment of a negative value to the z process. In what follows, we will consider new formulations for the equations for a z process that will allow a z process to learn to assume the inhibitory state.

section 7.3 Logics

Having described the states of the various processes in an outstar, we are now ready to introduce the function $\mathcal{L}(\bar{x}_c, \bar{x}_i) = \bar{z}_{ci}$. $\mathcal{L}$ describes how the state of a z process at an arrowhead is determined from the states of the prediction signal at the arrowhead and x process at the adjacent node. Throughout this discussion the state of a prediction signal will be denoted by $\bar{x}_c$. The state of the adjacent x process will be denoted by $\bar{x}_i$, and the state of the z process will be denoted by $\bar{z}_{ci}$. The choice for the subscripts was motivated by the geometry of an outstar, but the discussion is not limited to outstars. It applies to all networks which may be built from embedding field elements. Throughout, the function $\mathcal{L}$ will be called a "logic". We will introduce several distinct logics and they will be distinguished by subscripts, i.e. $\mathcal{L}_i$.

A logic is a tabular function. That is, we tabulate all the possible combinations of prediction signal states and x processes states and assign a z process state to this combination. For example, the logic $\mathcal{L}_0$, for the excitory biased outstars we dealt with previously is defined by:

Definition of the Excitory Biased Logic, $\mathcal{L}_0$

$\bar{x}_c$	$\bar{x}_i$	$\mathcal{L}_0(\bar{x}_c, \bar{x}_i) = \bar{z}_{ci}$
0	0	0
+1	0	0
0	+1	0
+1	+1	+1
0	-1	0
+1	-1	0

(The inhibitory prediction signal state $\bar{x}_c = -1$ has been excluded from consideration for reasons of consistency as explained in section 7.2)

The reasons for calling this an excitory logic are clear. The only states allowed for the z process are the ambient state $\bar{z}_{ci} = 0$, and the excitory state $\bar{z}_{ci} = +1$. The ambient state is passive. The z process does not actively learn to be in the ambient state. Therefore the only state which the z process can actively learn is the excitory state. Thus the z process is biased to learn only the excitory state.

The excitory biased logic, $\mathcal{L}_0$, is implemented in an outstar by the equation:

7.3.1 $$\dot{z}_{ci}(t) = -uz_{ci}(t) + v\,[x_c(t-\tau) - \Gamma_c]^+\,[x_i(t) - \Gamma_x]^+$$

where either or both thresholds can be zero.

The driving functions in equation 7.3.1 is:

$$v\,[x_c(t-\tau) - \Gamma_c]^+\,[x_i(t) - \Gamma_x]^+$$

This function is always non negative. It can actively drive the z process only when the prediction signal and the adjacent x process are both in the excited state. Additionally, because the driving function is always non negative, it can only drive the z process in the direction of increasing positive amplitudes. Thus our tabular definition of $\mathcal{L}_0$ conveniently summarizes the effects of equation 7.3.1 on the outstar.

Note that $\mathcal{L}_0$ only describes the immediate effect of the states of the prediction signal and the adjacent x process on the z process. It does not describe the current state of a z process based on the entire past history of the prediction signal and x process states. That is, $\mathcal{L}_0$ only tell us in which direction the z process will be driven by the signals at a given time.

We shall now consider other logics for z processes. A general approach would be to consider all the possible assignments of $\bar{z}_{ci}$ states to each of the six distinct combinations of $\bar{x}_c$ and $\bar{x}_i$ states.

However, this results in 3^6 logics. We will therefore have to use some judgement in selecting the logics to be considered.

A key tenet of embedding field theory is that an excited prediction signal and an excited x process should result in an excitory z process. Thus we will only consider logics in which:

$$\mathcal{L}_i(\bar{x}_c = +1, \bar{x}_i = +1) = +1$$

Also, we have always started experiments which the z processes in the ambient state. That is, the initial conditions on the z processes have always been small or zero. We have interpreted those initial conditions as a state of initial ignorance. It would be senseless to allow a learning machine to develop from initial ignorance to learning something by itself. For this reason we will only consider logics in which:

$$\mathcal{L}_i(\bar{x}_c = 0, \bar{x}_i = 0)$$

This reduces the possible logics to $3^4 = 81$. There are no overriding reasons for excluding broad categories of the remaining logics. However, 81 logics is just too many to consider. We will only consider those which show promise in this study. These logics are defined in the table below:

Table 7.3.1

		$\mathcal{L}_0$	$\mathcal{L}_1$	$\mathcal{L}_2$	$\mathcal{L}_3$
$\bar{x}_c$	$\bar{x}_i$	$\bar{z}_{ci}$	$\bar{z}_{ci}$	$\bar{z}_{ci}$	$\bar{z}_{ci}$
0	0	0	0	0	0
+1	0	0	0	-1	-1
0	+1	0	0	-1	0
+1	+1	+1	+1	+1	+1
0	-1	0	0	-1	0
+1	-1	0	-1	-1	-1

$\mathcal{L}_0$ is the excitory biased logic we have considered previously. $\mathcal{L}_1$ is the logic resulting from removing the non negative restriction on the driving function in equation 7.3.1:

7.3.2 $$\dot{z}_{ci}(t) = -uz_{ci}(t) + vx_c(t - \tau)x_i(t)$$

As the tabulation of $\mathcal{L}_1$ shows, if $x_i(t)$ is negative, $z_{ci}(t)$ will learn inhibition. $\mathcal{L}_1$ can be considered a neutrally biased logic because the z process is not biased in favor of excitation or inhibition.

$\mathcal{L}_1$ is interesting, but of dubious value. Suppose that all the z processes in a network are in the ambient state at the beginning of an experiment. That is, the network is in a state of initial ignorance at the beginning of an experiment. Then a z process in this network can not possibly assume the inhibitory state. The reason is that the only states for input pulses are $\bar{P} = +1$ and $\bar{P} = 0$. The input pulses can only drive x processes in the network can assume are $\bar{x}_i = +1$ and $\bar{x}_i = 0$ due to input pulses. Therefore the prediction signals in the net work can only assume states $\bar{x}_c = +1$ and $\bar{x}_c = 0$. The combination of states $\bar{x}_c = +1$, $\bar{x}_i = -1$ can not occur. By the tabulation of $\mathcal{L}_1$, the state $\bar{z}_{ci} = -1$ can not be attained.

Thus the logic $\mathcal{L}_1$ is effectively equal to the logic $\mathcal{L}_0$. If we allowed the permanent assignment of negative values to z processes in a network governed by $\mathcal{L}_1$, then it is possible for the learning z processes in the network to learn inhibition. However, this requires the artificiality of a z process with a permanently assigned value.

$\mathcal{L}_3$ defined in table 7.3.1 is particularly interesting in an outstar. As can be seen from the tabulation, z processes in a network governed by $\mathcal{L}_3$ can learn inhibition from a state of initial ignorance without the use of z processes with permanently assigned negative

values. The two assignments:

$$\mathcal{L}_3(\bar{x}_c = +1, \bar{x}_i = 0) = -1$$
$$\mathcal{L}_3(\bar{x}_c = +1, \bar{x}_i = -1) = -1$$

insure this. In an outstar, these assignments mean that a command node can learn to inhibit grid nodes which do not correspond to events in the pattern associated with the command event. Consider a command event c which usually occurs with the pattern $\vec{\theta}$ in the environment. Let the grid events $\{i_c\}$ be the events which compose this pattern. Let the grid events $\{j_0\}$ be the remaining events represented by grid nodes. Then the assignment:

$$\mathcal{L}_3(\bar{x}_c = +1, \bar{x}_i = +1) = +1$$

means that the z processes $z_{ci_c}(t)$ associated with the grid nodes included in the pattern will learn excitation. The assignment:

$$\mathcal{L}_3(\bar{x}_c = +1, \bar{x}_i = 0) = -1$$

means that the z processes $z_{cj_0}(t)$ associated with the grid nodes not in the pattern will learn inhibition. Further, the assignment:

$$\mathcal{L}_3(\bar{x}_c = +1, \bar{x}_i = -1) = -1$$

insures that once these z processes have learned inhibition, they will continue to do so. The result is that after having learned the pattern, presentation of the command event alone will result in the grid nodes included in the pattern being excited. The grid nodes not included in the pattern will be inhibited. If a random mistake occurs in the pattern, the learned inhibition will cause it to be supressed.

We will consider an outstar governed by $\mathcal{L}_3$ in detail in the next chapter. The rest of this chapter will be devoted to an outstar governed by $\mathcal{L}_2$.

section 7.4 Formulation of the z Process Conforming to Logic $\mathcal{L}_2$

The logic $\mathcal{L}_2$ is defined by the tabulation:

Table 7.4.1

$\bar{x}_c$	$\bar{x}_i$	$\mathcal{L}_2(\bar{x}_c, \bar{x}_i) = \bar{z}_{ci}$
0	0	0
+1	0	-1
0	+1	-1
+1	+1	+1
0	-1	-1
+1	-1	-1

In this section we shall develop a formulation for a z process that will conform to this tabulation. However, we might inquire beforehand if this is a worthwhile endeavor. The large number of inhibiting assignments makes $\mathcal{L}_2$ appear somewhat useless. In the discussion of $\mathcal{L}_3$ in the previous section we saw that the following assignments in table 7.4.1 are useful:

$\bar{x}_c$	$\bar{x}_i$	$\mathcal{L}(\bar{x}_c, \bar{x}_i) = \bar{z}_{ci}$
0	0	0
+1	0	-1
+1	+1	+1
+1	-1	-1

We only have to establish the possible usefulness of the other two assignments:

7.4.1 $\mathcal{L}_2(\bar{x}_c = 0, \bar{x}_i = +1) = -1$

7.4.2 $\mathcal{L}_2(\bar{x}_c = 0, \bar{x}_i = 0) = -1$

Assignment 7.4.1 above says that a z process will learn inhibition if a grid node is excited and the prediction signal is not. This combination can only occur if a pattern not corresponding to the command event is on the grid. Thus learning to inhibit this pattern by prediction when the command event is presented is useful. Assignment 7.4.2,

however, can get us into trouble. Suppose there are two command nodes V_{c1} and V_{c2} sharing the same grid. Let the command events c_1 and c_2 represented by these nodes usually occur with the distinct patterns $\vec{\theta}_1$ and $\vec{\theta}_2$ respectively. Let the event represented by grid node i_1 be an event which is included in pattern $\vec{\theta}_1$ but not included in pattern $\vec{\theta}_2$. Then we can expect that excitement of V_{c2} will result in the x processes of the grid nodes assuming the values describing $\vec{\theta}_2$. Additionally, because of assignment 7.4.1, node i_1 will be inhibited. Therefore assignment 7.4.2 will result in $z_{c_1 i_1}(t)$ learning inhibitions. If this is learned sufficiently well, subsequent excitement of V_{c1} will result in grid node i_1 being inhibited even though it is part of the pattern $\vec{\theta}_1$ associated with c_1.

This vividly illustrates some of the problems we can get into with logic $\mathcal{L}_2$. It is not the only one. If it happens that the command node or the grid nodes in an outstar are randomly excited for some time then $\mathcal{L}_2$ will cause all the z processes in the outstar to learn inhibition. When we get around to teaching the outstar the pattern associated with the command event, we will have to overcome this initial inhibitory biasing. In a real environment, this will probably be the case. Our outstar will be "born" with all of its z processes in the ambient state. It will then spend a period of time in the environment before "going to school". In this period the random occurance of the command event and grid events is highly unlikely. Therefore, when the outstar "goes to school" all of its z processes will probably be inhibitory biased.

In order to prevent this inhibitory biasing from destroying the outstar's ability to learn when it goes to school, we will limit its effect. That is, we will limit the maximum negative amplitude

of a z process to a value that will insure that positive associations can not be completely inhibited. This rather vague statement will become clearer as we progress in the study of an outstar governed by $\mathcal{L}_2$.

A formulation for the z processes in an outstar that conforms to $\mathcal{L}_2$ is:

7.4.1 $$\dot{z}_{ci}(t) = -uz_{ci}(t) + v\left(a(x_2(t-\tau) + x_i(t))^2 - b(x_c(t-\tau) - x_i(t))^2\right)$$

with $b > a$; $a > 0$

Expanding the right hand side of equation 7.4.1 we get:

7.4.2 $$\dot{z}_{ci}(t) = -uz_{ci}(t) + v\left(-(b-a)x_c^2(t-\tau) - (b-a)x_i^2(t) + 2(a+b)x_c(t-\tau)\,x_i(t)\right)$$

with $b > a$; $a > 0$

From equation 7.4.2 it can be seen that this formulation conforms to $\mathcal{L}_2$.

It is interesting exactly how this formulation came about. In the progress of the experimental study for this thesis report, the author began thinking of simulating an outstar on an analogue computer. At that time the idea of logics had not been thought of. The author was interested only in simulating an excitory biased outstar on an analogue computer. To do this the z process driving function:

$$vx_c(t-\tau)x_i(t)$$

had to be simulated. The product of two varying signals is implemented on an analogue computer by means of square law devices. For example, the product xy is implemented by forming the sums:

$$x + y \quad \text{and} \quad x - y.$$

These sums are then scaled by constant factors a and b. Each sum is sent through a separate square law device and then the difference is

formed:

$$a(x + y)^2 - b(x - y)^2$$

expanded, this is:

$$(a - b)x^2 + (a - b)y^2 + 2(a + b)xy$$

Thus, by selecting the scaled factors a and b such that:

$$a = b$$

the result of this process is:

$$2(a + b)xy$$

Scaling this by 1/(2(a +b)) results in the desired product.

It was recognized that an outstar so simulated with $a \neq b$ would have some of the desirable properties of $\mathcal{L}_2$. A digital simulation of an outstar with the formulation 7.4.1 for the z processes was run. The results were confusing and in an attempt to clearly define the properties of this outstar the idea of logics and processes' states was conceived. Having developed this concept, it was realized that it was a handy description of the possibilities for formulating other z processes. Additionally, it was a convenient method of predicting what an outstar with various z process formulations would do.

The z process formulation given in equations 7.4.1 or 7.4.2 has some interesting properties other than those described by the tabulation of $\mathcal{L}_2$. The z process driving function in equation 7.4.1 is:

$$D(t) = v\left(a(x_c(t - \tau) + x_i(t))^2 - b(x_c(t - \tau) - x_i(t))^2\right)$$

This is composed of two competing processes. The process driving the z process in the direction of an excited state is $a(x_c(t - \tau) + x_i(t))^2$. Competing with it is the process $-b(x_c(t - \tau) - x_i(t))^2$ which drives the z process in the direction of an inhibited state.

Of particular concern to us is the point where these competing driving functions exactly balance one another. This point is achieved when:

$$a(x_c(t-\tau) + x_i(t))^2 = b(x_c(t-\tau) - x_i(t))^2$$

Let μ be the ratio of the amplitude of a prediction signal at an arrowhead and the adjacent node x process, i.e.:

$$\mu = \frac{x_i(t)}{x_c(t-\tau)}$$

then:

$$\left(\frac{\mu x_i + x_i}{\mu x_i - x_i}\right)^2 = b/a$$

or:

$$\left(\frac{\mu + 1}{\mu - 1}\right)^2 = b/a$$

since $b/a > 1 > 0$:

$$\frac{\mu + 1}{\mu - 1} = \pm\sqrt{b/a}$$ which is a real value.

Using the positive square root, we get:

$$\mu = \frac{\sqrt{b/a} + 1}{\sqrt{b/a} - 1} = \mu_0^+ > 1$$

Using the negative square root, we get the inverse:

$$\mu = \frac{\sqrt{b/a} - 1}{\sqrt{b/a} + 1} = \mu_0^-$$

Note that:

$$0 < \mu_0^- < 1$$

This calculation shows us that there are two ratios, μ_0^+ and μ_0^- where the competing driving functions are balanced. Note that $\mu_0^+ = 1/\mu_0^-$ which is as it should be from the definition of μ. For a ratio between the prediction signal and the x process of μ where falls in the range:

$$\mu_0^- < \mu < \mu_0^+$$

the total driving function D(t) is positive. Thus the z process is being driven in the excitory direction. Note that the bounds μ_0^- and μ_0^+ of this region are both positive. Since we do not allow negative prediction signals, this means that D(t) is positive only when both $x_c(t-\tau)$ and $x_i(t)$ are positive in conformity with $\mathcal{L}_2$. Outside the region $\mu_0^- < \mu < \mu_0^+$, D(t) is negative and the z process is being driven in the inhibitory direction.

The ratios μ_0^+ and its reciprocal μ_0^- are called the cross over ratios for obvious reasons. By specifying a and b to result in a particular cross over ratio, we can specify a sort of "floating" threshold on the z process. The thresholds we have considered previously have all been "fixed". That is, the amplitude of the process they were thresholding was compared to their fixed value. If it was greater than this fixed value we got a different result than when it was less. The floating threshold in the z process under consideration is a function of the ratio of the amplitudes of the prediction signals and the x process. If this ratio falls in a certain range we get one result and if the ratio falls outside this range we get another. The range is completely determined by the constants a and b.

One further analytic property of D(t) is that it is a convex function of the ratio μ. It therefore has a maximum with respect

to μ which we compute:

$$\frac{\partial D(t)}{\partial \mu} = -2\mu(b - a) - 2(a + b) = 0$$

or the maximum of D(t) with respect to μ occurs at:

$$\mu_{max} = \frac{a + b}{a - b}$$

note that $\mu_0^- < \mu_{max} < \mu_0^+$.

This says that the maximum "force" driving a z process in the excitory direction occurs when the prediction signal and the x process are in the ratio, μ_{max}, to one another. There is no minimum to D(t). Thus the driving function D(t) seems to be biased in favor of driving the z process in the inhibitory direction. To compensate for this and to cover the initial inhibitory biasing of this z process, we will artificially bound D(t) on the negative side. That is, we will use a driving function $D'(t)$ defined by:

$$D'(t) = \delta_1(M_z + z_{ci}(t))\, D(t)$$

where $M_z > 0$

and where:

$$\delta_1(y) = \begin{cases} 1 \text{ if } y \geq 0 \\ 0 \text{ if } y < 0 \end{cases}$$

By the proper selection of M_z, $z_{ci}(t)$ will be prevented from assuming large negative values that would totally inhibit the learning of excitory associations.

section 7.5 Specification of the Parameters in an Outstar Conforming to Logic $\mathcal{L}_2$

By incorporating the equation for a z process developed in the previous section, we get the equations governing an outstar conforming to logic $\mathcal{L}_2$:

7.5.1 $\dot{x}_c(t) = -\alpha x_c(t) + P_c(t)$

7.5.2 $\dot{x}_i(t) = -\alpha x_i(t) + P_i(t) + \beta z_{ci}(t)x_c(t-\tau)$

7.5.3 $\dot{z}_{ci}(t) = -uz_{ci}(t) + v\delta_{-1}(M_z + z_{ci}(t))\left(a(x_c(t-\tau) + x_i(t))^2 - b(x_c(t-\tau) - x_i(t))^2 \right)$

With this formulation, the z processes in the arrowheads of the directed edges from the command node can learn inhibition. If they do, then the excitement of the command node will result in direct inhibition of the grid nodes. For this reason, the outstar governed by equations 7.5 will be called a directly inhibiting outstar. We will run the same experiment that we have used on other outstars. Therefore the parameters of the directly inhibiting outstar are specified to be the same as in the other outstars except where there are special considerations to be made:

Input parameters:

The input shape is rectangular

$A = 10$

$\delta = 0.3$ seconds

Network parameters:

$\alpha = 3.3333$ seconds^{-1}

$\beta = 1$

$\tau = 0.3$ seconds

Network parameters continued:

$N = 3$

Initial condition on all variables is zero.

The presentation rate for presentations and/or predictions will be 1.8 seconds. u will be specified such that the decay time 1/u for the z processes will be twice the presentation rate:

$u = 0.278$ sec. $= 1/((2)(1.8 \text{ sec.}))$

To specify a and b we must select the cross over ratio $\mu_0^+ = 1/\mu_0^-$.

$\mu_0^+ = \dfrac{x_i(t)}{x_c(t - \tau)}$ is the ratio between those functions at which the competing driving functions in the z process balance. A cross over ratio of $\mu_0^+ = 11.5$ was selected arbitrarily. Thus:

$b/a = \left((\mu + 1)/(\mu - 1)\right)^2 = 1.414$

Arbitrarily, b was selected to be $b = 1$.

Therefore $a = 0.707$.

With these parameters, v was experimentally determined on the two presentations mean well learning criteria. The value of v so determined was:

$v = 0.25$

M_z the lower bound on negative excursions of the z processes requires some thought. M_z should be specified luch that an amplitude of $z_{ci}(t) = -M_z$ will not prevent learning of excitory associations. Consider equation 7.5.2 for the x processes when $z_{ci}(t) = -M_z$:

$$\dot{x}_i(t) = -\alpha x_i(t) + P_i(t) - \beta M_z x_c(t - \tau)$$

If the node V_i is being excited by an input pulse we want the combination of inputs to V_i,

$$P_i(t) - \beta M_z x_c(t - \tau)$$

to be sufficiently positive to drive $x_i(t)$ to values such that:

$$x_i(t) > \frac{x_c(t - \tau)}{\mu_0^+} = \frac{x_c(t - \tau)}{11.5}$$

If this condition is met, then the driving function for $z_{ci}(t)$ will be positive and $z_{ci}(t)$ will move away from the value $z_{ci}(t) = -M_z$ in the excitory direction. In such a situation, the outstar will always be able to learn that the command node is excitorally associated with a grid event by sufficiently many presentations.

Analytically, the maximum amplitude for $x_c(t - \tau)$ is $(A/\alpha)(1 - e^{-1})$. If we make $P_i(t) = \beta M_z(A/\alpha)(1 - e^{-1})$, then we could expect the inhibitory input $\beta M_z x_c(t - \tau)$ and the excitory input $P_i(t)$ to approximately cancel. In this case, $\beta M_z = /(1 - e^{-1}) = 5.28$. Since $\beta = 1$, we therefore want $M_z < 5.28$ at least. To allow room for errors, $M_z = 2.10$ was selected.

To investigate the effect of random occurances of the command event in inhibitorally biasing the outstar before it "goes to school", the command node alone was excited once before presentation of the pattern.

section 7.6 Experiments with a Directly Inhibiting Outstar

Figure 7.6.1 shows the results of performing an experiment with the directly inhibiting outstar specified in the last section. Note that excitement of the command node alone at the beginning of the experiment results in small negative amplitudes for the z processes. The directly inhibiting outstar is thus slightly inhibitorally biased before "going to school". "School" begins with the second presentation of the command event. From the $x_2(t)$ trace it can be seen that the pattern $V_c \rightarrow V_1$ was approximately well learned in two presentations. Event 1 is not presented. The $z_{c1}(t)$ trace shows that the outstar has learned to directly inhibit grid node V_1.

Event 2 was presented with $\varphi = 0$ presentation phase with respect to the arrival of the prediction signal. (Presentation phase has been explained in section 3.5.) Event 3 was presented with presentation phase $\varphi = 0.6$ seconds after event 2. As can be seen from the $x_3(t)$ and $z_{c3}(t)$ traces, the outstar has learned to inhibit grid node V_3.

The experiment was continued to test the resistance of the directly inhibiting outstar to random mistakes in the pattern. Figure 7.6.2 shows the results. Event 1 is the simulated random mistake. As can be seen from the $x_1(t)$ and $z_{c1}(t)$ traces, the direct inhibition the outstar learned before the occurance of this mistake resulted in little damage to the pattern. $z_{c1}(t)$ rose to a small positive amplitude which is decaying. The prediction following occurance of the mistake did not cause $z_{c1}(t)$ to increase. Thus we may conclude that the outstar will forget the mistake entirely in time.

The experiment was continued to test the correctability of the

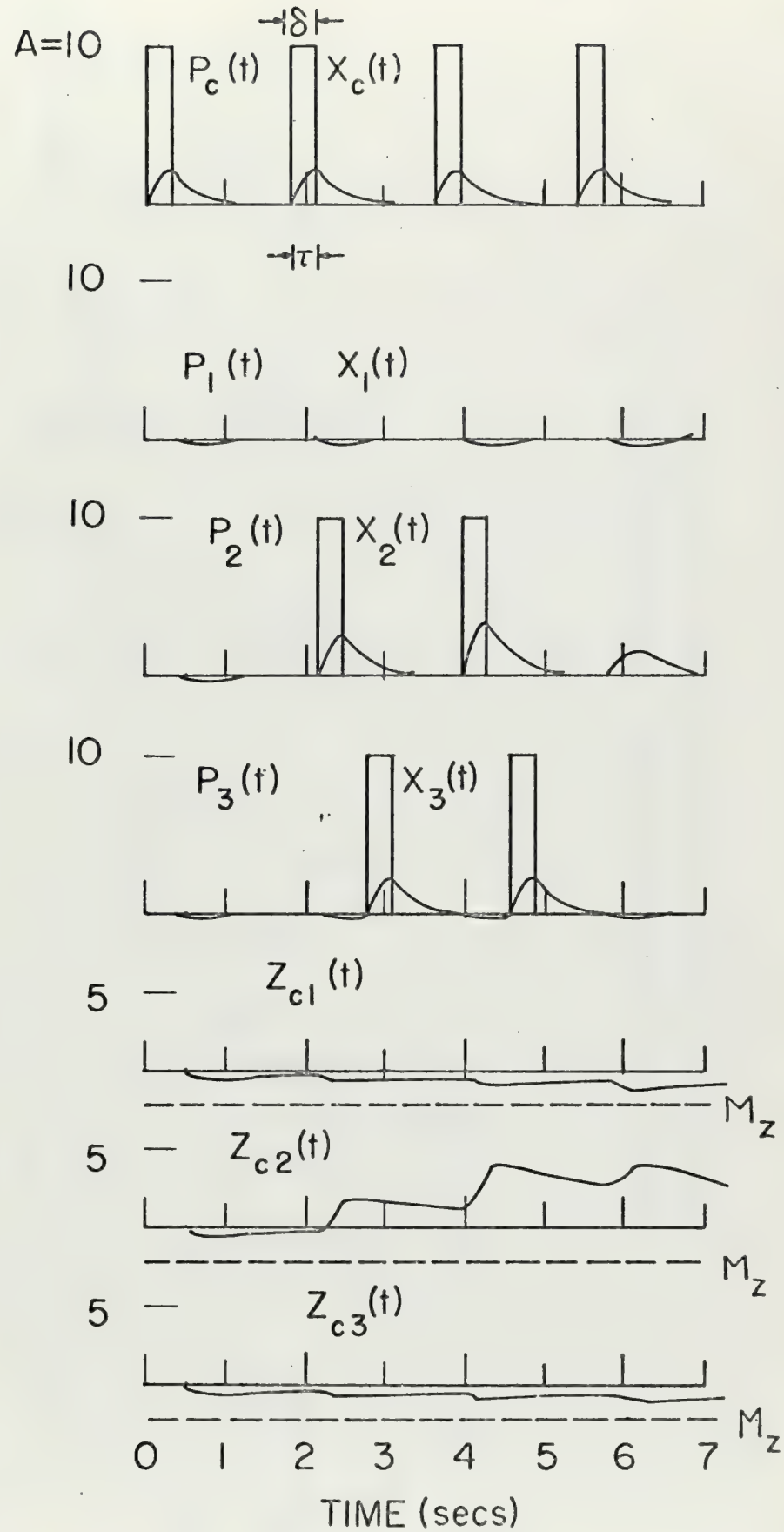

Figure 7.6.1. Results of an experiment conducted with an outstar governed by logic $\mathcal{L}_3$.

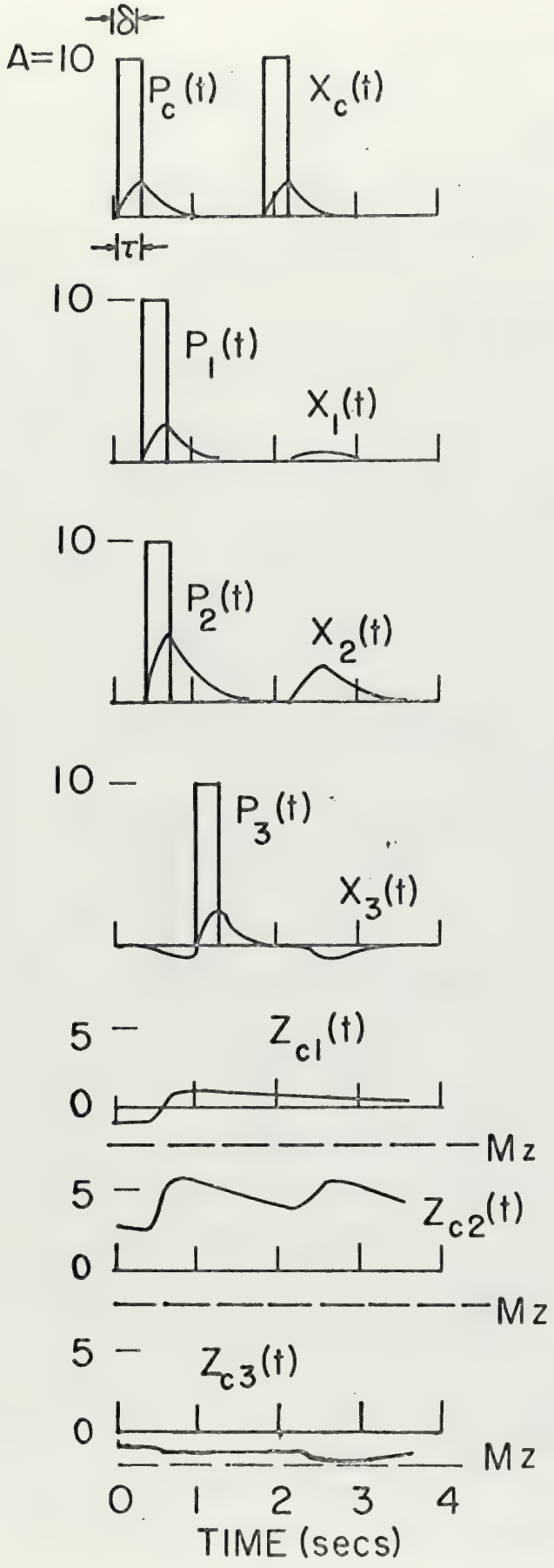

Figure 7.6.2. Result of presenting a simulated random mistake in the previously learned pattern $V_c \rightarrow V_2$. Event 1 is the mistake.

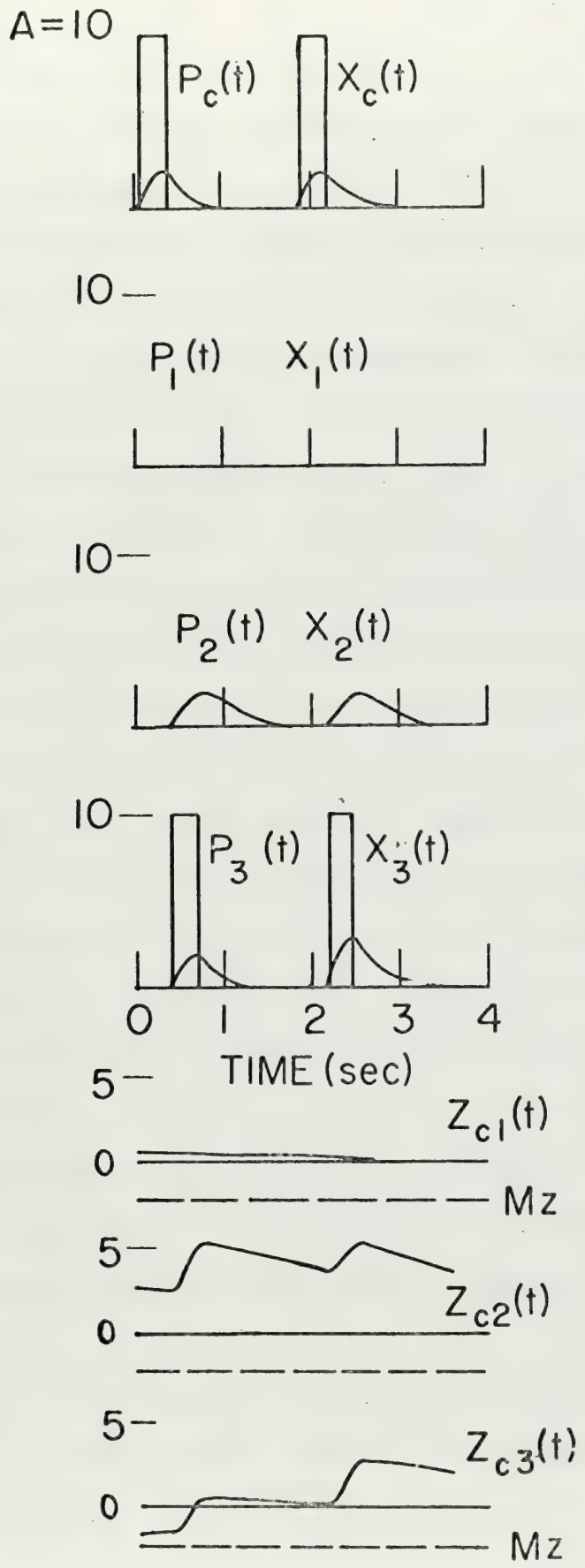

Figure 7.6.3. The result of attempting to correct the previously learned pattern $V_c \rightarrow V_2$ with the correcting pattern $V_c \rightarrow V_3$.

directly inhibiting outstar. Figure 7.6.3 shows the results. An attempt was make to correct the previously learned pattern $V_c \rightarrow V_2$ with the correcting pattern $V_c \rightarrow V_3$ by presenting $V_c \rightarrow V_3$ twice. Figure 7.6.3 shows that the attempt was unsuccessful. The first presentation of $V_c \rightarrow V_3$ was treated like a random mistake. The previously learned inhibition of V_3 was sufficient to prevent $z_{c3}(t)$ from rising to much of a positive amplitude. The next presentation of $V_c \rightarrow V_3$ did result in a healthy increase in $z_{c3}(t)$. Further presentations of $V_c \rightarrow V_3$ will result in it being learned better. However, $V_c \rightarrow V_2$ was not "unlearned" during this time. Both excitements of the command node resulted in approximately well learned responses by $x_2(t)$.

The only method by which this directly inhibiting outstar can correct a pattern is to forget the old pattern while learning the new pattern. From the $z_{c2}(t)$ trace we can see that the presentation rate for $V_c \rightarrow V_3$ was just right to result in "pumping up" $z_{c2}(t)$ such that $V_c \rightarrow V_2$ remained well learned during the correction attempt. Thus the outstar could not forget $V_c \rightarrow V_2$ while learning $V_c \rightarrow V_3$. The addition of lateral inhibition and/or increasing the forgetting rate u would probably increase the correctability, but these options were not investigated.

In the discussion of the logic $\mathcal{L}_2$ in section 7.4, it was noted that random excitation of the grid nodes without excitation of the command node might result in inhibition of a learned pattern. The assignment:

$$\mathcal{L}_2(\bar{x}_c = 0, \bar{x}_i = +1) = -1$$

is the source of this possible trouble. It was decided to see if this was indeed a problem. All the grid nodes were excited twice without

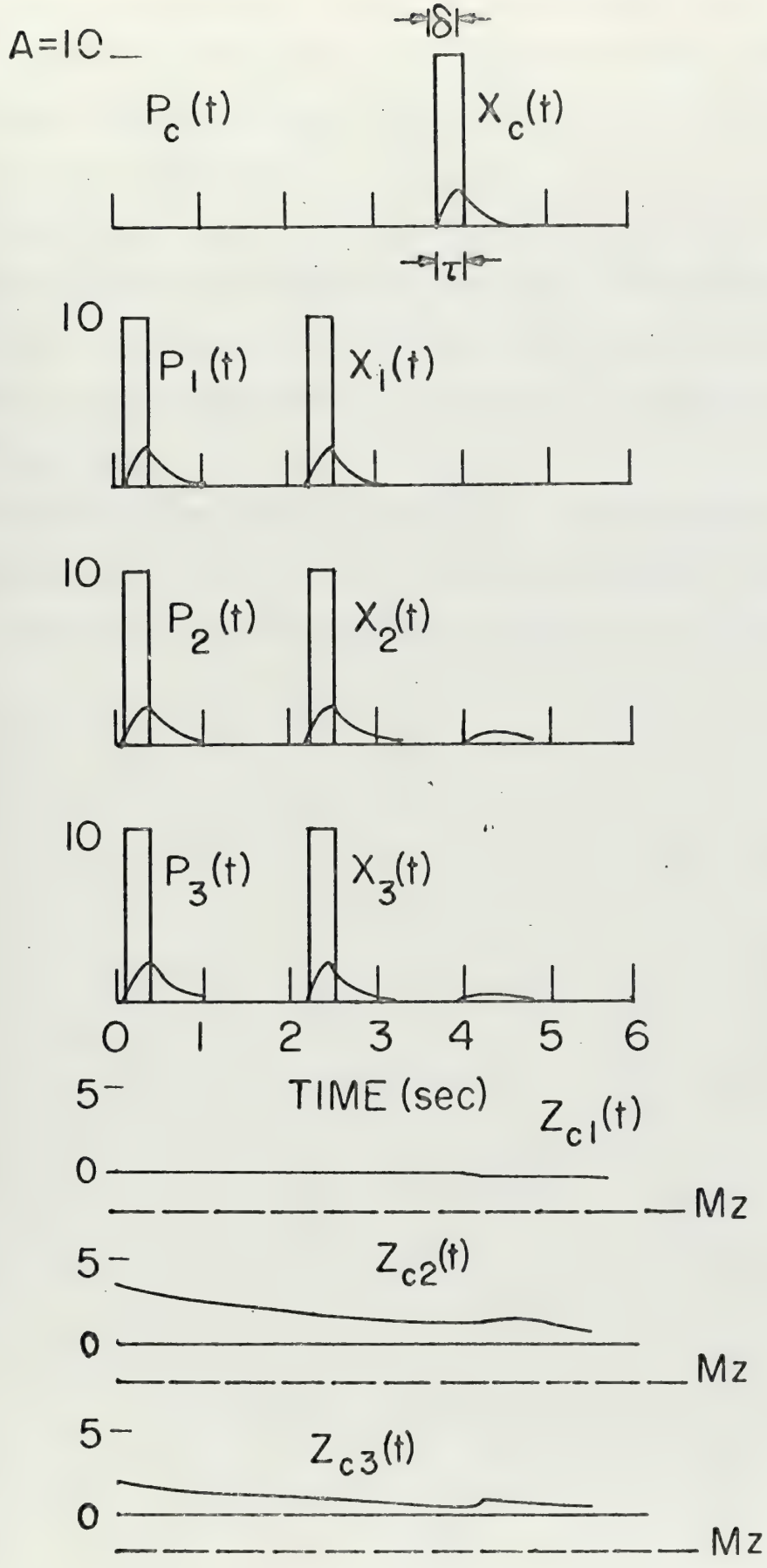

Figure 7.6.4. Result of excitement of grid nodes alone on the previously learned pattern $V_c \rightarrow (V_2, V_3)$.

exciting the command node. The command node was then excited to see what would be predicted on the grid. Note that because of the unsuccessful correction attempt, the outstar had learned $V_c \rightarrow (V_2, V_3)$ at the end of figure 7.6.3.

Figure 7.6.4 shows the result. $z_{c2}(t)$ and $z_{c3}(t)$ were very slightly driven in the direction of inhibition by the grid node excitements. However, as the prediction shows, the pattern $V_c \rightarrow (V_2, V_3)$ is still in the outstar's memory. It can still be completely recovered by "pumping up".

This result does not mean that there is no problem with random excitements of the grid nodes in an outstar conforming to $\mathcal{L}_2$. It only means that it is not a significant problem in the outstar under study.

section 7.7 Generality of the Formulation of the z Process Conforming to Logic $\mathcal{L}_2$

The z process formulation conforming to logic $\mathcal{L}_2$ that we have used is:

7.7.1 $$\dot{z}_{ci}(t) = -uz_{ci}(t) + v\,\delta_{-1}(M_z + z_{ci}(t))\left(a(x_c(t-\tau) + x_i(t))^2 - b(x_c(t-\tau) - x_i(t))^2\right)$$

where:

$$\delta_{-1}(y) = \begin{cases} 1 \text{ if } y \geq 0 \\ 0 \text{ if } y < 0 \end{cases}$$

As was shown in section 7.5, setting a = b in equation 7.7.1 will result in:

7.7.2 $$\dot{z}_{ci}(t) = -uz_{ci}(t) + \delta_{-1}(M_z + z_{ci}(t))2v(a+b)x_c(t-\tau)x_i(t)$$

Equation 7.7.2 describes a z process conforming to the neurtrally biased logic $\mathcal{L}_1$ of table 7.3.1. By setting $M_z = 0$ in equation 7.7.2, we get the excitory logic $\mathcal{L}_0$ of table 7.3.1 which has been the logic we have used in the simple and laterally inhibiting outstars. Thus the z process formulated by equation 7.7.1 is rather genreal. By specifying the parameters a, b, and M_z we have a choice of which logic and what type of outstar we shall get.

The general application of equation 7.7.1 does not end there. By appropriate specification of the parameters a, b, M_z, and v we can make a z process governed by it "practically inhibitorally biased".

Suppose, for example, that we wished to make a laterally inhibiting outstar. We connect all of the grid nodes with directed edges and arrowheads. Previously we have used z processes with a permanently assigned negative value to get laterally inhibiting prediction signals. However, we can now make all the z processes in the network conform

to equation 7.7.1. By proper selection of a, b, and v we can make the z processes in the laterally inhibiting arrowheads negative most of the time.

To do so, we depend on the statistics of the environment. It is unlikely that ant two x processes in the grid will be excited to identically equal amplitudes for very many times in succession. Therefore, by specifying the cross over factors $\mu_0^+ = 1/\mu_0^- \tilde{=} 1$, we can be almost certain that the z processes in the arrowheads will learn inhibition.

An experiment was conducted to test this conclusion. Two nodes, V_1 and V_2 were connected by a directed edge as shown at the bottom of figure 7.7.1. The originating node, V_1, was excited four times in succession by input pulses. The "receiving" node, V_2, was excited twice exactly when the prediction signal arrived at the arrowhead. The parameters used in the experiment were:

Input parameters:

Input pulse shape is rectangular

$A = 10$

$\delta = 0.3$ seconds

Network parameters:

All initial conditions were zero

$\alpha = 3.3333$ seconds^{-1}

$\beta = 1$

$u = 0.278$ seconds^{-1}

$\tau = 0.3$ seconds

$v = 1.0$

$a = 0.12$

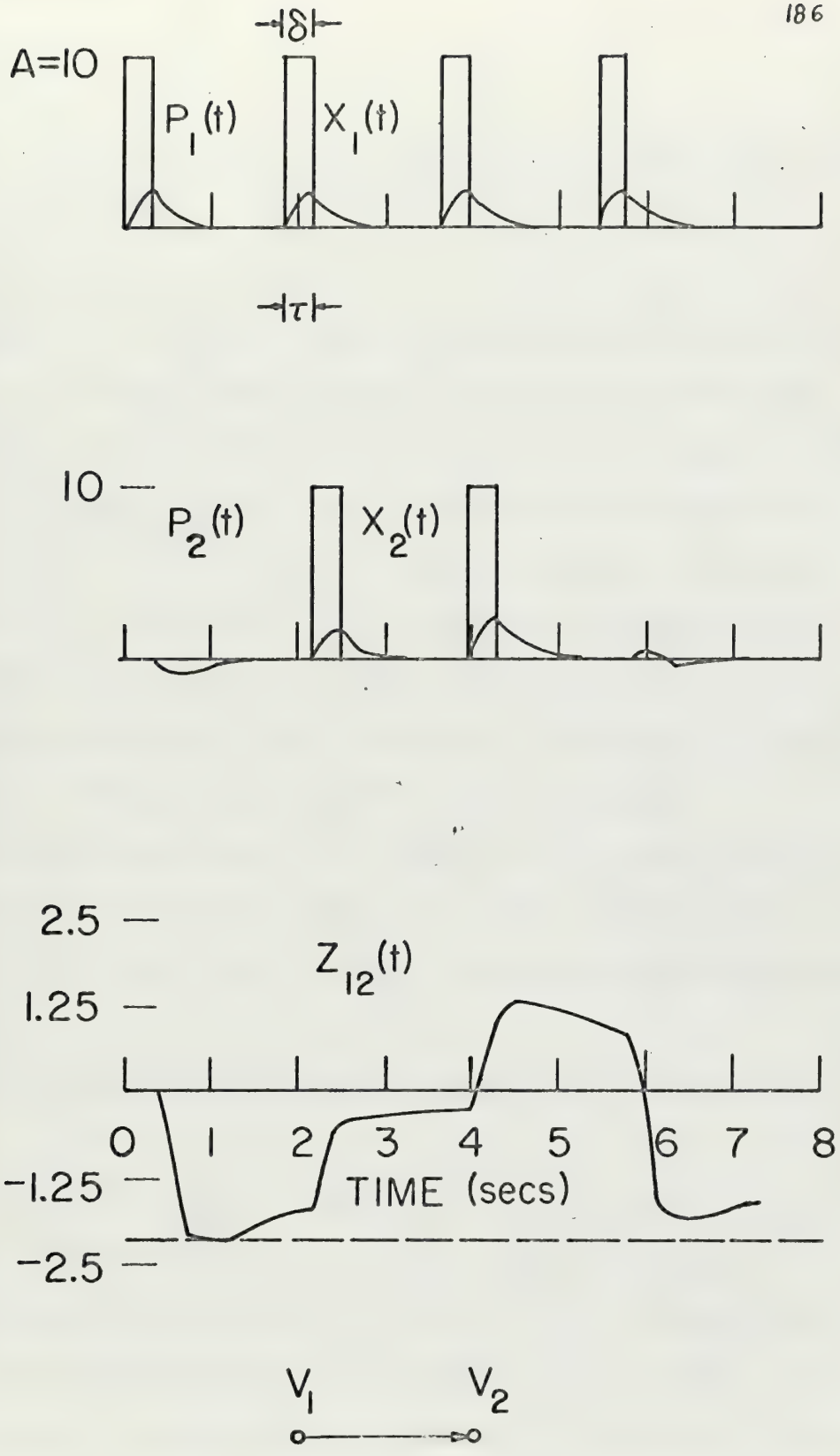

Figure 7.7.1. Demonstration of a z process which learns inhibition.

Network parameters continued:

$b = 1.08$

$M_z = 2.10$

From the selection of a and b, the cross over ratio $\mu_0^+ = 1/\mu_0^-$ was computed to be:

$\mu_0^+ = 2$

Figure 7.7.1 shows the result. The initial excitement of V_1 alone resulted in the $z_{12}(t)$ process being driven to its negative limit, $-M_z$. The two presentations of event 2 exactly at the time that the prediction signal $x_1(t - \tau)$ arrived at the arrowhead resulted in $z_{12}(t)$ being driven to a positive amplitude. However, the fourth excitement of V_1 resulted in $z_{12}(t)$ returning to inhibitory values. Thus we may conclude that the $z_{12}(t)$ process will behave as an inhibitory process most of the time. Note also that we did not have to specify the cross over factor to be exactly 1 to get this result.

Of course, specifying a = 0 in equation 7.7.1 would make the z process always inhibitorally biased. The above experiment was conducted to show that we did not have to go to this extreme to get the desired results.

If we go to the other extreme and specify b = 0 in equation 7.7.1, we get:

7.7.3 $$\dot{z}_{ci}(t) = -uz_{ci}(t) + va\,\delta_{-1}(M_z + z_{ci}(t))(x_c(t - \tau) + x_i(t))^2$$

This formulation will result in the z process being driven to positive amplitudes when ever $x_c(t - \tau)$, or $x_i(t)$, or both, are non zero. Thus we can replace the permanently assigned positive z processes in the command node cascade in an avalanche with "learning" z processes that are governed by the same general equation as all the other z

processes in the avalanche.

The z process formulation given by equation 7.7.1 is therefore general enough to be used in all the applications we have found for z processes in outstars and avalanches. We could specify that all the z processes in a network be governed by this formulation. The special features of the network such as a command cascade or lateral inhibition can be implemented by appropriate selections for the parameters a, b, and M_z. Thus the design of an outstar or an avalanche could be reduced to specification of these parameters at each of the arrowheads in the network.

CHAPTER 8 THE CHEMICAL OUTSTAR

section 8.1 Introduction

At this point there are three outstanding promises made in the previous chapters. In the introduction to chapter one, it was promised that this thesis would examine Grossberg's theoretical proposal for the neurophysiological processes that allow a living organism to learn. In chapter five it was promised that a solution to "pulse lengthening" in a cascade of nodes would be developed. In chapter seven it was promised that an examination of a logic corresponding to logic $\mathcal{L}_3$ in table 7.4.1 would be made.

We shall keep these promises in this chapter. A synthesis of all three will be developed and we shall examine its performance.

section 8.2 The Analogy Between Embedding Field Networks and the Nervous System of Living Organisms

Figure 8.2.1 shows the analogy between embedding field network elements and the elements of the nervous system of a living organism. A thorough perusal of figure 8.2.1 would explain this analogue to the reader better than volumes of words.

For the uninitiated, a brief description of the neurophysiological elements and processes shown in figure 8.2.1 is offered. The dark cell body and axon shown is an interneuron in the spinal column of a vertebrate. The light cell body and axon is a motoneuron. Neurons are living cells. They occur in organisms in a variety of shapes. However, they always consist of a reasonably elongated part called an axon, and a "fatter" part called the cell body. The cell body contains the cell's nucleus. An interneuron and a motoneuron were chosen for figure 8.2.1 because they have been extensively studied and the information shown was easy to collect.

The traces shown are voltages recorded by microelectrodes inserted into the interneuron and the motoneuron at the places shown. These recordings correspond to the following sequences of events: The interneuron is excited by an electrical signal delivered to the cell body by a microelectrode. This signal results in the membrane potential of the cell body rising from its resting potential of approximately -70 mV. There are two parts to this positive increase in the cell body membrane potential: The excitory post synaptic potential, EPSP, and the action potential (spike). The EPSP is the lower trace which is shown as a solid line. If the EPSP does not rise to suprathreshold

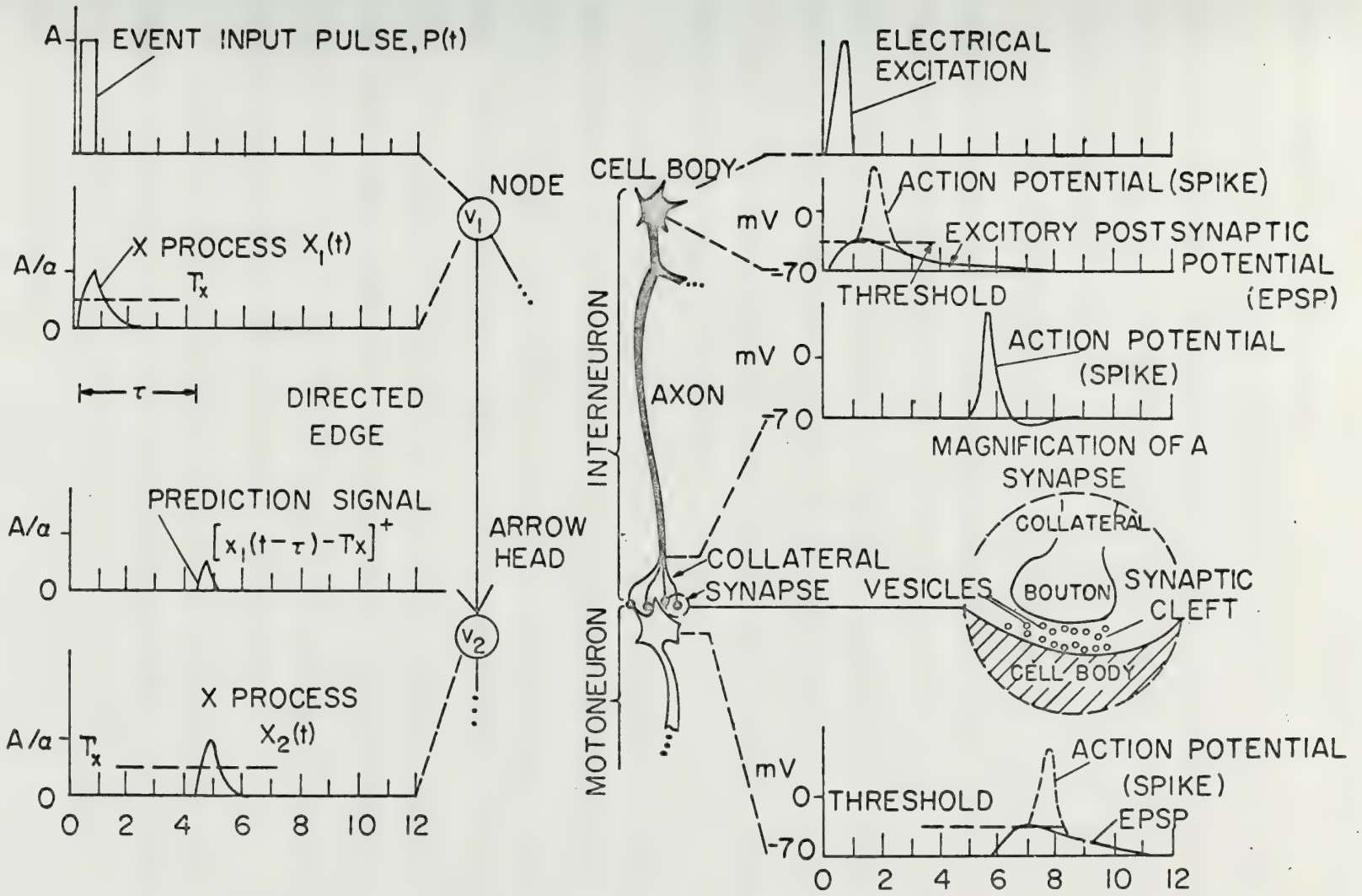

Figure 8.2.1. Comparison of the elements of embedding field theory and the elements of the nervous system of a vertebrate. An interneuron is shown synapsing on a motoneuron in the spinal column of a vertebrate.

values, then it is the only signal recorded at the cell body. Further a subthreshold EPSP does not result in an action potential (spike) being propagated down the ason.

When the EPSP rises to suprathreshold values, a spike is propagated down the axon. In addition, the spike is "reflected" back into the cell body giving rise to the dotted line spike trace shown superimposed on the EPSP.

The spike is formed at the point where the cell body narrows down to form the axon. It propagates down the axon at a finite velocity which is on the order of 5 meters/sec. to 100 meters/sec. The type of neuron and the covering on the axon determines the propagation velocity. In a particular type of neuron, the propagation velocity is fixed. All spikes are transmitted at the same velocity. Spikes also always have the same amplitude and shape.

The end of an axon generally breaks up into a number of collaterals. Each collateral ends in a swelled portion called a bouton. These boutons are located immediately adjacent to another neuron's cell body. The bouton-cell body junction is called a synapse. For this reason the geometric arrangement of the neurons shown is described as an interneuron "synapsing" on a motoneuron. We have shown the spike propagated down the axon as it arrives at the synapse. Note that it is delayed due to the finite transmission velovity.

A spike arriving at a synapse causes the adjacent cell body membrane potential to rise from its resting potential with an EPSP. If the EPSP rises to suprathreshold values, a spike is propagated down this neuron's axon.

There is a short delay between the arrival of a spike at the synapse and the beginning of an EPSP at the adjacent cell body. This is because the cell body being synapsed upon is not excited electrically by the spike. Instead, the spike causes the release of a chemical substance in the space between the bouton and adjacent cell body. This chemical substance is called transmitter. It causes the EPSP in the synapsed upon cell body by changing the cell body's permeability to different ionic species.

A magnification of a synapse is shown. The space between the bouton and the cell body is called the synaptic cleft. Under an electron microscope, the synaptic cleft is revealed to hold a number of small particals called vesicles. It is currently believed that these vesicles are packages of transmitter which burst open when a spike arrives at the synapse.

The reason for these voltage traces is relatively easy to understand. A neuron is surrounded by an interstitial fulid in which various ions are dissolved. The interior of a neuron is also a fluid like substance in which ions are soluble. The boundary between the interior of the neuron and the interstitial fulid is a membrane which is selectively permeable to ions. In a neuron at rest, the membrane is permeable to potassium ions, K^+, but reasonably impermeable to sodium ions, Na^+. There is additionally a "sodium pump" in the membrane which continuously ejects Na^+ ions from the neuron's interior. To maintain electrical and chemical equilibrium of the overall system, there is a higher concentration of K^+ inside the neuron than outside. The reverse is true for Na^+. The result is that the interior of the neuron is approximately 70 milli volts negative with respect to the interstitial fluid.

Electrical stimulation of the membrane results in a sudden change in the membrane permeability. The membrane becomes permeable to Na^+ ions and they diffuse into the neuron. This results in a sudden increase in the voltage of the neuron's interior with respect to the interstitial fluid. In a very short time the membrane regains its impermeability to Na^+ ions. K^+ ions then diffuse out of the neuron to redress the equilibrium and the potential across the membrane drops to the resting potential. The net effect is a small loss of K^+ ions and a small increase of Na^+ ions inside the neuron. The sodium pump will redress this in short time. Thus with microelectrodes inserted into the neuron the potential across the membrane can be measured and electrical traces similar to those shown can be recorded.

Release of the trandmitter substance in the synaptic cleft by a spike causes similar membrane permeability changes which result in an EPSP.

Next to the neurons we have shown the geometrical elements and processes which occur in embedding field elements. Grossberg has proposed the following analogy between the neurophysiological phenomena in an organism and embedding field theory:

Embedding Field Theory	Living Organism
Geometric elements:	
node	cell body
directed edge	axon
arrowhead	synapse
Processes:	
x process	cell body membrane potential
prediction signal	action potential (spike)
amplitude of z process	amount of transmitter substance available in synaptic cleft

Except for the last correspondence, figure 8.2.1 shows that the analogy is in general very good. There are differences in detail which we will take the time to explain here.

The x processes shown are not divided into an EPSP and a superimposed spike. Further, the maximum amplitude of the prediction signal is directly proportional to the amplitude of the x process which, in turn, is directly proportional to the amplitude of the input pulse . The amplitude of a spike on an axon is constant and independent of the amplitude of the signal exciting the cell body.

However, the situation we have shown on the interneuron is the response to a single excitation of short duration and limited amplitude. In the usual case the EPSP is suprathreshold for a reasonably long time. This results in a barrage of spikes being propagated down the axon. The frequency of these spikes is proportional to the strength of the stimulus exciting the cell body. In Grossberg's proposal, the amplitude of the portion of the x process that is suprathreshold is considered to be proportional to the spiking frequency in a neuron. Thus a prediction signal represents a barrage of spikes.

section 8.3 Summary of the Theoretical Proposal for the Neurophysiological Process of Learning in Living Organisms

We have seen that an outstar network composed of embedding field elements is capable of learning. The key to this ability is the z process at an arrowhead. The z process at an arrowhead correlates the prediction signal arriving at the arrowhead with the x process at the adjacent node. It remembers this correlation in its amplitude and allows prediction signals to excite the adjacent node proportional to its amplitude. By writing down the equations governing the embedding field network shown in figure 8.2.1, we can see this clearly:

8.3.1 $$\dot{x}_1(t) = -\alpha x_1(t) + P_1(t)$$

8.3.2 $$\dot{x}_2(t) = -\alpha x_2(t) + P_2(t) + \beta z_{12}(t)[x_1(t-\tau) - \Gamma_x]^+$$

8.3.3 $$\dot{z}_{12}(t) = -uz_{12}(t) + v[x_1(t-\tau) - \Gamma_x]^+[x_2(t) - \Gamma_x]^+$$

where:

$$[y]^+ = \begin{cases} y \text{ if } y > 0 \\ 0 \text{ if } y \leq 0 \end{cases}$$

From the $x_2(t)$ trace is figure 8.2.1, we can conclude that $z_{12}(t)$ has already learned that V_1 and V_2 are associated. That is, $z_{12}(t) > 0$ and is of sufficient amplitude to result in a well learned prediction response by $x_2(t)$.

In order for the interneuron in figure 8.2.1 to excite the noto-neuron with spikes, there must be transmitter substance in the synaptic clefts. If we make the amount of transmitter substance released by a barrage of spikes proportional to $\beta z_{12}(t)[x_1(t-\tau) - \Gamma_x]^+$ then the equations governing the embedding field network could accurately

describe the nervous network. If we further made the amount of transmitter substance available for release proprotional to the amplitude of $z_{12}(t)$, then equation 8.3.3 could describe how, why, and how much transmitter substance is available in the synaptic cleft. Grossberg has proposed this as a concrete theoretical explanation of the neurophysiological phenomena underlying learning in living organisms. His proposal is that transmitter substance is produced in a synaptic cleft at a rate proportional to the correlation of the frequency of spikes arriving at the bouton and the membrane potential and/or spiking frequency of the adjacent cell body. He has proposed additional refinements and an exact mechanism which gives this result in reference 4.

It is doubtful that the ability of an interneuron to excite a motoneuron in the spinal column of vertebrates is learned. As we have said, the neurons selected for figure 8.2.1 were selected because of the extensive information that has been collected on them. However, the arrangement of neurons in the medulla, cerebellum, and cerebrum of vertebrates is similar and we do know that learning occurs in these organs. The similarity between the embedding field network and the nervous network in figure 8.2.1 is uncanny. Grossberg has shown theoretically, and we have shown experimentally, that embedding field networks can learn. Thus Grossberg's proposal could explain learning in organisms at the microscopic level. The proposal is even more attractive when it is recalled that embedding field theory originated at a model for the macroscopic psychological phenomena of learning.

This thesis originally intended to simulate Grossberg's proposal in detail and compare it to existing neurophysiological experimental

data. However, the time was not available. A simplistic stab was made in this direction. The reason was that nervous networks are capable of transmitting a signal through a cascade of neurons without "pulse lengthening" occuring. To solve this problem in an embedding field node cascade, an attempt was made to model the embedding field elements more closely to neurophysiological elements. At the same time, attempts to implement logic $\mathcal{L}_3$ of table 7.4.1 in an outstar were being made. The simplistic model of neurophysiological phenomena proved to be an $\mathcal{L}_3$ logic. Because of these diverse reasons, the simplistic model arrived at in this thesis is quite different from Grossberg's proposal. In the next section we shall derive this model in a somewhat logical manner. The reader may be assured that this was not the historical progress of the model.

section 8.4 A Simplistic Model for the Neurophysiological Phenomena in a Nervous Network Based on Embedding Field Theory

Suppose that we had two neurons, V_1 and V_2, arranged as in figure 8.2.1. Suppose further that excitements of the first neuron, V_1, only results in one spike being generated per excitement. Also suppose that we could excite the cell body of the second neuron, V_2, with an input. As in embedding field theory, we are not concerned here with how these inputs are delivered to the cell bodies. For the sake of argument, suppose that transmitter substance is produced in the synaptic cleft at a rate proportional to the correlation between the membrane potential of a bouton and the membrane potential of the adjacent cell body, V_2. For the purposes of this discussion, we will assign a value of zero to the resting membrane potential at the bouton and let $x_2(t)$ be the membrane potential of the V_2 cell body. Let $z_{12}(t)$ be the "amount" or "concentration" of transmitter substance present in the synaptic cleft. From our previous work we have a choice of two formulations for $z_{12}(t)$:

8.4.1 $$\dot{z}_{12}(t) = -uz_{12}(t) + vx_1(t-\tau)x_2(t)$$

and the more general formulation:

8.4.2 $$\dot{z}_{12}(t) = -uz_{12}(t) + v\,\delta_1(M_z + z_{12}(t)) \left[a(x_1(t-\tau) + x_2(t))^2 - b(x_1(t-\tau) - x_2(t))^2\right]$$

Now, we run into a problem. $x_1(t-\tau)$ and $x_2(t)$ are voltages. $z_{12}(t)$ is the rate of production of a chemical transmitter substance. What are the chemical reactants which produce the transmitter substance? How does it come about that a chemical substance is being produced at a rate proportional to the product of voltages?

In our brief description of how membrane potentials come about, we saw that these potentials are due to changes in the ionic permeability of the neurons' membranes. Suppose that an ion or substance diffuses or is released from the bouton when the membrane permeability is changed by arrival of a spike. We will call this substance "B" substance. Suppose further that a different ion or substance diffuses or is released from the cell body when its membrane permeability is changed by an EPSP or spike. We will call this substance "C" substance. Suppose further that "B" substance and "C" substance are the reactants which produce the transmitter substance. Since the transmitter substance results in excitation of neuron V_2, we will call it "excitory transmitter substance", or simply "E" substance.

How do the B and C substances combine to produce E substance, and why would the rate for this reaction be proportional to the product of voltages? The rate of reaction for biochemical reactions may be governed by many things, including voltages. Due to the complexities of biochemical processes, we could blatantly assume that the rate of reaction for the combination of B and C substances into E substance is proportional to the product, or the squares of the sum and difference, of two voltages. However, we need not make this blatant assumption. It is possible to allow B and C substances to combine according to a very simple chemical reaction and this will result in all the desired properties for production of E substance. The remainder of this section will be devoted to this simple chemical reaction and its implications.

Let B and C substances combine to form E substance according to the chemical reaction:

8.4.3 $\quad b \cdot B + c \cdot C \rightleftharpoons 1 \cdot E$

where b is the number of moles of B and c is the number of moles of C required to produce one mole of E.

Let this reaction occur instantly at body temperatures. That is, if b moles of B and c moles of C are released into the synaptic cleft at time t_0, then at any time $t > t_0$ only the end product of one mole of E will be present in the cleft.

We will investigate the implications of equation 8.4.3 for the production of E substance. The investigation will involve a number of tricky conservation of reactants and end product equations. For simplicity , we will make b = c = 1 in equation 8.4.3. That is:

8.4.4 $\quad 1 \cdot B + 1 \cdot C \rightleftharpoons 1 \cdot E$

Equation 8.4.4. will be used throughout. However it must be kept in mind that equation 8.4.3 is the general situation and that we will be investigating a special case.

Let $\dot{b}_{12}(t)$ be the number of moles of B substance released from a bouton into the synaptic cleft per second. Let $\dot{c}_{12}(t)$ be the number of moles of C substance released from the cell body per second into the cleft. We can relate $\dot{b}_{12}(t)$ and $\dot{c}_{12}(t)$ to the membrane potentials, $x_1(t - \tau)$ and $x_2(t)$.

The biochemical process which results in membrane potentials is the selective permeability of the membranes. A positive increase in a membrane potential is due to an increase in the membrane's permeability to sodium ions, Na^+. A decrease in membrane potential is due to a decreased permeability to Na^+ ions. As we discussed in section 8.2, the net effect of a spike or an EPSP on a neuron is a slight increase of Na^+ ions inside it and a compensating decrease of potassium, K^+. Now, suppose that B and C substances are held inside the membrane

when it is at rest potential. Suppose further that they diffuse through the membrane with K+ ions to compensate for a net increase of Na+ ions. Since K+ ions diffuse out of a membrane when the membrane potential is decreasing, we can say that:

(a) $\dot{b}_{12}(t) > 0$ when $\dot{x}_1(t - \tau) < 0$

(b) $\dot{c}_{12}(t) > 0$ when $\dot{x}_2(t) < 0$

Since the rate of diffusion of K+ ions is proportional to the rate of change of membrane potential, let us go a bit further and say that:

(c) $\dot{b}_{12}(t) = [-\dot{x}_1(t - \tau)]^+$

(d) $\dot{c}_{12}(t) = [-\dot{x}_2(t)]^+$

where:

$$[y]^+ = \begin{cases} y \text{ if } y > 0 \\ 0 \text{ if } y \leq 0 \end{cases}$$

In other words, this says that the rate of release of B and C into the synaptic cleft is directly proportional to the rate of decrease of membrane potential.

Now, what happens to the B and C substance when they are released into the synaptic cleft? If both are being released at the same time, then E substance will be produced. This exactly what we want. It says that E substance will be procuded if both $x_1(t - \tau)$ and $x_2(t)$ are decreasing at the same time. Although it ignores the increasing leading edge of $x_1(t - \tau)$ and $x_2(t)$, it does correlate the decreasing trailing edges. Further, this process corresponds to known physical facts. That is, when membrane potentials are decreasing, at least one substance from inside the membrane in diffusing out of it.

However, there is a catch. Suppose a spike has excited the bouton recently, but no EPSP or spike has excited the adjacent cell body.

Then B substance will have been released into the synaptic cleft and there will be a net amount of it present for all time after arrival of the spike at the bouton. Thus, if a few days later, the adjacent cell body is excited by an EPSP or a spike, E substance will be produced. In embedding field terms, the association $V_1 \rightarrow V_2$ will be learned. One of the key tenets of embedding field theory is that $V_1 \rightarrow V_2$ can only be learned when V_1 and V_2 have been excited in close temporal proximity. Thus, we can not allow excess B or C substances to accumulate in the cleft.

There are three methods of preventing excess B or C substance from accumulating in the cleft. It can diffuse out of the cleft, it can be readsorbed into the bouton or cell body from which it came, or, it can be rendered inactive by chemical reactions. There is no reason for prefering one of these methods to another here. We will arbitrarily choose the chemical reaction and say that B and C substances are deactivated at a finite rate to prevent accumulation.

Let $\bar{b}_{12}(t)$ be the number of moles of B in the cleft at time t. Let $\bar{c}_{12}(t)$ be the number of moles of C in the cleft at time t. Then we will say that:

8.4.5 $$\dot{\bar{b}}_{12}(t) = -w_b \bar{b}_{12}(t)$$

8.4.6 $$\dot{\bar{c}}_{12}(t) = -w_c \bar{c}_{12}(t)$$

We now have a "correlating" process. The amount of E substance in the cleft, $z_{12}(t)$, will grow when a spike excites the bouton in close temporal proximity to the excitement of the adjacent cell body. It will not grow if they are not in close temporal proximity.

We must now develop a mathematical description of the production of E substance in the cleft as a function of the membrane potentials

$x_2(t)$ and $x_1(t-\tau)$. Thus far we have reached the following results:

8.4.7 $1 \cdot B + 1 \cdot C \rightleftharpoons 1 \cdot E$ (instantaneous rate)

8.4.8 $\dot{b}_{12}(t) = [-\dot{x}_1(t-\tau)]^+$

8.4.9 $\dot{c}_{12}(t) = [-\dot{x}_2(t)]^+$

8.4.10 $\dot{\bar{b}}_{12}(t) = -w_b \bar{b}_{12}(t)$

8.4.11 $\dot{\bar{c}}_{12}(t) = -w_c \bar{c}_{12}(t)$

where:

$x_1(t-\tau)$ is the membrane potential of the bouton.

$x_2(t)$ is the membrane potential of the adjacent cell body.

$\dot{b}_{12}(t)$ is the number of moles of B released into the cleft from the bouton per second.

$\dot{c}_{12}(t)$ is the number of moles of C released into the cleft from the cell body per second.

$\bar{b}_{12}(t)$ is the net number of moles of B in the cleft at time t .

$\bar{c}_{12}(t)$ is the number of moles of C in the cleft at time t .

Because of 8.4.7, either $\bar{b}_{12}(t)$ or $\bar{c}_{12}(t)$ is zero at any given time. Also because of 8.4.7:

8.4.12 $\dot{z}_{12}(t) = [\min(\bar{b}_{12}(t), \bar{c}_{12}(t))]^+$

where:

$$[\min(x, y)]^+ = \begin{cases} x \text{ if } x \leq y \text{ and } x > 0 \\ y \text{ if } y \leq x \text{ and } y > 0 \\ 0 \text{ if } x \leq 0 \text{ OR } y \leq 0 \end{cases}$$

This simply says that if there is $\bar{b}_{12}(t)$ of B substance in the cleft, and we release $\bar{c}_{12}(t) < \bar{b}_{12}(t)$ of C substance into the cleft, then instantaneously all of the C will be used up to produce E. $\dot{z}_{12}(t)$ is restricted to be postive because there simply can not be a negative number of moles of B or C in the cleft.

Equation 8.4.12 will describe $z_{12}(t)$ as a function of $x_1(t-\tau)$ and $x_2(t)$ if we can develop equations relating $\bar{b}_{12}(t)$ and $\bar{c}_{12}(t)$ to $x_1(t-\tau)$ and $x_2(t)$ respectively. Let us consider the conservation of B in the cleft:

(i) $\dot{b}_{12}(t) = [-\dot{x}_1(t-\tau)]^+ dt$ of B substance is released into the cleft per time interval dt.

(ii) $[\min(\bar{b}_{12}(t), \bar{c}_{12}(t))]^+ dt$ of B substance is converted to E substance instantaneously in time interval dt.

(iii) The reaction to produce E substance is instantaneous. Therefore if there is $\bar{b}_{12}(t)$ of B substance in the cleft and $\bar{c}_{12}(t)$ of C is added at $t = t_0$, then at $t > t_0$ there can be at most $[\bar{b}_{12}(t) - \bar{c}_{12}(t)]^+$ of B in the cleft. This is the amount of B substance which will be available for deactivation. Therefore there is:

$$-w_b[\bar{b}_{12}(t) - \bar{c}_{12}(t)]^+ dt$$

of B substance deactivated per time interval dt.

Therefore:

$$8.4.13 \quad \dot{\bar{b}}_{12}(t) = [-\dot{x}_1(t-\tau)]^+ - w_b[\bar{b}_{12}(t) - \bar{c}_{12}(t)]^+ - [\min(\bar{b}_{12}(t), \bar{c}_{12}(t))]^+$$

Similarly:

$$8.4.14 \quad \dot{\bar{c}}_{12}(t) = [-x_2(t)]^+ - w_c[\bar{c}_{12}(t) - \bar{b}_{12}(t)]^+ - [\min(\bar{b}_{12}(t), \bar{c}_{12}(t)]^+$$

Equations 8.4.13 and 8.4.14 coupled with 8.4.12 completely describe the process whereby the voltages $x_1(t-\tau)$ and $x_2(t)$ are converted into the chemical substance E. As they are rather complicated, a system diagram was drawn and is shown in figure 8.4.1.

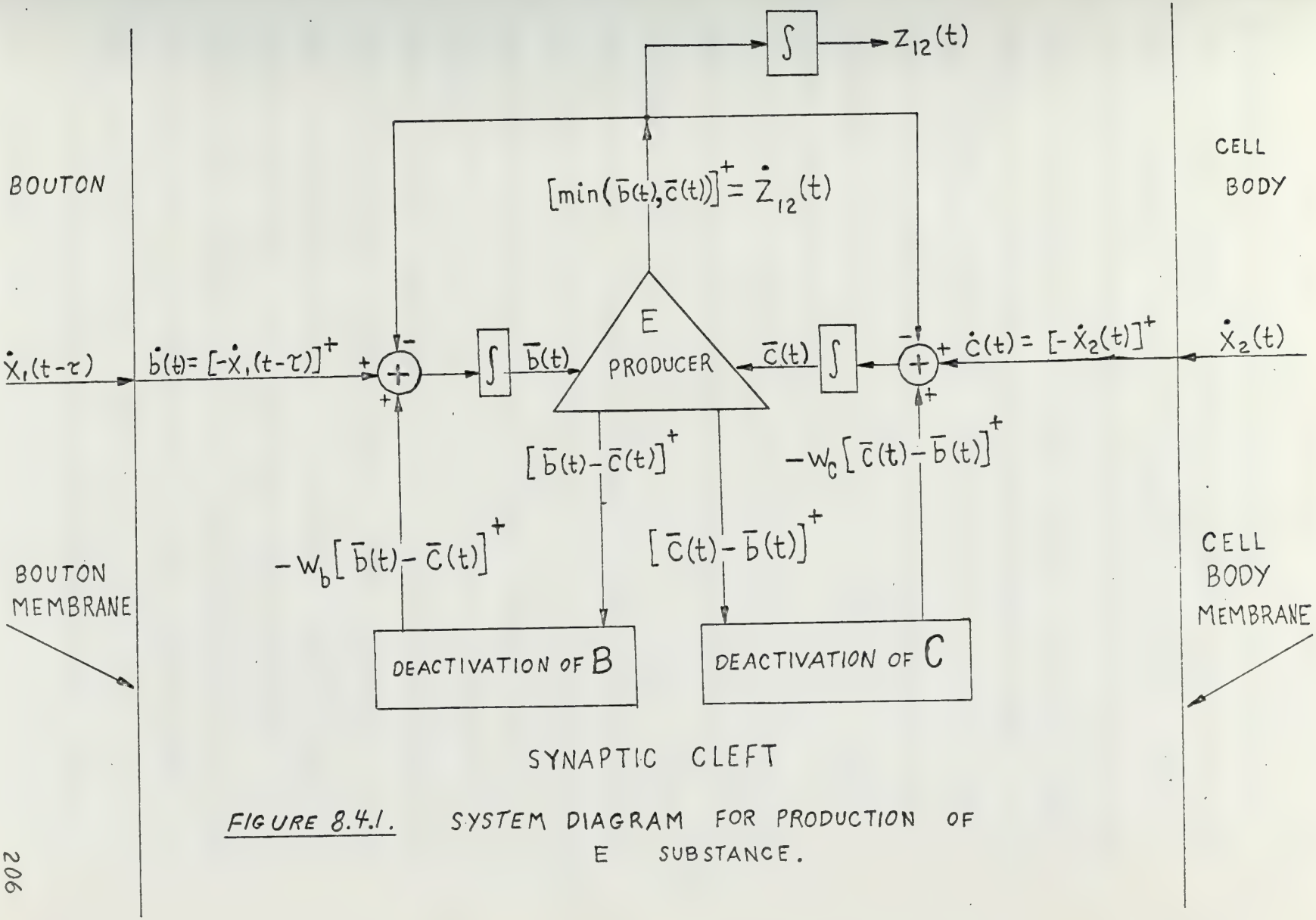

FIGURE 8.4.1. SYSTEM DIAGRAM FOR PRODUCTION OF E SUBSTANCE.

A signal from one neuron is transmitted to another by the release of transmitter substance in the synaptic cleft. Having developed a model for the production of transmitter substance, we must not model how this substance is used in the transmission of signals. Let us assume that the transmitter substance produced by our reaction is contained in the vessicles in the synaptic cleft. Under normal circumstances, it is safely packaged in these vessicles and unable to affect the permeability of the adjacent cell body membrane. However, when a spike arrives at the bouton, the vessicles suddenly burst and the transmitter is released to attack the cell body membrane. How does the spike cause the vessicles to burst?

Again since we are dealing with a biochemical system, there is no obvious method. Let us consider the events associated with the arrival of the spike at the bouton and see if there is any reason for the vessicles to burst. Arrival of the spike at the bouton begins with a rapid diffusion of Na^+ ions into the bouton. Here we have two possible reasons for the vessicles to burst. Firstly, before the arrival of the spike, the bouton and the cell body are at zero potential to one another. When the spike begins to arrive at the bouton the potential of the bouton rapidly increases relative to the potential of the cell body. Thus we could conceive of the vessicles being pulled apart by electrostatic forces. This would require dipolar vessicles. One end of the vessicle would have to be at a different potential with respect to the other end. If transmitter were released by this method, then it would most likely be released before the spike peaks.

On the other hand, we could conceive of the vessicles bursting due to the sudden infusion of Na^+ into the bouton. The detailed

mechanism would require that the normal Na+ concentration in the synaptic cleft be greater than that inside the bouton as is the case with the interstitial fluid surrounding the neuron. Then the beginning of the arrival of a spike at the bouton would cause the Na+ to diffuse out of the cleft into the bouton. Since the volume of the cleft is small compared to that of the bouton, this process would rapidly deplete the cleft of Na+. If sodium is required to keep the vessicle together they would come apart when a spike arrives at the bouton. Another mechanism that would have the same result would be to surround the vessicles with a membrane that is permeable to Na+ and H_2O. Then the sudden depletion of Na+ in the cleft would also deplete the vessicles of Na+. The result would be an osmotically compensating insurge of H_2O into the vessicles. With sufficient Na+ depletion, enough H_2O will enter the vessicles to burst them similarly to hemolysis in red blood cells. (Ref. 12 , p.13) Again this method would release transmitter most likely before the spike peaks.

We could conceive of other mechanisms to cause vessicles to burst. However, we have two likely candidates which cause them to burst before the spike peaks. Our process for the production of transmitter begins to operate after the spike has peaked and begun to decay.

If the process which releases transmitter operates at the same time as the production process, we will be releasing the transmitter that we produce. Thus, to make our system work well, we must separate the transmitter release and production process. For this practical reason, and the fact that it could work, we will release transmitter when the bouton membrane potential is increasing. That is, transmitter will be released when: $\dot{x}_1(t - \tau) > 0$

We must now decide how much transmitter is released. For simplicity let us assume that all the transmitter in the cleft is released when the bouton membrane potential begins to increase. We will further assume that all the released transmitter immediately changes the permeability of the adjacent cell body membrane and results in an immediate increase in the cell body's membrane potential. Note that this implies that arrival of the spike at the bouton causes an impulsive excitement of the adjacent cell body.

We need to decide one further thing. Release of one mole of E substance will result in a cell membrane potential of how many volts? We will arbitrarily sat that release of one mole of E will result in a cell body membrane potential increase of $\underline{a}$ volts.

In summary, our transmitter releasing process does the following: Suppose that there is $z_{12}(t)$ moles of E present in the cleft. Then any increase of the bouton membrane potential above resting potential will cause the release of $z_{12}(t)$ moles of E. This will in turn cause an immediate increase in the adjacent cell body membrane potential of $az_{12}(t)$ volts. The E released is used up causing the $x_2(t)$ membrane potential to increase. Thus $z_{12}(t) = 0$ immediately after release of the E.

In order to use this simplistic model for the production and release of transmitter in the synaptic cleft, we must also model the membrane potential responses of cell bodies and axons. At the beginning of the modeling process, we said that we were only interested in the propagation of a single spike across the synaptic cleft. Our model for the membrane response at other parts of the system thus need only account for a single spike. Rather than going through the laborious process of finding

processes which will exactly duplicate the membrnae potential traces shown in figure 8.2.1, we will adopt the formulation for x processes at a node in an embedding field. Further, we will not consider thresholds in this study.

With these assumptions, suppositions, and modeling results, we are in a position to write down a complete set of equations governing this simplistic model for a nervous network. We will summarize the notations used and then write down the equations.

The equations amd notations will be presented in a generalized form. Since this is just a reformulation of the embedding field network equations, we will number the cell bodies in a nervous network and refer to them as the "V_i" cell body. All synapses between boutons connected to the V_i cell body by axons and the V_j cell body will be referred to by the dual subscript ij. The first, i, subscript shows the direction a signal is coming from and the second subscript shows the direction it is traveling toward across the synapse.

Chemistry:

B substance is a chemical substance released from a bouton into a synaptic cleft when the bouton's membrane potential is decreasing.

C substance is a chemical substance different from B substance which is released from the cell body into synaptic clefts when the cell body membrane potential is decreasing.

E substance is excitory transmitter substance. It is produced by the instantaneous reaction:

$$1 \cdot B + 1 \cdot C \rightleftharpoons 1 \cdot E$$

At all times when the bouton membrane potential is at resting potential or decreasing, the E substance is stored in the synaptic cleft and is

unable to affect membrane potentials. When the bouton membrane potential is increasing, all the E substance in the cleft is immediately released. When it is released it immediately caused an increase in the adjacent cell body membrane potential of $\underline{a}$ volts per mole of E substance released. The E substance releasee is used up causing the cell body membrane potential to increase.

Variables:

$P_i(t)$ is an input signal delivered directly to the V_i cell body from the environment.

$x_i(t)$ is the cell body membrane potential of the V_i cell body in the nervous network.

$x_i(t - \tau)$ is the membrane potential of the boutons connected to the V_i cell body by axons.

$z_{ij}(t)$ is the number of moles of E substance present in the synaptic cleft between boutons connected to the V_i cell body by axons and the V_j cell body.

$\overline{b}_{ij}(t)$ is the net amount of B substance in moles in the ij synaptic cleft at time t.

$\overline{c}_{ij}(t)$ is the net amount of C substance in moles in the ij synaptic cleft at time t.

Constants:

α is the decay rate for membrane potentials.

w_b is the deactivation rate for B substance in a synaptic cleft.

w_c is the deactivation rate for C substance in a synaptic cleft.

$\underline{a}$ is the released transmitter effectiveness factor on a cell body membrane potential. One mole of E substance released in a synaptic cleft results in an increase in the adjacent cell body's membrnae

potential of a volts.

τ is the interval between origination of a spike at a cell body and its arrival at the boutons attached to that cell body by axons.

The equations governing the system's performance:

8.4.15 $$\dot{x}_i(t) = -\alpha x_i(t) + P_i(t) + a\sum_j R(\dot{x}_j(t-\tau))z_{ji}(t)$$

where:

$$R(\dot{x}_j(t-\tau))z_{ji}(t)$$

is a special function defined by:

$$R(\dot{x}_j(t-\tau))z_{ji}(t) = \begin{cases} 0 \text{ if } x_j(t-\tau) \leq 0 \\ \text{an impulse of amplitude } z_{ji}(t) \text{ when } \dot{x}_j(t-\tau) > 0 \end{cases}$$

8.4.16 $$\dot{z}_{ji}(t) = [\min(\bar{b}_{ji}(t), \bar{c}_{ji}(t))]^+ - R(\dot{x}_j(t-\tau))z_{ji}(t)$$

where:

$$[\min(x, y)]^+ = \begin{cases} x \text{ if } x \leq y \text{ and } x > 0 \\ y \text{ if } y \leq x \text{ and } y > 0 \\ 0 \text{ if } x < 0 \text{ or } y < 0 \end{cases}$$

8.4.17 $$\dot{\bar{b}}_{ji}(t) = [-\dot{x}_j(t-\tau)]^+ - w_b[\bar{b}_{ji}(t) - \bar{c}_{ji}(t)]^+ - [\min(\bar{b}_{ji}(t), \bar{c}_{ji}(t))]^+$$

where:

$$[y]^+ = \begin{cases} y \text{ if } y > 0 \\ 0 \text{ if } y \leq 0 \end{cases}$$

8.4.18 $$\dot{\bar{c}}_{ji}(t) = [-\dot{x}_i(t)]^+ - w_c[\bar{c}_{ji}(t) - \bar{b}_{ji}(t)]^+ - [\min(\bar{b}_{ji}(t), \bar{c}_{ji}(t)]^+$$

section 8.5 Experiments with the Simplistic Neurophysiological Model

Equations 8.4.15 through 8.4.18 look formidable. They were simulated on a digital computer and it was experimentally verified that they work. A simple network consisting of one neuron, V_1, synapsing on another, V_2, was used. Since the method for the excitement of a cell body by transmitter substance is an impulse, the external inputs $P_1(t)$ and $P_2(t)$ were specified to be impulses of amplitude 10. The remaining parameters were selected arbitrarily to be:

$\alpha = 3.3333 \text{ sec.}^{-1}$

$\tau = 0.3$ sec.

$w_b = \infty$

$w_c = 0.5$

$a = 1.0$

Figure 8.5.1 shows the results. The impulse input $P_2(t)$ was presented to cell body V_2 exactly at the instant that the first spike $x_1(t - \tau)$ arrived at the 1,2 synapse. Thus the signals $x_1(t - \tau)$ and $x_2(t)$ exactly correlated. Therefore the amount of B substance entering the cleft per second was exactly equal to the amount of C substance. Thus all the B and C substance was used up instantly to produce E as is shown by the zero $\bar{b}_{12}(t)$ and $\bar{c}_{12}(t)$ traces. The amount of E produced was exactly enough to cause $x_1(t - \tau)$ to exactly correlate with $x_2(t)$ on the second response. Again all B and C was used up producing E and the amount of E produced was the same as before.

Since all the B and C substance was used up instantly to produce E, we can analytically compute the traces in figure 8.5.1. The response

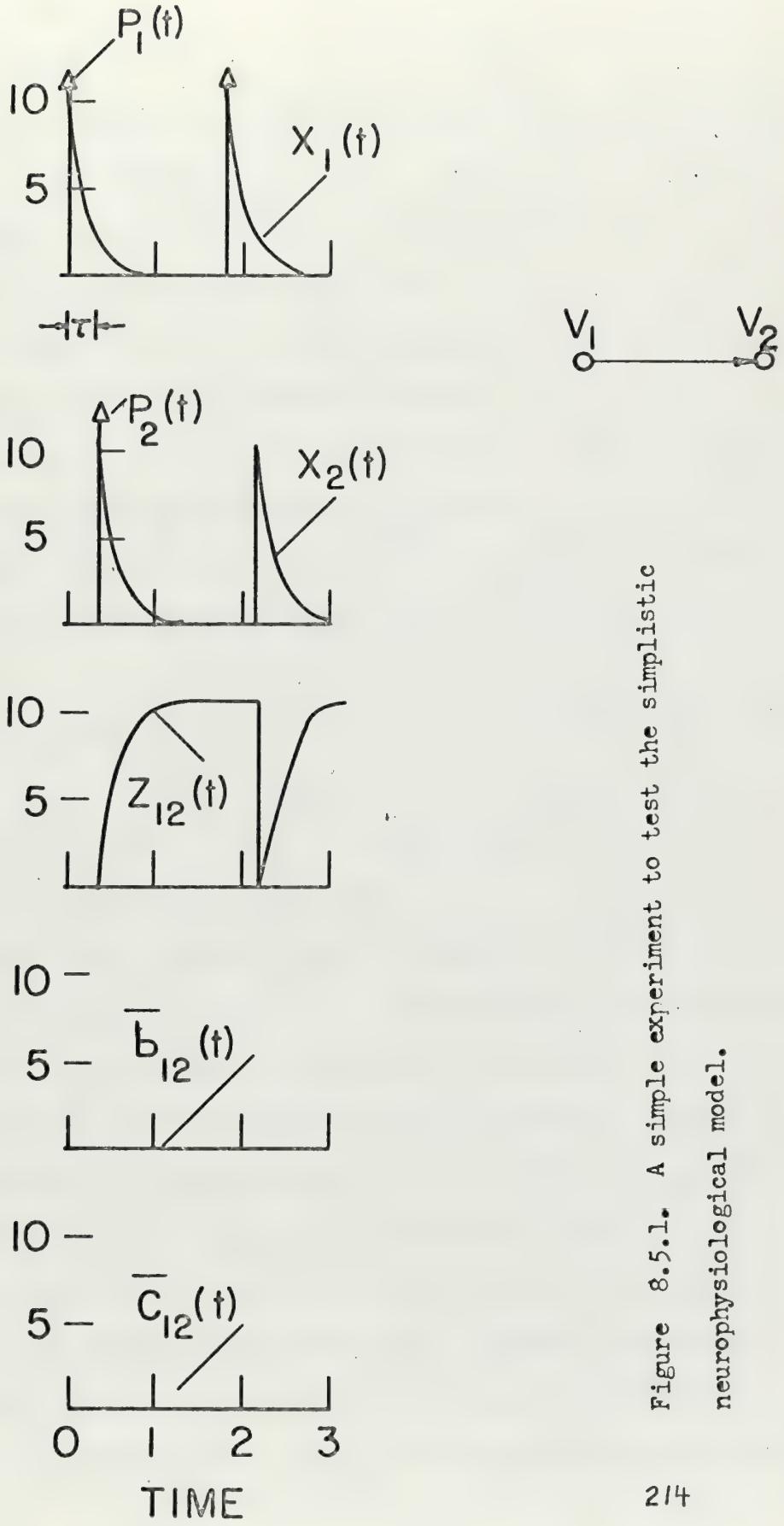

Figure 8.5.1. A simple experiment to test the simplistic neurophysiological model.

of V_1 to an impulse is:

$$x_1(t) = 10e^{-\alpha[t - 0.1]^+} \qquad \text{for } t \geq 0.1 \text{ sec.}$$

Allowing for the transmission delay between cell body v and the bouton, the bouton membrane potential is:

$$x_1(t - \tau) = 10e^{-\alpha[t-0.4]^+} \qquad \text{for } t \geq 0.4 \text{ sec.}$$

The response of V_2 to the impulse $P_2(t)$ is:

$$x_2(t) = 10e^{-\alpha[t-0.4]^+} \qquad \text{for } t \geq 0.4 \text{ sec.}$$

The amount of B entering the synaptic cleft is:

$$\dot{b}_{12}(t) = [-\dot{x}_1(t - \tau)]^+ = 10\alpha e^{-\alpha[t-0.4]^+} \qquad \text{for } t \geq 0.4 \text{ sec.}$$

similarly, the amount of C entering the cleft is:

$$\dot{c}_{12}(t) = [-\dot{x}_2(t)]^+ = 10\alpha e^{-\alpha[t-0.4]^+} \qquad \text{for } t \geq 0.4 \text{ sec.}$$

Since all the B and C entering the cleft is instantly used up producing E,

$$\dot{z}_{12}(t) = \dot{b}_{12}(t) = \dot{c}_{12}(t)$$

or:

$$z_{12}(t) = \int_{0.4}^{t} 10\alpha e^{-\alpha[t-0.4]^+} dt = 10(1 - e^{-\alpha[t-0.4]^+})$$

which is exactly what figure 8.5.1 shows.

The second $x_2(t)$ response is due to release of E by the sudden increasing leading edge of $x_1(t - \tau)$. This results in the instantaneous release of all E in the cleft as is shown by the z trace. From equation 8.4.15, the release of the E results in an instantaneous increase in the amplitude of $x_2(t)$ to a value of $az_{12}(t)$. As $a = 1.0$ and $z_{12}(t) = 10.5$, $x_2(t)$ suddenly jumps to a value of 10.5 as shown. When the sharp increasing leading edge of $x_1(t - \tau)$ is over, no more transmitter is released and the production process begins to produce E substance. The amplitudes are the same as in the first response and the same amount of E is produced again. As long as the amplitude of the impluse

exciting V_1 is kept at a value of 10, the same traces will be produced for as many excitements of V_1 as we desire. We will analytically prove this statement shortly.

If we consider the traces $x_1(t)$, $x_1(t - \tau)$, and $x_2(t)$ to be spikes, then the assumption that the input impulses amplitudes will remain constant is realistic. Spikes are always of the same amplitude and duration in a particular species of neurons. Note that once the transmitter substance was formed, arrival of the spike $x_1(t - \tau)$ at the bouton had the same effect as an input impulse on $x_2(t)$. Thus we may consider that our input impulses, $P_1(t)$ and $P_2(t)$ are the effects of spikes arriving at boutons synapsing on V_1 and V_2 which already have 10 molar units of E substance present in their synaptic clefts.

Figure 8.5.1 shows the result of the special case of a spike arriving at the 1,2 synapse at exactly the same time that V_1 is excited by an input impulse. To check the ability of these networks to learn when the input impulse to a cell body is delivered at a time different from the instant that a spike arrives at the synapse, another experiment was performed. One cell, V_c, was arranged so that it synapses on 5 other cell bodies in an outstar arrangement. The parameters in the network were kept the same as in the previous experiment. Figure 8.5.2 shows the arrangement of the neurons and the results.

The amount of B substance in the clefts, $\bar{b}_{ci}(t)$, was zero at all times. This is because the deactivation rate for B, w_b, was infinite. In the simulation, it was considered that the amount of B entering the cleft in an infinitesimal time interval, dt, was made available to react with any C present to form E. If there was any B left over after this reaction, it was immediately deactivated before any more

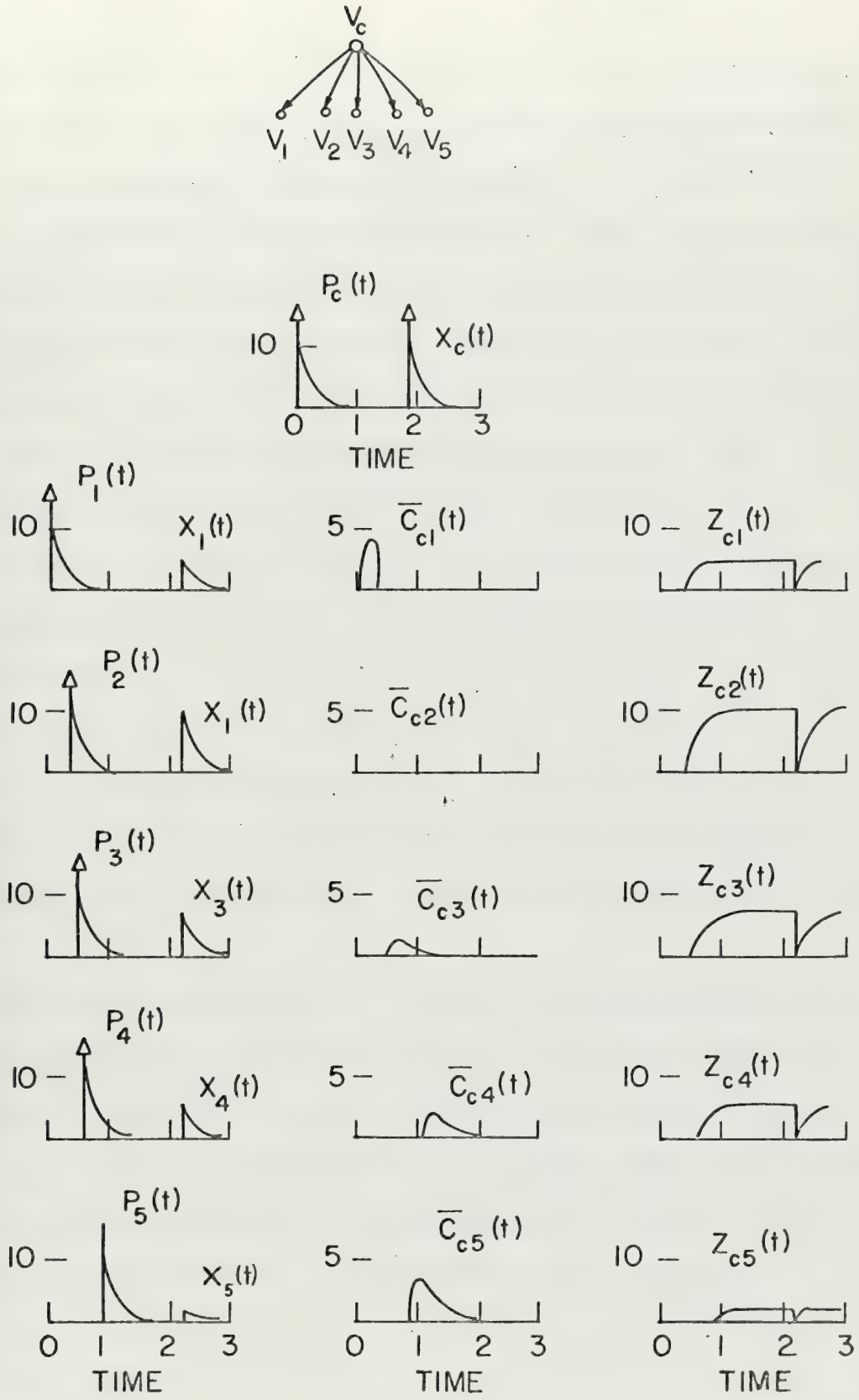

Figure 8.5.2. A more complex experiment with the simplistic neurophysiological model.

B entered the cleft in the next infinitesimal time interval.

Nevertheless, figure 8.5.2 is a good look at the processes going on in this model. The $\bar{c}_{c1}(t)$ and $\bar{c}_{c2}(t)$ traces show the instantaneousness of the E production reaction. V_1 was excited by an input impulse before the spike from V_c arrived at the boutons. Thus C was released into the c,1 synaptic cleft and began to be deactivated. When the spike arrived at the c,1 bouton, B was released into the cleft. Since there was more B being released into the cleft than there was C present in the cleft, all the C was instantly used up producing E. Thus $\bar{c}_{c1}(t)$ suddenly drops to zero when the spike arrives at the c,1 bouton at t = 0.4. However, enough of the C released by V_1 had already been deactivated when the spike arrived to allow $z_{c1}(t)$ to rise to a value of only 5.

The traces associated with V_2 are exactly the same as those associated with V_2 in the previous experiment. The spike arrived at the c,2 bouton at exactly the same instant that the $P_2(t)$ input impulse was delivered to V_2. Thus all the C and B released was used up producing E.

The traces associated with V_3, V_4, and V_5 show what happened when the input impulses are delivered to the cell bodies after arrival of the spike at the boutons. Because of the infinite deactivation rate for B, there was no accumulation of B in the cleft. Thus only the amount of B entering the cleft when these cell bodies were escited is available for reaction with C to form E. Remember that the B entering the cleft is:

$$\dot{b}_{c3}(t) = [-\dot{x}_c(t - \tau)]^+$$

and the C entering the cleft is:

$$\dot{c}_{c3}(t) = [-\dot{x}_3(t)]^+$$

V_3 was excited by the input impulse $P_3(t)$ at time $t = 0.5$. The spike arrived at the bouton at $t = 0.4$. Because of the infinite deactivation rate for B, all the B which entered the cleft before $t = 0.5$ was deactivated instantly. Thus the B available for reaction with the C which begins to enter the cleft after $t = 0.5$ is:

$$\dot{b}_{c3}(t) = [-\dot{x}_c(t-\tau)]^+ = 10\alpha e^{-\alpha 0.1} e^{-\alpha[t-0.5]^+} \text{ for } t \geq 0.5$$

The C which enters the cleft after $t = 0.5$ is:

$$\dot{c}_{c3}(t) = [-\dot{x}_3(t)]^+ = 10\alpha[e^{-\alpha[t-0.5]^+} \text{ for } t \geq 0.5 \text{ sec.}$$

Thus, the amount of C entering the cleft is a factor of $e^{0.1\alpha}$ greater than the B entering the cleft. The reaction $1 \cdot B + 1 \cdot C \rightleftharpoons 1 \cdot E$ is instantaneous and the coeficients of unity mean that $[\min(\dot{b}_{c3}(t), \dot{c}_{c3}(t)]^+$ of B is converted to E immediately upon entering the cleft. Since $b_{c3}(t)$ is less than $c_{c3}(t)$, all of the B is converted to E. Knowing this, we can analytically compute the amount of E produced:

$$\dot{z}_{c3}(t) = [\min(\bar{b}_{c3}(t), \bar{c}_{c3}(t))]^+ = \dot{b}_{c3}(t)$$

This last conclusion is a technical point. Since all the B entering the cleft is immediately used up, there can be no accumulation of B and $\bar{b}_{c3}(t)$ is technically zero. However, in an infinitesimal time interval, dt, $\dot{b}_{c3}(t)dt$ of B did enter the cleft. We must hypothesize an infinitesimal accumulation of B in the cleft of:

$$d\bar{b}_{c3}(t) = \dot{b}_{c3}(t)dt$$

Since $d\bar{b}_{c3}(t) < \bar{c}_{c3}(t)$ at all times, the amount of E produced during the time interval dt is:

$$dz_{c3}(t) = d\bar{b}_{c3}(t) = \dot{b}_{c3}(t)dt$$

Thus $\dot{z}_{c3}(t) = \dot{b}_{c3}(t)$.

The E produced at any time $t > 0.5$ is:

$$z_{c3}(t) = \int_{0.5}^{t} \dot{b}_{c3}(t)dt = \int_{0.5}^{t} [-\dot{x}_c(t-\tau)]^+ dt$$

$$= \int_{0.5}^{t} 10\alpha e^{-0.1\alpha} e^{-\alpha[t-0.5]^+} dt$$

$$= 10e^{-0.1\alpha}(1 - e^{-\alpha[t-0.5]^+}$$

For times sufficiently greater than $t = 0.5$, the E produced is:

$$z_{c3}(t >> 0.5) = 10e^{-0.1\alpha}$$

for $\alpha = 3.3333$, this gives us:

$$z_{c3}(t >> 0.5) \cong 7.2$$

which agrees very well with the experimental reaults shown on the $z_{c3}(t)$ traces in figure 8.5.2.

Since there was more C than B entering the c,3 cleft, and since C was deactivated at a finite rate, there is an accumulation of C in the cleft. The $\bar{c}_{c3}(t)$ trace shows this accumulation and its deactivation.

The traces associated with V_4 and V_5 are similar to those associated with V_3. The only difference is that V_4 and V_5 were excited by input impulses at progressively later times than V_3.

The second response shown on all the traces is a "prediction" response. The command cell body, V_c, was excited by an input impulse alone. The spike so generated traveled down the axons to the "grid" cell bodies, V_1 through V_5. When it arrived, it instantly released all the transmitter E substance in the synaptic cleft. Each of the "grid" cell bodies was excited to a membrane potential of $z_{ci}(t = 2.2)$. In this case, there was no time difference between the arrival of the

spike at the boutons and the excitement of the grid cell bodies. Both events occured at t = 2.2. Thus the amount of B being released into the clefts which could react with C to form E was:

$$\dot{b}_{ci}(t) = [-\dot{x}_c(t - \tau)]^+ = 10\alpha e^{-\alpha[t-2.2]^+} \quad \text{for } t \geq 2.2$$

However, the amount of C being released into the clefts at the same time was:

$$\dot{c}_{ci}(t) = [-\dot{x}_i(t)]^+ = az_{ci}(t = 2.2)\alpha e^{-\alpha[t-2.2]^+} \quad \text{for } t \geq 2.2$$

In all cases, the amount of C being released was less than or equal to the amount of B being released. Thus:

$$\dot{z}_{ci}(t) = az_{ci}(t = 2.2)\alpha e^{-\alpha[t-2.2]^+} \quad \text{for } t \geq 2.2$$

or:

$$z_{ci}(t) = az_{ci}(t = 2.2)\int_{2.2}^{t} \alpha e^{-\alpha[t-2.2]^+} dt =$$

$$az_{ci}(t = 2.2)(1 - e^{-\alpha[t-2.2]^+})$$

for t sufficiently greater than t = 2.2:

$$z_{ci}(t >> 2.2) \tilde{=} az_{ci}(t = 2.2)$$

which is what the $z_{ci}(t)$ traces in figure 8.5.2 show. Note that the effect of a prediction excitement of the grid cell bodies is to produce the exact amount of E after excitement as there was before the excitement. In this sense, the network is self-sustaining. We can continue to excite the grid cell bodies with prediction spikes for as long as we want. The result will be the same as the prediction response shown.

Because the amount of B being released was always greater than or equal to the amount of C being released during the prediction excitement, there is no accumulation of C in the clefts. The $\bar{c}_{ci}(t)$ traces are therefore zero during the prediction excitement.

section 8.6 Inhibition and an $\mathcal{L}_3$ Logic

We now have a simplistic model of a nervous system that is a synthesis of some neurophysiological facts, some assumptions, and embedding field theory. Although much thought went into the modeling process, we can not pretend the model is accurate. The fact that the model does work is a powerful argument for a deeper study of the embedding field theoretical assumptions concerning learning at the microscopic level in living organisms.

The time was not available for that deeper study. Shortly, we will drop the neurophysiological names that have been attached to the elements and processes in this model and consider it to be an embedding field network only. Before we do so, there is one further neurophysiological phenomena which occurs in nervous systems. At the microscopic level, inhibition consists of depressing the cell body membrane potential below the resting potential. Figure 8.6.1 shows a common inhibiting arrangement in the spinal column of vertebrates. The two large light neurons are motoneurons. The dark neuron is a Renshaw cell. The sequence of events shown on the traces is as follows: The cell body of motoneuron V_1 is excited by a spike. Its membrane potential rises with an EPSP and a reflected spike. This spike is propagated down V_1's axon. A collateral breaks off of this axon and synapses on the Renshaw cell's body. Arrival of the spike at this synapse excited the Renshaw cell body which fires a burst of spikes. These spikes propagate up the Renshaw cell's axon. The Renshaw cell's axon breaks up into two collaterals. One synapses on the V_1 cell body and another synapses on the V_2 cell body. When the burst of spikes

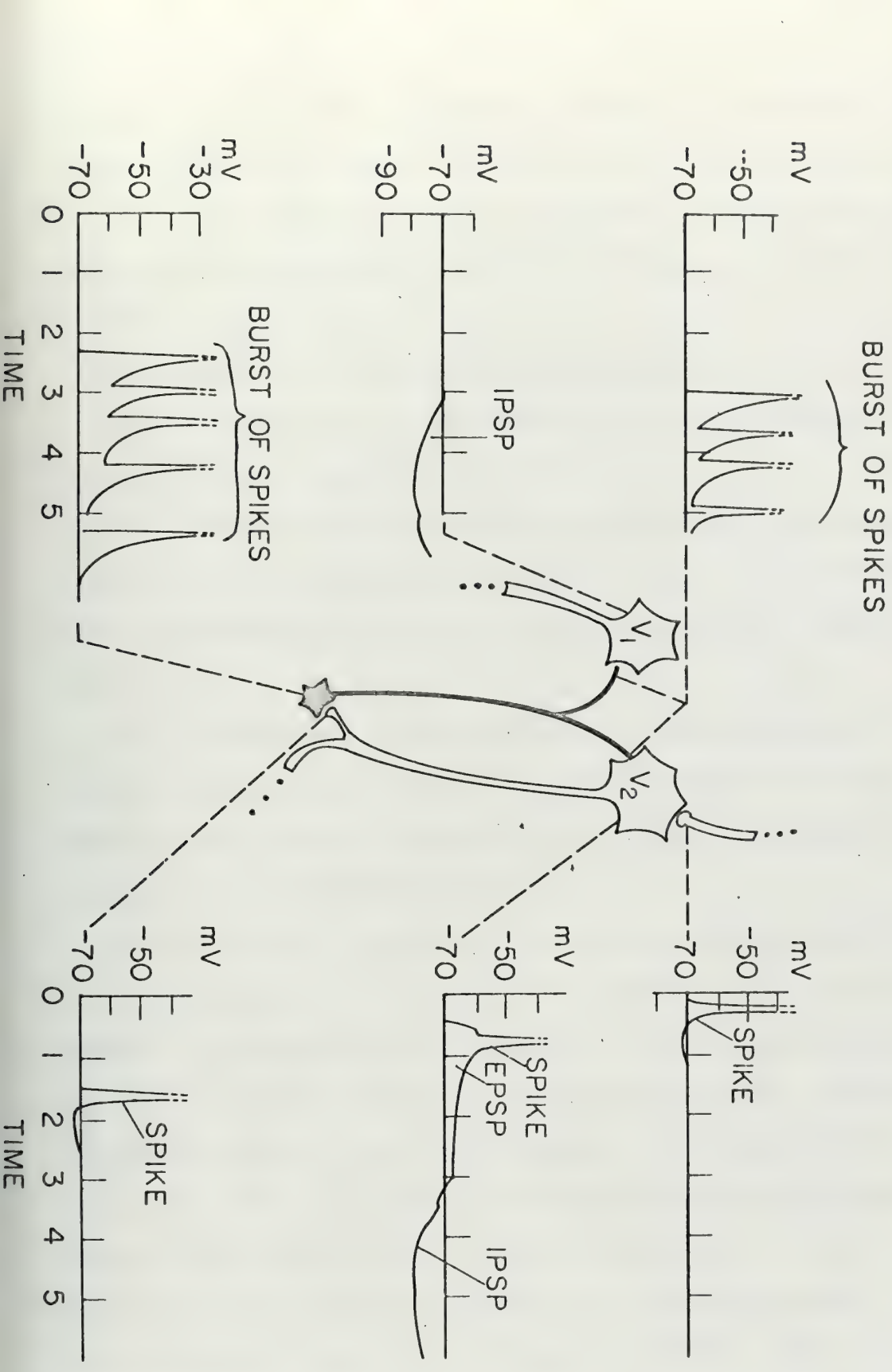

Figure 9.7.1. A common inhibitory arrangement in the spinal column of vertebrates. The dark neuron is a Renshaw cell. The light neurons are motoneurons.

arrives at these synapses, inhibitory transmitter is released. The inhibitory transmitter causes a decrease in the membrane potentials of V_1 and V_2 below resting potential. The membrane potential traces which are below resting potential are called inhibitory post synaptic potentials or IPSP's.

The important things we want to note from figure 8.6.1 are:

(a) The Renshaw cell's body membrane potential increases in the positive direction when it is excited.

(b) The spikes propagated along the Renshaw cell's axon are similar to the spikes along the motoneuron's axons. In particular they are increases in the positive direction of the axon's membrane potential.

(c) A transmitter substance is releasee by these spikes. It causes a decrease in the motoneuron's cell body membrane potential. This decrease in membrane potential does not cause any change in the motoneuron's axon membrane potentials.

These facts show that there is no negative membrane potential propagated anywhere in the system. All propagating signals are positive signals. In the discussion of allowable prediction signal states in section 7.2, we did not allow the propagation of negative amplitude prediction signals. We made this restriction on the grounds of consistency and the fact that negative amplitude prediction signals were not needed in an outstar. In the nervous system of living organisms, negative amplitude "prediction" signals do not occur. Thus our restriction on the allowable states of prediction signals in embedding field networks is consistent with neurophysiological data.

The inhibitory transmitter substance released by the Renshaw cell's burst of spikes is considered to be a chemical substance that is different from the excitory transmitter which excites the motoneuron's cell bodies. There are at least three chemical substances which act as transmitter in nervous systems. They are acetycholine, epinephrine, and norepinephrine. In one part of the body, and with one species of neuron, one of the substances may act as an excitory transmitter and another may act as an inhibitory transmitter. In another part of the body and with another species of neuron, their effects may reverse.

With these few facts in mind, we will now invent a simplistic model for inhibition which we shall add to our previous model. Firstly, we will postulate an inhibitory transmitter substance H which is different from our excitory transmitter substance E. Since the H and E may reverse their roles in other parts of the nervous system, we want the processes for production and release of H to be similar to those for E. Therefore we will assume that H substance is stored in the synaptic cleft. It is released when the adjacent bouton membrane potential is increasing, i.e., when $\dot{x}(t - \tau) > 0$. We will further assume that the release of one mole of H will result in an instantaneous increase in the adjacent cell body membrane potential of γ volts. Note that this is an <u>increase</u> of γ volts. We have specified that the release of one mole of E will result in an instantaneous cell body membrane ptoential increase of $\underline{a}$ volts. By specifying a or γ positive or negative, we can specify their effects in various parts of our system. However, normally γ will be assigned a negative value.

We must now invent a process which will produce H substance from chemical substances available in the synaptic cleft. To do this we will look closely at the Renshaw cell bouton-motoneuron synapse in figure 8.6.1. The effect of H substance is a decrease in the motoneuron's cell body membrane potential. This is caused by an increase in the cell body membrane's permeability to K+ and Cl- ions. With the sodium pump working to eject Na+, the net effect is an increase of K+ ions inside the cell body. Remember that we allowed C substance to be released when the cell body membrane potential was above resting potential, but decreasing. When the cell body membrane potential is above resting potential but decreasing, K+ ions are diffusing out of the cell body. Thus we have sort of tied the release of C substance to the diffusion of K+ ions out of the cell body. Now, when the cell body's membrane potential is decreasing below resting potential, K+ ions are diffusing into the cell body. Thus we may assume that no C substance is being released into the synaptic cleft when the cell body membrane potential is decreasing below rest potential. We will make the further assumption that no C substance is released at any time when the cell body's membrane potential is below resting potential. Thus C substance can not be involved in the production of H substance. We could postulate another chemical substance which is released from the cell body into the synaptic cleft when the cell body membrane potential is below resting potential. This is a valid option, but we will not investigate it further.

Since the Renshaw cells' spikes are the same as all other spikes, B substance is being released from the Renshaw cells' boutons. Thus B substance could be a reactant in the production of H. Suppose that

there is a substance, S, which is always present in large quantities in the synaptic cleft. Suppose further that a substance reacts with B substance according to:

8.6.1 $\quad 1 \cdot B + 1 \cdot S \rightleftharpoons 1 \cdot H$

Suppose further that this reaction is fast, but not as fast as the reaction producing E substance. Then excitation of a bouton with a spike will release B substance. If there is C substance present in the cleft, then $[\min(\dot{b}(t), \bar{c}(t))]^+$ of E substance will be produced. If there is any B left over after this reaction, it will combine with S to form H. In the experiments of section 8.5 we saw that an accumulation of B in the cleft is not necessary for learning. (The accumulation of B in those experiments was always zero because the deactivation rate for B, w_b, was infinite.) Further, if we make this postualtion, then the logic governing the performance of the elements in the network will be an $\mathcal{L}_3$ logic.

An $\mathcal{L}_3$ logic conforms to the following tabulation:

Table 8.6.1

$\bar{x}_c$	$\bar{x}_i$	$\mathcal{L}_3(\bar{x}_c, \bar{x}_i) = \bar{z}_{ci}$
0	0	0
0	+1	0
+1	0	-1
+1	+1	+1
+1	-1	-1
0	-1	0

In the current context, this tabulation means that there is no transmitter substance, E or H, produced when the bouton membrane potential is at resting potential, or $\bar{x}_c = 0$. This is independent of whatever the adjacent cell body membrane potential may be. However, when the

bouton membrane potential is above resting potential, there are three cases: When the adjacent cell body membrane potential is at or below resting potential, inhibitory H transmitter substnace is formed. If the adjacent cell body membrane potential is avove resting potential, but decreasing, then excitory E substance is formed.

Thus the reaction $1 \cdot B + 1 \cdot S \rightleftharpoons 1 \cdot H$ accomplishes one of the stated aims of this chapter - the implementation of an $\mathcal{L}_3$ logic. We will therefore adopt it as the chemical reaction producing H substance in the model.

The alert reader may have noticed that we have already accomplished the third aim of this chapter. We have already invented a process which does not cause "pulse lengthening" of a signal being transmitted through a neuron or embedding field node cascade. Consider a cascade of N neurons, $V_1, V_2, \ldots, V_N$. The V_{j-1} neuron synapses on the V_j neuron. The V_1 neuron is the "starting" neuron. Suppose that each of the j-1,j synaptic clefts in the cascade contains A moles of E substance. Let the E effectiveness factor, a, be a = 1.0. For simplicity let the H effectiveness factor, γ, be $\gamma = 0$, so that we do not have to worry about inhibition. Let the "starting" neuron, V_1, be excited by an input impulse of amplitude A at time t_1. Then:

$$x_1(t) = \begin{cases} 0 \text{ for } t < t_1 \\ Ae^{-t} \text{ for } t \geq t_1 \end{cases}$$

This signal will arrive at the 1,2 synapse at $t_1 + \tau$. It will cause the release of all the E substance present. Thus:

$$x_2(t) = \begin{cases} 0 \text{ for } t < t_1 + \tau \\ Ae^{-at} \text{ for } t \geq t_1 + \tau \end{cases}$$

Since $x_2(t)$ and $x_1(t-\tau)$ are identical, A moles of E will be produced in the 1,2 cleft by the E production process after $t = t_1+\tau$. The same argument holds for each pair of neurons, V_{j-1}, V_j, in the cascade. Thus:

$$x_j(t) = \begin{cases} 0 \text{ for } t < t_1 + (j-1)\tau \\ Ae^{-\alpha t} \text{ for } t \geq t_1 + (j-1)\tau \end{cases}$$

Except for the time delay, $(j-1)\tau$, the signal is transmitted through the cascade unchanged. There is no "pulse lengthening". Additionally, the self-sustaining property of the E production insures that we can propagate any number of signals through the cascade without distortion. (Note, this last statement is true only if there is a time interval between consecutive signals which is large enough to allow the E production process to produce approximately A moles of E before the next signal is started at the "starting" neuron. In practice, making this interval $3/\alpha$ seconds is sufficient.)

The reason that such a cascade does not distort a signal is simple. The input signal to the "starting" neuron is an impluse. The "prediction" input signal to all the cell bodies in the cascade is also an impulse. This is because the effect of the release of A moles of E in a synaptic cleft is an instantaneous increase of the adjacent cell body membrane potential of A volts. The effect of an input impulse is an instantaneous increase of the cell body membrane potential of A volts. Thus the effect of an input impulse and a "prediction" excitement are the same.

Having modeled an arbitrary mechanism, we will now drop the neurophysiological names assigned to the elements and processes of the nodes and replaced them with embedding field names. To do so, we must add a "synaptic cleft" between the arrowheads of the embedding field

theory and the adjacent node. This is added to give us a definite place for the chemical reactions we have invented to occur. We will denote the synaptic cleft between the N_{ji} arrowhead and the V_i node by S_{ji}. Because our model works according to chemical reactions, we will call a network composed of elements from this model a chemical embedding field network. We list here a complete description of the processes. There are several new variables in the following equations. They are defined after the equations.

Equations for the chemical embedding field network processes:

8.6.2 $$\dot{x}_i(t) = -\alpha x_i(t) + P_i(t) + a\sum_j R(\dot{p}_j(t-\tau))z_{ji}(t) + \gamma\sum_j R(p_j(t-\tau))h_{ji}(t)$$

where $R(\dot{p}_j(t-\tau))y(t)$ is a special function defined by:

$$R(\dot{p}_j(t-\tau))y(t) = \begin{cases} 0 \text{ if } \dot{p}_j(t-\tau) \leq 0 \\ \text{an impulse of amplitude } y(t) \text{ when } \dot{p}_j(t-\tau) > 0 \end{cases}$$

8.6.3 $$p_j(t-\tau) = [x_j(t-\tau)]^+$$

8.6.4 $$\dot{z}_{ji}(t) = [\min(\dot{\bar{b}}_{ji}(t), \bar{c}_{ji}(t))]^+ - R(\dot{p}_j(t-\tau))z_{ji}(t)$$

where:

$$[\min(x, y)]^+ = \begin{cases} x \text{ if } x \leq y \text{ and } x > 0 \\ y \text{ if } y \leq x \text{ and } y > 0 \\ 0 \text{ if } x < 0 \text{ or } y < 0 \end{cases}$$

8.6.5 $$\dot{h}_{ji}(t) = [\dot{\bar{b}}_{ji}(t) - [\min(\dot{\bar{b}}_{ji}(t), \bar{c}_{ji}(t)]^+]^+ - R(\dot{p}_j(t-\tau))h_{ji}(t)$$

8.6.6 $$\dot{\bar{b}}_{ji}(t) = [-\dot{p}_j(t-\tau)]^+ - [\min(\dot{\bar{b}}_{ji}(t), \bar{c}_{ji}(t))]^+$$

where:

$$[y]^+ = \begin{cases} y \text{ if } y > 0 \\ 0 \text{ if } y \leq 0 \end{cases}$$

8.6.7 $$\dot{\bar{c}}_{ji}(t) = [-\dot{\overline{[x_i(t)]^+}}]^+ - w_c[\bar{c}_{ji}(t) - \bar{b}_{ji}(t)]^+ - [\min(\bar{b}_{ji}(t), \bar{c}_{ji}(t)]^+$$

Definition of the variables:

$x_i(t)$ is the conventional x process which occurs at node V_i.

$p_j(t - \tau)$ is the prediction signal at the arrowheads connected to node V_j by directed edges. Since we do not allow negative amplitudes for prediction signals, $p_j(t - \tau) = [x_j(t - \tau)]^+$. Only the first derivative, $\dot{p}_j(t - \tau)$ is used in the above equations.

$P_i(t)$ is the conventional event input impulse. In this study of the chemical embedding field networks, $P_i(t)$ will be constrained to be an impulse of amplitude A.

$z_{ji}(t)$ is the amount of excitory transmitter substance, E, in the S_{ji} synaptic cleft.

$h_{ji}(t)$ is the amount of inhibitory transmitter substance, H, in the S_{ji} synaptic cleft.

$\bar{b}_{ji}(t)$ is the amount of B substance in the S_{ji} synaptic cleft.

$\bar{c}_{ji}(t)$ is the amount of C substance in the S_{ji} synaptic cleft.

Definition of the constants:

α is the decay rate for x processes.

a is the effectiveness factor for E substance. Release of 1 unit of E in the synaptic cleft will result in an instantaneous increase in the amplitude of the adjacent nodes' x process of $\underline{a}$.

γ is the effectiveness factor for H substance. Release of 1 unit of H in the synaptic cleft will result in an instantaneous increase in the amplitude of the adjacent nodes' x process of γ. γ will have negative values throughout the rest of this study.

τ is the transmission delay due to finite transmission velocities on directed edges. A signal which originates at the V_i node at time t_i

will arrive at the arrowheads connected to this node at time $t_i + \tau$.

w_c is the rate constant for deactivation of C substance.

Discussion:

Equations 8.6.2 through 8.6.7 are a mathematical description of the processes we have invented in this chapter. They are different from equations 8.4.15 through 8.4.18 because they include the addition of the inhibitory processes.

The functions $a\sum_j R(\dot{p}(t-\tau))z_{ji}(t)$ and $\gamma\sum_j R(p_j(t-\tau))h_{ji}(t)$ in equation 8.6.2 say that when the prediction signal $p_j(t-\tau)$ arriving at the N_{ji} arrowhead is increasing, all the E and H substances in the S_{ji} synaptic cleft is released instantly. The release of these substances at time t_0 causes an instant increase in the amplitude of the adjacent $x_i(t)$ process of $az_{ji}(t_0) + \gamma h_{ji}(t_0)$.

E substance is produced in the synaptic cleft according to the instantaneous reaction:

$1\cdot B + 1\cdot C \rightleftharpoons 1\cdot E$

Because the unit coeficients in this equation, the maximum amount of E that can be produced at any time is the minimum of the reactants available. Equation 8.6.6 says that the amount of B being released into the S_{ji} cleft per second is $[-\dot{p}_j(t-\tau)]^+$. That is, the amount of B being released from the N_{ij} arrowhead into the S_{ji} cleft is directly proportional to the decrease per second in the amplitude of the prediction signal at the N_{ji} arrowhead. The B substance thus released is first made available for reaction with C to form E. If there is any B left over after this reaction, it reacts with S substance to form H substance. S substance is always present in large quantities in the

cleft. Equation 8.6.5 says this mathematically.

The amount of C released into the S_{ji} cleft per second is directly proportional to the decrease per second in the amplitude of the adjacent V_i nodes' x process, provided that x process is positive. The term $[-\overline{[\dot{x}_i(t)]^+}]^+$ in equation 8.6.7 says this. The amount of C present in the cleft is first made available to react with any B present to form E. If there is any C left over after this reaction, it is deactivated at rate w_c. Equation 8.6.7 states this mathematically.

Although equations 8.6.3 through 8.6.7 are complicated and describe a complicated set of simultaneous processes, they are fairly straight forward to simulate on a digital computer. In the next section, we shall study an outstar network governed by these equations.

section 8.7 A Chemical Outstar

An outstar composed of chemical embedding field elements was set up. The standard experiment that has been performed in the other outstars studied was performed. The events inputs to the nodes were specified to be impulses of amplitude A = 10. From equations 8.6.2 through 8.6.7, there are five network parameters to be specified: α, τ, a, δ, and w_c. α and τ were specified as in the past:

$\alpha = 3.333$ sec.$^{-1}$

$\tau = 0.3$ sec.

The deactivation rate for C substance, w_c, was arbitrarily specified to be:

$w_c = 0.5$ sec.$^{-1}$

Since an excitory transmitter (E) substance effectiveness factor of a = 1.0 has resulted in self-sustaining systems in the past, a was specified to be:

a = 1.0

The specification of the new inhibitory transmitter (H) substance effectiveness factor, δ, will require some discussion. The chemical outstar conforms to logic $\mathcal{L}_3$ tabulated in table 8.6.1. The three assignments in that table which can cause the "z" processes to be driven to non ambient states are:

8.7.1 $\mathcal{L}_3(\bar{x}_c = +1, \bar{x}_i = +1) = +1$

8.7.2 $\mathcal{L}_3(\bar{x}_c = +1, \bar{x}_i = 0) = -1$

8.7.3 $\mathcal{L}_3(\bar{x}_c = +1, \bar{x}_i = -1) = -1$

In the current context, 8.7.1 says that an excited prediction signal at an arrowhead and an excited x process at the adjacent node results

in the production of E substance. This is equivalent to driving a "z" process in the excitory direction. The other two assignments say that when the prediction signal is in an excited state and the adjacent node x process is in an ambient or inhibited state, H substance will be produced. This is equivalent to driving a conventional "z" process in the inhibitory direction. In the last chapter, we introduced the idea that an outstar may have its grid nad command nodes randomly excited before it "goes to school" to learn a pattern. According to the $\mathcal{L}_3$ logic, random excitement of the grid nodes can not change the "z" process state. However, random excitement of the command node can result in the outstar learning to directly inhibit all the grid nodes according to assignments 8.7.2 and 8.7.3. In a real environment we can expect this to be the case before the outstar "goes to school". Thus the outstar will be inhibitorally biased before we try to teach it a pattern. We must insure that this inhibitory biasing is not so great as to prevent the outstar from learning a pattern.

To facilitate this discussion, we will prove the following lemma:

Lemma 8.7.1

Let a node V_1 have an arrowhead N_{12} impinging on another node V_2. Let the fundtions $z_{12}(t) = h_{12}(t) = 0$. Let node V_1 be excited by a positive impulse of amplitude A_1 at time t_1. Let node V_2 be excited at time $t_2 = t_1 + \tau$ by an input impulse of amplitude A_2 which may be negative. Then the amount of H substance in the S_{12} synaptic cleft at times $t >> t_1 + \tau = t_2$ is:

$$h_{12}(t >> t_2) \cong \begin{cases} 0 \text{ if } 0 < A_1 < A_2 \\ A_1 - A_2 \text{ if } 0 < A_2 < A_1 \\ A_1 \text{ if } A_2 \leq 0 \end{cases}$$

And the amount of E substance in the S_{12} synaptic cleft at times $t >> t_1 + \tau = t_2$ is:

$$z_{12}(t >> t_2) \cong \begin{cases} A_1 \text{ if } 0 < A_1 < A_2 \\ A_2 \text{ if } 0 < A_2 < A_1 \\ 0 \text{ if } A_2 \leq 0 \end{cases}$$

Proof:

The input impulse to node V_1 results in a prediction signal arriving at the arrowhead at time $t_1 + \tau = t_2$ which is:

$$p_1(t) = \begin{cases} 0 \text{ for } t < t_2 \\ A_1 e^{-\alpha[t-t_2]^+} \text{ for } t \geq t_2 \end{cases}$$

The input impulse to node V_2 results in an $x_2(t)$ process:

$$x_2(t) = \begin{cases} 0 \text{ for } t < t_2 \\ A_2 e^{-\alpha[t-t_2]^+} \text{ for } t \geq t_2 \end{cases}$$

The amount of B substance released into S_{12} is:

$$\dot{b}_{12}(t) = [-\dot{p}_{12}(t)]^+ = \begin{cases} 0 \text{ for } t < t_2 & \text{for } t < t_2 \\ A_1 \alpha e^{-\alpha[t-t_2]^+} & \text{for } t \geq t_2 \end{cases}$$

The amount of C substance reseased into S_{12} is:

$$\dot{c}_{12}(t) = [-[\dot{x}_2(t)]^+]^+ = \begin{cases} 0 \text{ for } t < t_2 \\ 0 \text{ for } t \geq t_2 \text{ if } A_2 \leq 0 \\ A_2 \alpha e^{-\alpha[t-t_2]^+} \text{ for } t \geq t_2 \end{cases}$$

Thus the amount of E being formed is:

$$z_{12}(t) = \int_{t_2}^{t} [\min(\dot{b}_{12}(t), \dot{c}_{12}(t))]^+ dt$$

$$= \begin{cases} 0 \text{ for } t \geq t_2 \text{ if } A_2 = 0 \\ A_2(1 - e^{-\alpha[t-t_2]^+} \text{ for } t \geq t_2 \text{ if } 0 < A_2 < A_1 \\ A_1(1 - e^{-\alpha[t-t_2]^+} \text{ for } t \geq t_2 \text{ if } 0 < A_1 < A_2 \end{cases}$$

Thus for $t >> t_2$:

$$z_{12}(t >> t_2) \cong \begin{cases} 0 \text{ if } A_2 \leq 0 \\ A_2 \text{ if } 0 < A_2 < A_1 \\ A_1 \text{ if } 0 < A_1 < A_2 \end{cases}$$

The amount of H being formed is equal to the amount of B left over after the E production reaction.

$$h_{12}(t) = \int_{t_2}^{t} \left[\dot{b}_{12}(t) - \left[\min(\dot{b}_{12}(t), \dot{c}_{12}(t)) \right]^+ \right]^+ dt$$

$$= \begin{cases} 0 \text{ if } A_1 < A_2 \text{ for all } t \\ (A_1 - A_2)(1 - e^{-\alpha[t-t_2]^+}) \text{ if } 0 < A_2 < A_1 \text{ for } t \geq t_2 \\ A_1(1 - e^{-\alpha[t-t_2]^+}) \text{ if } A_2 \leq 0 \text{ for } t \geq t_2 \end{cases}$$

Thus for $t >> t_2$:

$$h_{12}(t >> t_2) \cong \begin{cases} 0 \text{ if } A_1 < A_2 \\ A_1 - A_2 \text{ if } 0 < A_2 < A_1 \\ A_1 \text{ if } A_2 \leq 0 \end{cases}$$

Note that by lemma 8.7.1, $h_{12}(t > t_2) + z_{12}(t > t_2) \cong A_1$. Also note that immediately after arrival of a prediction signal at the N_{12} arrowhead, $h_{12}(t) = z_{12}(t) = 0$. Thus lemma 8.7.1 applies to the situations where there is H and/or E substance present in S_{12} before arrival of a prediction signal. Since arrival of a prediction signal causes the equivalent of input impulses of amplitudes $az_{12}(t)$ and $\gamma h_{12}(t)$ to be delivered to V_2, this lemma can be used in all cases by setting $A_2 = az_{12}(t) + \gamma h_{12}(t) + A_i$, where A_i is the amplitude of an external input impulse, if any.

Now, suppose we start our outstar in a state of initial ignorance. That is, $z_{ci}(0) = h_{ci}(0) = 0$. Let $0 > \gamma > -1$. We then excite the command node with an input impulse of amplitude A without exciting the

grid nodes. By lemma 8.7.1, $h_{ci}(t) = A$ and $z_{ci}(t) = 0$. Suppose we excite the command node again without exciting the grid nodes. When the prediction signal arrives at the N_{ci} arrowheads, all the transmitter substance is released. Thus the grid nodes are excited by impulses of amplitude $\gamma A < 0$. Then by lemma 8.7.1, A units of H will be produced in the synaptic clefts, S_{ci}. Thus, before the outstar "goes to school", the synaptic clefts contain A units of H and 0 units of E.

Now let the outstar "go to school". The command node and the grid nodes are excited with input impulses of amplitude A. The command prediction signal will cause a further impulse of amplitude $\gamma A < 0$ to excite each of the grid nodes. Thus the grid nodes will be excited by a total input of $A(1 + \gamma)$. Thus $A(1 + \gamma)$ of E will be produced. (Remember that $0 > \gamma > -1$)

Suppose we want the outstar to be able to directly inhibit a single occurance of a random mistake. To the outstar, the first presentation of the pattern after going to school is considered a random mistake. Thus we want as much of H produced as E. On this criteria, $\gamma = -0.5$ is specified. Now, let us present the pattern a second time. The total input impulse amplitude to the grid nodes in the pattern will be $A(1 + \gamma) + A\gamma + A = 0.5A - 0.5A + A = A$. Thus A units of E will be produced on the second presentation of the pattern. 0 units of H will be produced.

Thus by specifying $\gamma = -0.5$, we will have an outstar that is resistant to single occurances of random mistakes, but will learn a pattern well in two presentations. Therefore, for the experiment, γ is specified to be:

$$\gamma = -0.5$$

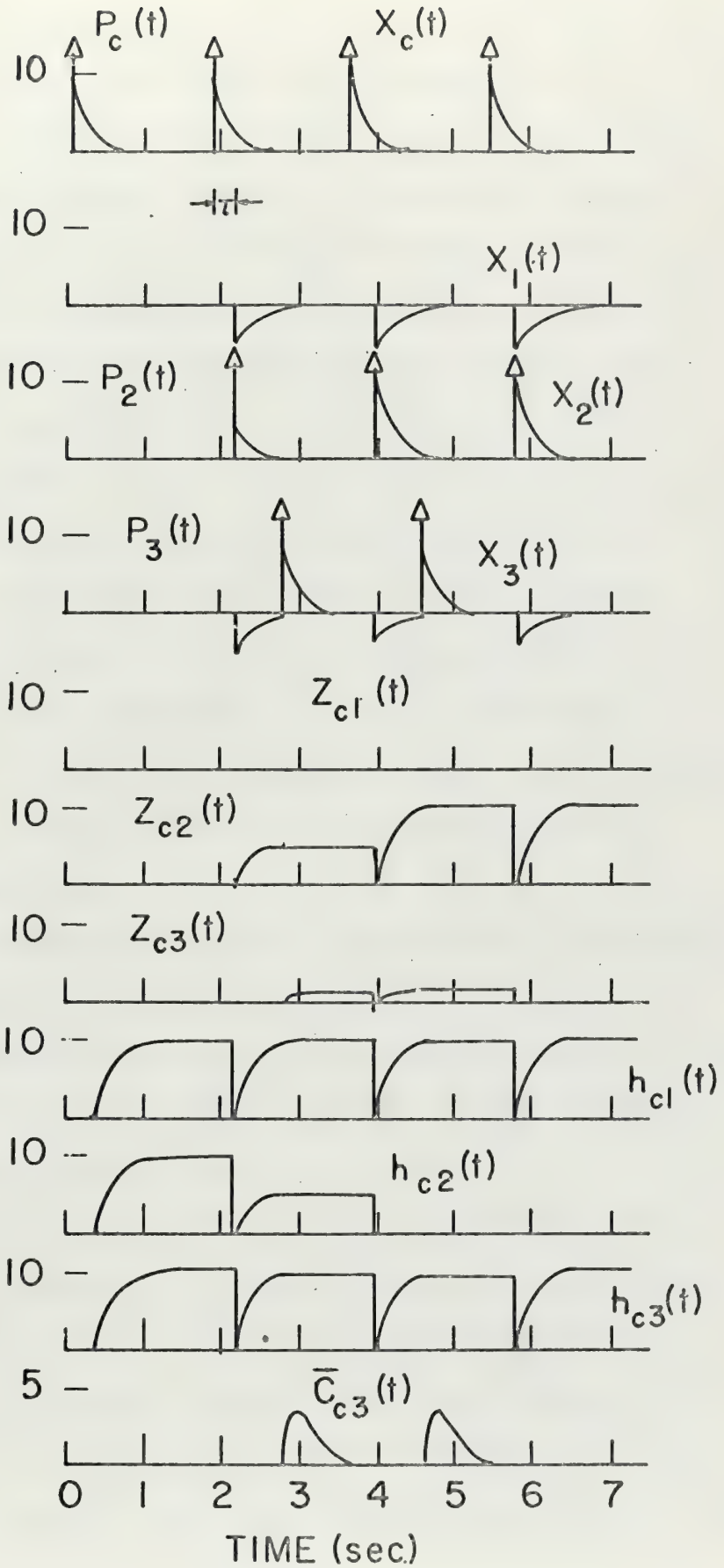

Figure 8.7.1. Teaching a chemical outstar the pattern $V_c \rightarrow V_2$. Note the inhibitory biasing before the outstar "goes to school".

Figure 8.7.1 shows the results of the first part of the experiment. The command node is excited once alone at the beginning of the experiment. The z traces show that no E was produced in the synaptic clefts. The h traces show that 10 units of H was produced in the clefts. Thus the outstar is inhibitorally biased before "going to school". "School" begins with the second command node excitement. Event 2 is presented exactly when the command prediction signal arrives at the arrowheads. Event 3 is presented $2/\alpha = 0.6$ seconds later. The pattern is presented twice.

In both presentations of the pattern, significantly more H is produced in the S_{c3} cleft than E. Since event 1 is not presented, 10 units of H are produced in the S_{c1} cleft. No E is produced in the S_{c1} cleft. On the first presentation of the pattern, the amount of E and H produced in the S_{c2} cleft approximately balance. On the second presentation of the pattern, 10 units of E are produced in the S_{c2} cleft and no H is produced.

The fourth excitement of the command nodes results in a prediction excitement of the grid. The third response on the grid x traces in this prediction excitement of the grid. From the results we can conclude that the outstar has learned the pattern $V_c \rightarrow V_2$. It has also learned to directly inhibit grid nodes V_1 and V_3.

The experiment was continued to test the random mistake in the previously learned pattern $V_c \rightarrow V_2$. Figure 8.7.2 shows the results. The direct inhibition of V_1 which the outstar had previously learned caused $x_1(t)$ to rise to a value of only 5. (The input impulse, $P_1(t)$ has an amplitude of 10.) The amounts of H and E produced in the S_{c1} cleft approximately balance. Thus when a prediction is excited by the

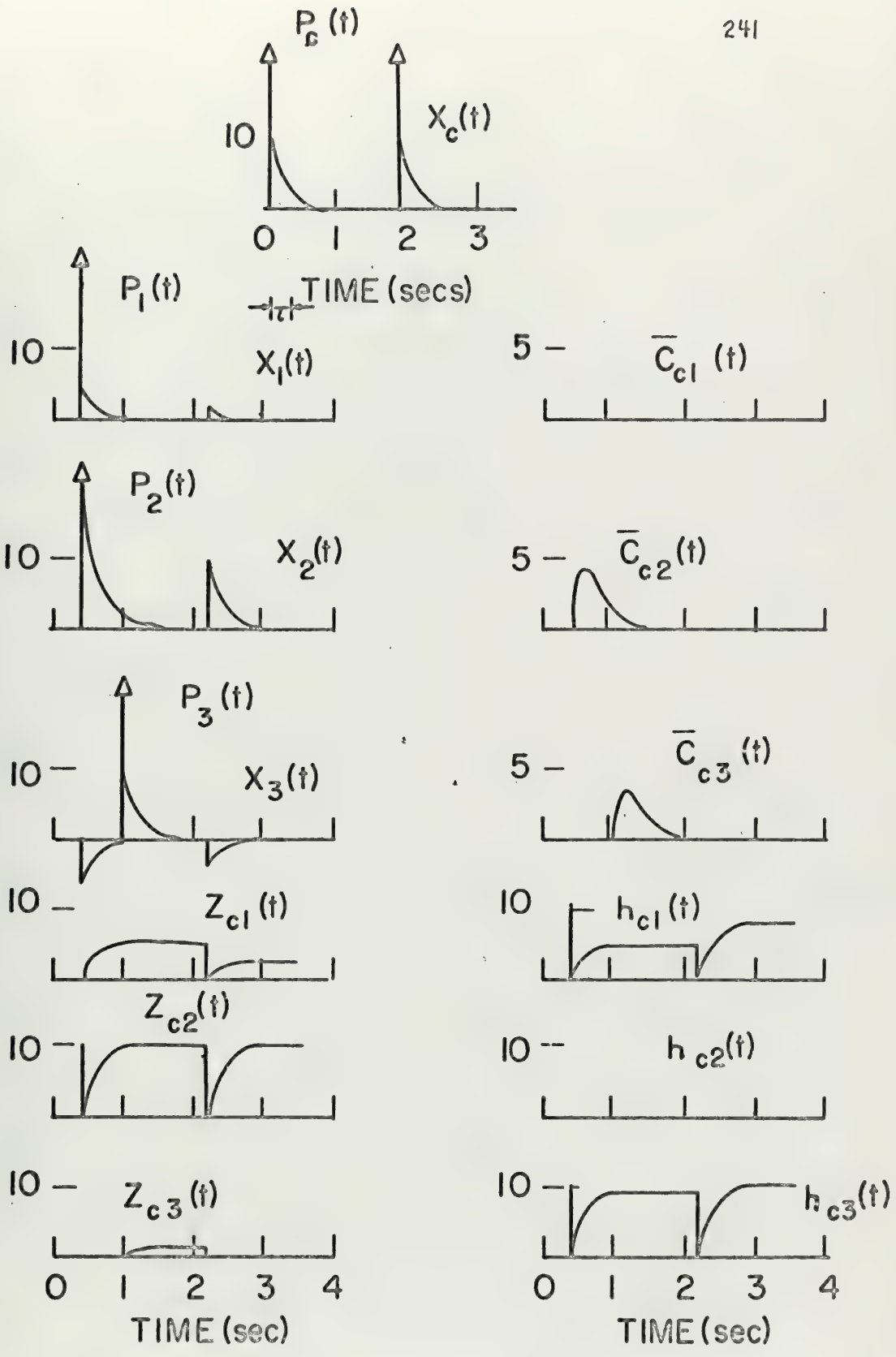

Figure 8.7.2. Resistance to random mistakes in a chemical outstar.

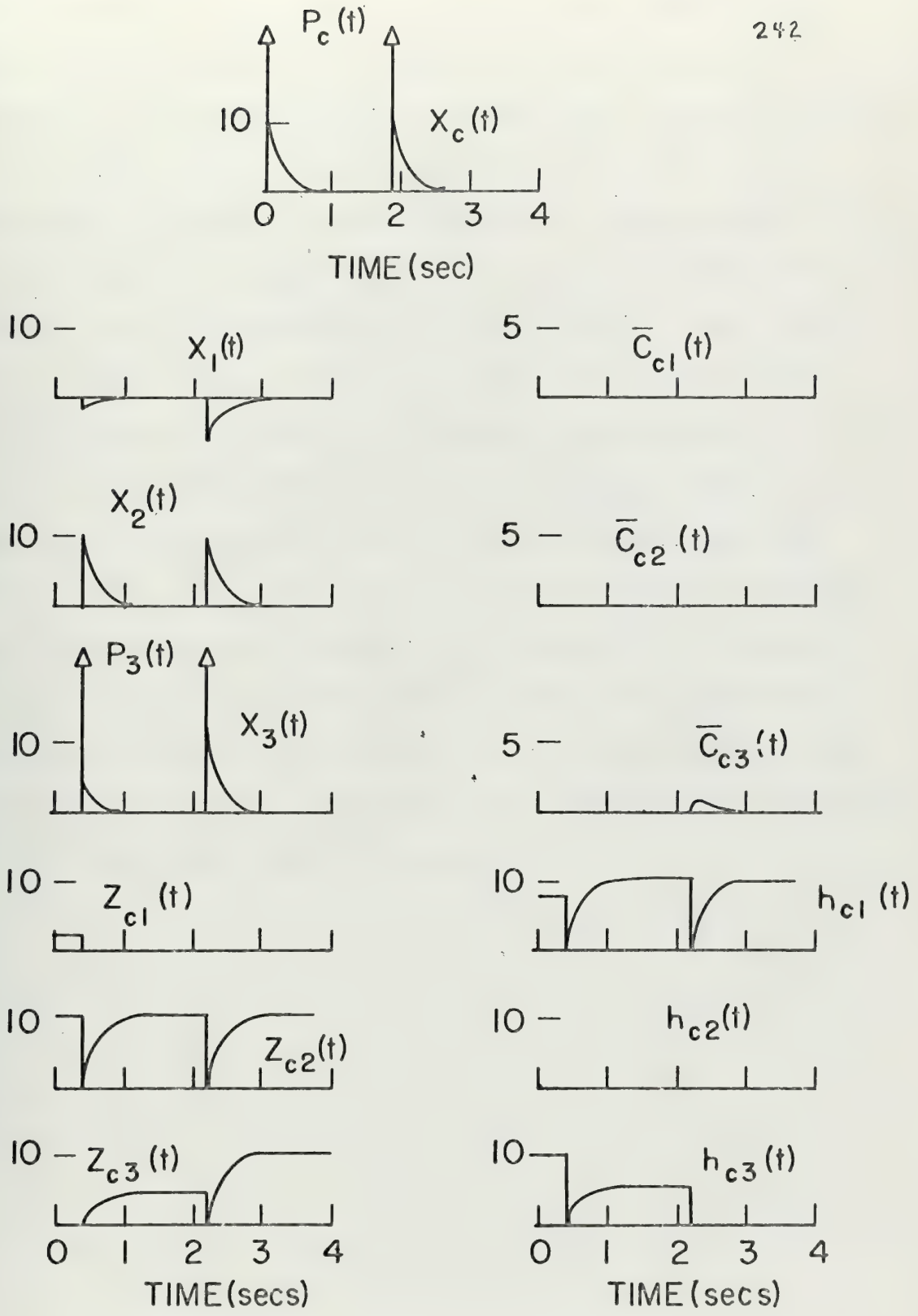

Figure 8.7.3. An unsucessful attempt to correct a previously learned pattern in a chemical outstar.

second excitement of the command node, $x_1(t)$ rises to only a slight positive value. The amount of H produced in S_{c1} during the prediction excitement is considerably more than the E produced. Further prediction excitements will result in inhibited amplitudes for $x_1(t)$. We may conclude that the outstar has good resistnace to random mistakes.

The experiment was continued to test the correctability of the outstar. The correcting pattern $V_c \rightarrow V_2$ was presented twice. Figure 8.7.3 shows the results. Although the outstar did learn the pattern $V_c \rightarrow V_3$, it did not "unlearn" the previously learned pattern $V_c \rightarrow V_2$. There is no "forgetting rate" in the chemical outstar. Thus the old pattern can not be forgotten. There is also no lateral inhibition in this outstar. Thus, this chemical outstar lacks the two mechanisms whereby previously learned patterns can be removed from its memory. This is a major drawback in this outstar. Further work with it would require investigations of the effects of a finite forgetting rate for the E and H substances in the synaptic clefts. Additionally, the effects of lateral inhibition should be investigated.

APPENDIX A

The Digital Simulation and its Accuracy

The equations which were simulated in this thesis were simultaneous nonlinear differential difference equations. They fell into three basic types:

A.1 $\dot{x}(t) = -\alpha x(t) + Ix(t)$

A.2 $\dot{y}(t) = -\alpha y(t) + z(t)x(t - \tau) + Iy(t)$

A.3 $\dot{z}(t) = -uz(t) + y(t)x(t - \tau)$

Figure A.1 shows a system flow diagram for this set of equations.

The key to the digital simulation is the algorithm used for the integrators. This thesis used a simple Euler rule algorithm. That is, the integral:

$$r(t) = \int \dot{r}(t)dt$$

was simulated by the algebraic equation:

$$r(t + h) = r(t) + \dot{r}(t)h$$

where h is the digital increment.

The Euler rule algorithm was adopted because it is easy to program on a high speed difital computer and the computations require comparatively little computations. The large number of experiments simulated in this thesis required efficient use of computation time. Most of the experiments involved at least seven variables and required over fifty increments. Thus the simplest and fastest integration algorithm was selected.

The sampled data "z" transforms for the equation:

A.4 $\dot{x}(t) = -\alpha x(t) + Ix(t)$

using an Euler rule integration algoritm is:

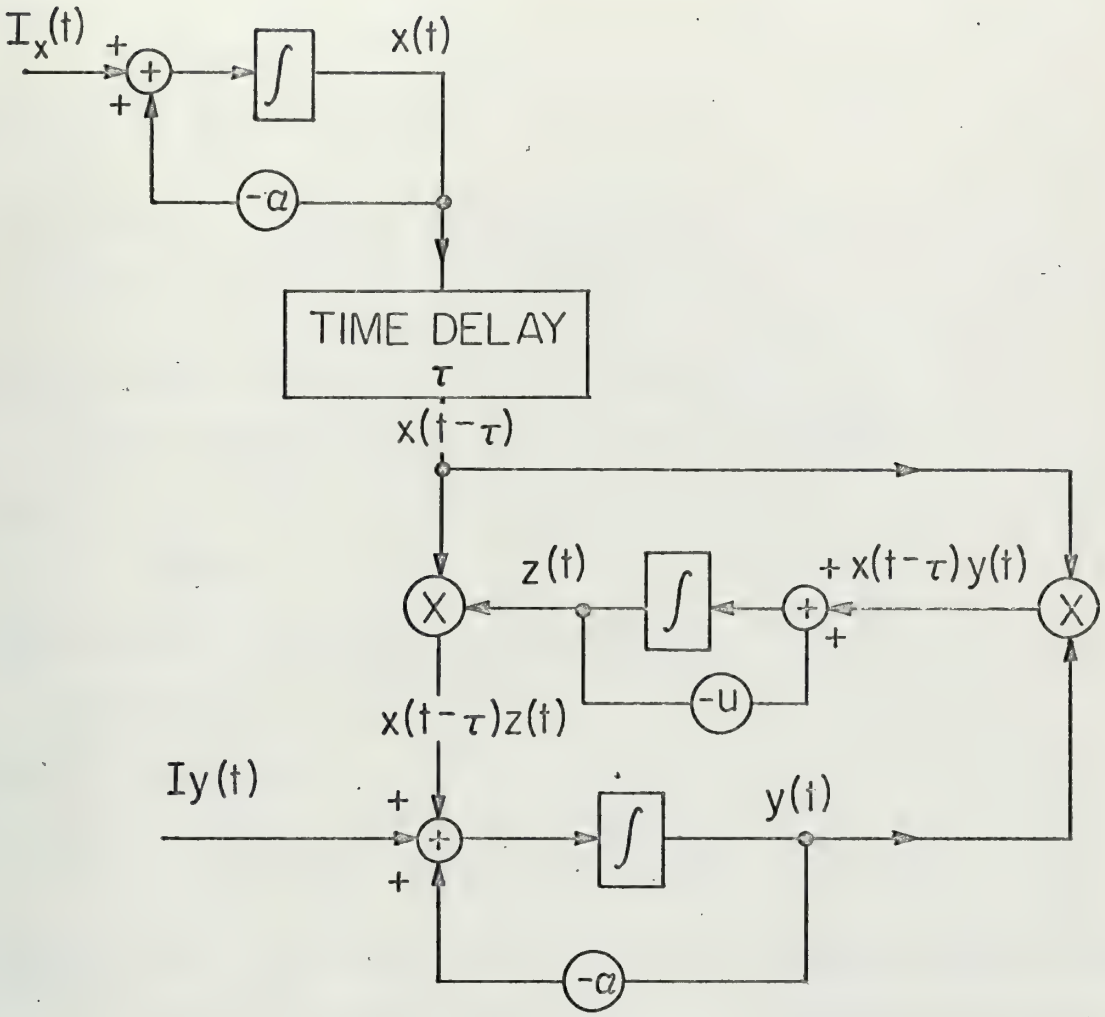

Figure A.1. A signal flow diagram for the simulation.

$$x^{\star}(z) = \left(h/(z - 1 + h\alpha)\right) I(z)$$

for:

$$Ix(t) = u_{-1}(t)$$

where:

$$u_{-1}(t) = \begin{cases} 0 \text{ for } t < 0 \\ 1 \text{ for } t \geq 0 \end{cases}$$

$x^{\star}(z)$ is:

$$x^{\star}(z) = \frac{h}{z}\left(\frac{z}{z - 1} + \frac{(1 - 1/(h\alpha))z}{z - 1 + h\alpha}\right)$$

The time varying function which this transforms to is:

$$x^{\star}(t) = (1/(\alpha))u_{-1}(t - h) + (h - 1/(\alpha))e^{-\gamma(t-h)}) \text{ for } t \geq 0$$

where:

$$\gamma = -1/(h)\ln(1 - h\alpha)$$

The continuous solution to A.4 when $Ix(t) = u_{-1}(t)$ is:

$$x(t) = (1/\alpha)(1 - e^{-\alpha t}) \quad \text{for } t \geq 0$$

For $t \geq h$, the ratio:

A.5
$$\frac{x^{\star}(t)}{x(t - h)} = 1 + \frac{\alpha h e^{-\gamma(t-h)}}{(1 - e^{-\alpha(t-h)}} \quad \text{for } t \geq h$$

computed at $(t - h) = 1/\alpha$ was used to check the accuracy of the amplitudes of the digitally simulated function $x^{\star}(t)$. The ratio γ/α was used to check the accuracy of the simulated decay rate, γ. The two most frequently used choices for α and h in this study were:

$\alpha = 3.3333, \quad h = 0.1$

and:

$\alpha = 1.6666, \quad h = 0.1$

The following table shows the accuracy of the simulation to a step input:

αh	$\gamma/\alpha = -(1/\alpha h)\ln(1-\alpha h)$;	$\frac{x^{*}(t)}{x(t)} = 1 + \frac{\alpha h e^{-\gamma(t-h)}}{(1 - e^{-\alpha(t-h)}}$
0.3333	1.170	1.163
0.166666	1.097	1.087

Since all of the input pulses used in the study were of duration $\delta = 1/\alpha$, the response of the x processes to input impulses is in error by at most 17%. The simulated decay rates are in error by at most 17% also.

No attempt was made to analytically compute the error in the simulated response of the x and z processes to non linear inputs. The results were self-consistent and agreed qualitatively with Grossberg's theoretical predictions. Throughout this study a qualitative feel for the networks studied and the parameters involved in them was the primary concern. As long as the simulation agreed qualitatively with theoretical expectations, little concern was given to the possibility of up to 20% amplitude errors in the computations.

The computations order and actual equations used to simulate equations A.1 through A.3 were:

A.5 $x(t + h) = x(t) + (I_x(t) - \alpha x(t))h$

A.6 $y(t + h) = y(t) + (I_y(t) - \alpha y(t) + z(t)x(t - \tau))h$

A.7 $z(t + h) = z(t) + (y(t + h)x(t + h - \tau))h$

where $t = hn$; where n is an integer.

τ was always chosen to be an integer multiple of h. The sequence A.5, A.6, A.7 was computed and then started again with A.5 for the next

incrementation. Thus the values for z(t) in A.6 were effectively delayed by h.

The digital computer used for the simulations reported was Digital Equipment Corporation PDP/9 with32K of core memory. The programs used were programed in the Digital Equipment Corporation's interpretive language FOCAL. The choice to use FOCAL was made because FOCAL allows the dimensions of matrices to be a variable that can be specified at run time. The programs used stored the value of each of the variables being computed after each incrementation. The stored values were outputed at the end of each run. Since the number of variables and the number of incrementations per run varied considerably, the ability to specify matrix dimensions in the programs immediately before the run was a great advantage.

The minimum accuracy in calculations performed by FOCAL is six digits. Since the sampled data error was on the order of 1%, six digits computation error was entirely sufficient.

REFERENCES

1. S. Grossberg, On the Serial Learning of Lists, Math. Biosc., 4 (1969), 201-253.
2. S. Grossberg, Some Physiological and Biochemical Consequences of Psychological Postulates, Proc.Natl. Acad. Sci. USA 60 (1968), 758-765.
3. S. Grossberg, A Prediction Theory for Some Nonlinear Functional-Differential Equations II. Learning of Patterns. J. Math. Anal. Appl. 22 (1968) 490-522.
4. S. Grossberg, On the Production and Release of Chemical Transmitters and Related Topics in Cellular Control, J. Theoret. Biol. (1969) 22, 325-364.
5. S. Grossberg, On Learning, Information, Lateral Inhibition, and Transmitters, Math. Biosc., 4, (1969) in press.
6. S. Grossberg, Some Networks Capable of Learning, Remembering, and Performing any Number of Complicated Motor Sequences and Reflexes by Respondant and Operant Conditioning.
7. S. Grossberg, Some Networks that Can Learn, Remember, and Reproduce Any Number of Complicated Space-Time Patterns, I, J. of Math. and Mechanics, in press.
8. S. Grossberg, Some Networks That Can Learn, Remember, and Reproduce Any number of Complicated Space-Time Patterns II.
9. S. Grossberg, On Learning of Spatiotemporal Patterns by Networks with Ordered Sensory and Motor Components: I-Excitory Components of the Cerebellum, J. of Math. and Physics., in press.

10. S. Grossberg, Embedding Fields: A New Theory Of Learning with Physiological Interpretations, J. Math. Psych., in press.

11. White, Handler, Smith, Principles of Biochemistry, McGraw-Hill, New York, 1968.

12. Physiology, ed. by E. E. Selkurk, Little, Brown and Company, Boston, 1966.

13. G. G. Simpson and W. S. Beck, Life, An Introduction to Biology, Harcourt, Brace, and World, New York, 1969.

Thesis 118518
F7854 Frasier
Computer simulated learning: a digital simulation of embedding field outstar networks.